ASSESSMENT OF CLIMATE CHANGE IMPACT ON WATER AVAILABILITY IN UPPER MAHAWELI RIVER BASIN, SRI LANKA

Faisal Musadiq

(208357P)

Degree of Master of Science

Department of Civil Engineering

University of Moratuwa

Sri Lanka

February 2022

ASSESSMENT OF CLIMATE CHANGE IMPACT ON WATER AVAILABILITY IN UPPER MAHAWELI RIVER BASIN, SRI LANKA

Faisal Musadiq

(208357P)

Supervised by

Dr P. K. C. De Silva

Thesis submitted in partial fulfillment of the requirements for the degree Master of Science in Civil Engineering

UNESCO Madanjeet Singh Centre for

South Asia Water Management (UMCSAWM)

Department of Civil Engineering

University of Moratuwa

Sri Lanka

February 2022

DECLARATION OF THE CANDIDATE AND SUPERVISOR

"I declare that this is my own work and this thesis does not incorporate without acknowledgement any material previously submitted for a Degree or Diploma in any other University or institute of higher learning and to the best of my knowledge and belief it does not contain any material previously published or written by another person except where the acknowledgement is made in the text".

Also, I hereby grant to University of Moratuwa the non-exclusive right to reproduce and distribute my thesis, in whole or in part in print, electronic or other medium. I retain the right to use this content in whole or part in future works (such as articles or books).

UOM Verified Signature

---------- 23/02/2022

Faisal Musadiq Date

The above candidate has carried out research for the Master's thesis under my supervision

UOM Verified Signature

---------- 25/02/2022

Dr P. K. C. De Silva Date

ABSTRACT

Assessment of Climate Change Impact on Water Availability in Upper Mahaweli River Basin, Sri Lanka

Climate change, population increase, and economic development will all have an impact on future water availability for drinking water supply, agriculture, and recreation activities, with different effects in different regions. The present study investigates the potential impact of climate change on future water availability in the Peradeniya sub-catchment of the Upper Mahaweli river basin. The hydrological modeling of this study was performed by Hydrologic Engineering Centre Hydrological Modelling systems (HEC-HMS). In this study, the entire catchment area was divided into three sub-basins to simulate runoff at the outlet of the catchment and the model results were calibrated and validated using historical streamflow data. Future runoff based on calibrated parameters was estimated after bias correction of climate rainfall data for representative concentration pathways (RCP) 4.5 and RCP 8.5 scenarios. Further, an assessment of water availability based on annual and seasonal periods was carried out from the model results.

The model calibration carried out from 1990 to 1994, indicated good model results in terms of objective functions where root mean square error (RMSE) is 0.60, Nash-Sutcliffe (NSE) is 0.62, and Percent Bias is -15%. Further, validation of model results from 1994 to 2000 yielded RMSE of 0.60, NSE of 0.52, and Percent Bias of 13.9 % indicating good model results. From the results obtained, it was identified that the water availability will increase for both scenarios RCP 4.5 and RCP 8.5 during the mid-century (2040-2060) and end-century (2080-2100) period. The annual water availability concerning the historical period will increase by 27.34 % during the mid-century period and will further increase by 42.06 % during the end-century period in the RCP 8.5 scenario. The seasonal water availability in mid-century compared to the historical period will be more affected during the first inter-monsoon (FIM) period with an average increase of 69 % and 83 % in RCP 4.5 and RCP 8.5 scenario, respectively. Whilst the seasonal water availability will decrease during the first inter-monsoon (FIM) in the end-century compared to the mid-century period by 26 % and 27 % in RCP 4.5 and RCP 8.5 scenarios, respectively. The findings of this study can be useful for the water managers and stakeholders to manage future water needs in the basin and reduce the future vulnerabilities associated with the increasing water availability in the basin.

Keywords: Climate Change, Precipitation-Runoff Process, HEC-HMS

DEDICATION

I dedicate this thesis to my Father and Mother for their dedicated partnership for success in my life.

ACKNOWLEDGEMENT

First and foremost, I thank Allah, the Almighty, for providing me with this chance and equipping me with the necessary skills to succeed.

Furthermore, I would like to convey my gratitude to Dr. P. K. C. De Silva, my research supervisor, for his research supervision as well as his warm and persistent encouragement throughout my research tenure. This thesis would not have been a success without his attentive supervision and ongoing coaching. I owe him a great debt of gratitude for his time, support, encouragement, and professional guidance during the research and writing of this thesis.

I shall never forget to express my gratitude to Center Chairman Prof. R. L. H. Lalith Rajapakse, who has always gone out of his way to assist me in carrying out my research. His unwavering support and encouragement are highly appreciated.

I would also like to thank Mr. H. W. Kumarasinghe and the other team at UMCSAWM for their encouragement, inspiration, support, assistance, and sacrifice of time and effort in assisting me in obtaining a master's degree.

Many of my colleagues with whom I worked and who supported me despite their work, as well as those who assisted me in attaining success in research and thesis writing, and all of the other people who helped me in various ways throughout my stay here, are indebted to me.

I would like to express my gratitude to Hamiduillah Arefi SAF (Afghanistan), and the University of Moratuwa for providing me with the opportunity to pursue a master's degree in Water Resource Engineering and Management at the UNESCO Madanjeet Singh Centre for South Asia Water Management (UMCSAWM), Department of Civil Engineering, and University of Moratuwa, Sri Lanka. Last but not least, I would like to express my gratitude to my family and friends for giving me the motivation to complete this thesis.

TABLE OF CONTENTS

LIST OF FIGURES

LIST OF TABLES

LIST OF ABBREVIATIONS

CMIP	Coupled Model Intercomparison Project
CORDEX	Coordinated Regional Climate Downscaling Experiment
DMC	Disaster Management Center
EP	Effective Precipitation
ERA	ECMWF Re-Analysis
GCM	General Circulation Model
GHG	Greenhouse Gas
HEC-HMS	Hydrologic Engineering Centre - Hydrologic Modeling System
IAM	Integrated Assessment Models
IDW	Inverse Distance Weightage Method
IPCC	Inter-governmental Panel for Climate Change
NSE	Nash Sutcliff Efficiency
PET	Potential Evapotranspiration
RCM	Regional Climate Model
RCP	Representative Concentration Pathways
RMSE	Root Mean Square Error
UNFAO	Food and Agriculture Organization of the United Nations
WAI	Water Availability Index
WMO	World Meteorological Organization

CHAPTER 1

1 INTRODUCTION

The total amount of freshwater which is available around the world is estimated to be 2.5 %. Around 68.7 % of this freshwater is related to the glaciers and 30.1 % is extracted from groundwater. The precipitation that pours over a certain area will drain as surface water into rivers, streams, and lakes, then penetrate into the groundwater, where it may be retrieved and consumed as a freshwater resource. Every day, nearly 9,000 billion liters of freshwater are consumed around the world (Richardson, 2017).

The usual method of storing water for household uses is to take water from a source and store it in a container or storage for different consuming purposes as it is a general practice in many parts of the world (Eric Mertens et al., 1990).

In the case of increasing population and climate change impacts, water shortages are caused in many regions of the world in the future. Sri Lanka has experienced climate change impacts that involve increasing temperature and variability of rainfall.

As people become more conscious of climate change, they are becoming more concerned about the future reliability of drinking water sources (Kristvik et al., 2019). The world's most challenging concern at the moment is the world's expanding population, which has an impact on freshwater supply while increased water use is one of the main causes of water scarcity (Sophocleous, 2004).

One of the fundamental topics in the global debate is the need for climate change information at the regional to a local level. This type of information is required to organize and assess the impact of climate change on human and natural systems. The impact of increased greenhouse gas concentrations will have an impact on the atmosphere's common circulation and the structure of planetary-scale dynamical processes (Giorgi & Gutowski, 2016).

Climate change will have an impression on rainfall intensity in the future. General circulation models can be used to explore the impact of climate change on water availability and water resources (Giorgi & Gutowski, 2016).

Therefore, the most crucial effects of climate on water sources are increasing of rainfall intensity, evaporation rates, earlier shorter runoff seasons, and also increased water temperature.

Scenario evaluations of water availability and demand sensitivity to climate change will provide estimates of how much more or less water will be accessible on the surface and in aquifers, as well as how much more or less water would be required by consumers if the climate changes by specific amounts. Climate, water supply, and water demand forecasts are based on a set of acceptable future assumptions, such as population and economic growth. Planners must be aware of these assumptions and prepare their plans accordingly, even though there are many unknowns. Strategic planning must include a risk assessment approach that leads to risk management (Molden et al., 2014).

Changes in climate, population increase, and economic growth will all influence future agricultural water availability, with various consequences in different areas. Changes in hydrological regimes (such as rainfall, actual evaporation, and runoff at the watershed and river basin sizes) will not only influence irrigation demand and supply but the non-agricultural customers will simultaneously become more competitive for freshwater in the future (Bharati et al., 2014).

The General Circulation Model (GCM) is the outcome of the multipart interaction between the atmosphere, cryosphere, hydrosphere lithosphere, and biosphere (Cubasch & Fischer-Bruns, 2005). The GCMs have been proven to be a crucial tool for assessing the effects of climate change.

Although the simulated scenarios are acceptable for regional to national scale investigations, their coarse spatial resolution makes them unsuitable for basin-level analyses. Several methodologies have been created to address this problem, but there is still a need to improve existing impact assessment study methods. Bias correction

has been effectively used to link the GCMs and impact assessment hydrological models in several parts of the world.

1.1 Problem Identification

Water availability and scarcity are the major concerns of the present world considering the increasing demand for multipurpose uses of water in households, agriculture, industry, and many more while the imbalances are making more water stress on communities. Considering the climate change impacts, the situation is getting even more challenging (Hoekstra et al., 2012).

Climate change has had a greater impact on Sri Lanka's economic, social, and agricultural sectors than on any other country in the area; the susceptibility is enormous due to the country’s strong reliance on hydropower generation, irrigation for agriculture, and home and human consumption (Seneviratne et al., 2010).

The upper Mahaweli river basin has a high fluctuation of precipitation which is discussed by a rainfall-runoff model and prediction for future water availability (Imbulana et al., 2018).

The Mahaweli Development Program (MDP) which was being implemented since 1977 in the study area was the largest and the most extensive physical and human resource development program ever implemented in Sri Lanka, MDP had focused on constructing a series of reservoirs, hydroelectricity plants and to develop a large area of land with irrigation, hydroelectricity plants and to develop a large area of land with irrigation. In the context of the water-climate-food-energy nexus, the MDP associated with Mahaweli water was demonstrating substantial failures due to the spatial and temporal impacts of climate variability, socioeconomic demands for water allocation, and distribution for paddy cultivation in dry zone areas (Shelton & Lin, 2019).

Two yearly monsoon seasons have an impact on the Mahaweli basin. The northeast monsoon (Maha) affects the area from December to February, while the southwest monsoon (Yala) affects the area from May to October. Annual rainfall in the top portions of the drainage basin is normally above 5,000 millimeters, although

precipitation in the lower reaches is typically on the order of 1600 millimeters (Tolisano et al., 2005).

Considering the climate change impact, the rainfall and streamflow trends have changed over time, which do not correspond to the ever-increasing demand for water. As a result of changing climate, temperature rises which means more evaporation will take place, and rainfall is getting intensified which causes several adverse environmental impacts and water shortage (WFP et al., 2020). Therefore, this study will fill the existing gap and give a better understanding of the water availability and variability due to climate change impacts.

1.2 Problem Statement

The Mahaweli Development Program which was aimed to supply water for different purposes is demonstrating substantial failures due to the spatial and temporal impacts of climate variability, socio-economic demands for water allocation, and distribution for paddy cultivation in dry zone areas. In addition, climate change raises more concerns for future water availability. The Peradeniya sub-catchment which is located in the upper Mahaweli basin is also affected by the climate change impacts. Therefore, an assessment of climate change impacts on water availability is necessary for sustainable water management of the study area.

1.3 Objectives

1.3.1 Main Objective

To assess the future water availability in the upper Mahaweli river basin in the Peradeniya sub-catchment, based on the RCM model and climate change scenarios (RCP 4.5 and RCP 8.5) in near future (2040-2060) and far future (2080-2100).

1.3.2 Specific Objectives

1. Developing a hydrological model based on daily precipitation and evapotranspiration to model streamflow using HEC-HMS.
2. Calibrating and validating the model performance using observed data.

3. Extracting the climate model data, performing bias correction and forecasting for future scenarios.
4. Predicting water availability due to the climate change impact in future.

1.4 Research Significance

1. Once the amount of available water is calculated, it will be useful for the water-balance calculations between the water availability and water demand.
2. The impact of climate change on the fluctuations of water availability will help to estimate water demand for future population growth.
3. It will be helpful to investigate the impact of climate change on streamflow fluctuation as a result of this research.

1.5 Research Scope

1. Simulation of future water availability for the wet and dry seasons.
2. Investigation on the potential impact of climate change on future water availability.

1.6 Outline of the Thesis

This thesis comprises of six chapters.

Chapter 1: This chapter covers the problem statement, research purpose, and research scope.

Chapter 2: Literature review relevant to this study on various topics such as climate change, water availability, and hydrological modeling are discussed in this chapter.

Chapter 3: This chapter provides a detailed description of the study area, highlights the methods utilized to obtain the research objectives, and describes the various datasets used in the study.

Chapter 4: The finding and results of this study are presented in this chapter, and it provides a critical review of the HEC-HMS model results and the impact of climate change on water availability.

Chapter 5: It includes a brief discussion based on the findings of this study and the analysis.

Chapter 6: Conclusions are presented based on the results obtained and recommendations are suggested for further research in the future.

CHAPTER 2

2 LITERATURE REVIEW

2.1 General

The quantity of water required to be continually present at a specific area (rivers, dams, lakes, reservoirs, and other water structures) for a certain amount and within a certain period is defined as water availability. To manage the water resources efficiently, it is necessary to understand the water availability in a catchment. The catchment is an exposed system at which the hydrological process happens in the hydrological cycle. In the management of sustainable water resources, spatial knowledge on water availability in a region is critical. Water availability in watersheds may be measured and monitored using geographic information systems throughout time and within a designated unit of space (Mirrah & Kusratmoko, 2017)

The majority of studies and assessments on water availability concentrate on blue water, or water that is accessible on the earth's surface and subsurface while the amount of water as river flow discharge is dependent on rainfall and catchment characteristics (Haque, 2018). The characteristics of the catchment, such as geological features, terrain, soil, land cover, and water availability will differ between the watersheds. To estimate the water availability in a region there are fundamental needs to water requirement, hydrological and hydrometeorological datasets. For this purpose, the index of water availability is used which indicates the relationship between human needs and water availability. The water availability index is the most important factor for controlling drinking water requirements in the region (Ekness & Randhir, 2015).

2.2 Past Studies Regarding Water Availability and Climate Change Impact

Climate change may have an impact on many components of the hydrological cycle, including water balance terms and runoff production, depending on the availability of water resources. Actual evapotranspiration and soil water storage which can be affected by changes in temperature and precipitation will subsequently affect agriculture, industry, and urban development programs (Abdo et al., 2009).

The impact of climate change on water resources is not only because of changes in amount and quality of streamflow, but it will be also related to the catchment characteristics, water requirement variation throughout the year, management of the systems, and the adaptation measures in the area (Tekleab et al., 2011).

Water availability in the Huong catchment, in Central Vietnam, was studied concerning climate change and population growth. The major objective of this research was to determine how much water is available in the Huong River Basin. The Hydrologic Engineering Centre Hydrological Modelling systems (HEC-HMS) model was used for simulating the rainfall-runoff response in association with climate forecasting. The regional climate model (RCM) is used for forecasting future rainfall, after bias correction.

For the study of climate change impact on flooding in Switzerland, HEC-HMS and Coupled Model Intercomparison Project (CMIP5) were employed to analyze the influence of climate change on flood happenings. The study by Bai et al. (2018), presented a framework combining the HEC-HMS and the CMIP5 general circulation models. The proposed approach is applied to the Nippersink Creek watershed, which demonstrates that precipitation for the low, medium and high emission scenarios are all more than the historic observation across 10, 25, 50, and 100 years.

Climate change significantly impacts meteorological parameters such as rainfall, temperature, and evaporation. The resulting change in meteorology affects hydrology and streamflow whereas changes in hydrologic components impact local and regional hydrology affecting ecological, social, and economic systems. Because hydrological impact studies require climate data at a precise spatial resolution, the GCMs data must be downscaled to a scale appropriate for catchment scales. As an example of

downscaling, Dhital et al. (2011) assessed climate change impact on the Bagmati river in Nepal using downscaled meteorological parameters from the statistical downscaling model (SDSM). In the Cianten watershed, Bogor District, a Geographic Information System (GIS) was used to estimate water availability and demand using rainfall and temperature data from 2007 to 2016, as well as elevation, slope, soil type, and land use data of the study area (Mirrah & Kusratmoko, 2017).

The study by Shrestha (2014), looked into the impact of climate change on Thailand's future water supplies. The whole country was divided into nine Hydrological Response Units (HRUs) for this study, and HEC-HMS was used to execute the hydrological modeling. Using observed and Climate Research Unit (CRU) data, trend analysis methods were utilized to investigate climate variability and trends from 1951 to 2015, and a mixture of spectral analysis techniques was used to predict temperature and precipitation using CRU data.

The flow duration curve can be used to examine water availability in a region (Ahmed, 2012). The curve can be created by charting the magnitude of each flow throughout the study period on the y-axis and the percentage of flows that equal or surpass that flow on the x-axis (hence, the term exceedance percentage). For big and peripheral rivers, a flow duration curve has been devised to indicate the river's 80 percent likelihood of water flow.

2.3 IPCC Fifth Assessment Report (AR5) and Future Scenarios

The Intergovernmental Panel on Climate Change (IPCC) started creating emission scenarios in 1996. According to these projections, several demographics, economic, and technical factors will influence future greenhouse gas and sulfur emissions. Four (4) possible narrative stories were produced by analyzing the links between the processes that affect pollution, their evolutions, and the perspective for scenario quantification (IPCC, 2007). According to the scenarios, the Representative Concentration paths (RCPs) propose Green House Gases (GHG) emissions into the atmosphere. The RCPs were created by feeding Integrated Assessment Models (IAMs) into a variety of climate model simulations in order to project their effects on the climate system. The RCPs are compatible with the vast variety of mitigation

possibilities examined in the literature. The RCPs Scenarios from the IPCC's special report on AR5 are listed below.

2.3.1 Representative Concentration Pathway RCP 2.6 (low emission)

Most models under RCP 2.6 indicate considerable net negative emissions, averaging approximately two (2) GtCO2/yr. RCP land-use scenarios demonstrate different ranges of conceivable futures, from increased green plants to increased desertification. Because of expected Policies to reduce air pollution and reduce greenhouse gas emissions, the RCP scenarios imply decreasing emissions for air pollutants, including sulfur dioxide (SO_2). Under RCP 2.6, the temperature will rise in the late 21st century (2081–2100) by 0.3 °C to 1.7 °C compared to 1986–2005. Earth System Models predict increasing ocean acidification in the late twenty-first century for all RCP scenarios.

As global mean surface temperature rises, it is clear that permafrost extent would decline at high northern latitudes. Permafrost near the surface is decreasing by 37 and 81 % under RCP 2.6 and RCP 8.5, respectively. All RCP scenarios predict that temperature rise will continue after 2100. The temperature will not change in high latitude due to no GHG emissions. The temperature change will exceed 2 °C in the late twenty-first century (2081–2100) concerning the base period 1850–1900 (Pachauri, Meyer & IPCC, 2014).

2.3.2 Representative Concentration Pathway RCP 4.5 (Intermediate emission)

In RCP 4.5, the temperature will increase about 1.5 °C by the late twenty-first century (2081–2100) concerning 1850–1900. The temperature will not increase by more than 2 °C. The majority of the plant will not be able to cope with the high projected changes in the climate system under this scenario. An increase in temperature will affect the hydrological cycle negatively and hence water availability. Therefore, this scenario is considered in this study.

2.3.3 Representative Concentration Pathway RCP 6.0 (Stabilizing Emission)

Temperature increment in the late twenty-first century (2081–2100) is predicted to increase 2 °C under RCP 6.0 and RCP 8.5, concerning 1850–1900. The temperature

change will range from 1.4°C to 3.1°C in the late twenty-first century (2081–2100) concerning 1986–2005. Climate change is mainly attributed to high emission scenarios such as RCP 4.5, RCP 6.0, and RCP 8.5 (Pachauri, Meyer & IPCC, 2014).

2.3.4 Representative Concentration Pathway RCP 8.5 (High Emission)

Temperature increment in the 21st century (2081–2100) is 1.5 °C for RCP 8.5 concerning 1850–1900. The temperature change ranges from 2.6 °C to 4.8 °C in 2081–2100 concerning 1986–2005 under RCP 8.5. Precipitation changes are not unidirectional. The high latitudes and the equatorial Pacific are likely to experience increasing average annual rainfall. Precipitation volume will decrease in mid-latitude dry regions, while opposite precipitation is projected for mid-latitude wet regions (Pachauri, Meyer & IPCC, 2014).

Droughts will likely become more common at the end of the twenty-first century in currently dry regions, according to RCP 8.5. Global mean sea-level rise will continue for several centuries after 2100 (Pachauri, Meyer & IPCC, 2014).

2.4 Coordinated Regional Climate Downscaling Experiment

Regional downscaling, according to the World Climate Research Programme (WCRP), is a chance to incorporate the larger scientific community in climate research. The coordinated regional climate downscaling experiment (CORDEX) has accelerated the downscaling process in this regard. The WCRP-CORDEX dataset for South Asia is supplied to aid the scientific community in predicting future climate patterns and to raise public awareness about climate change. The downscaled data after several quality checks are published on the CCCR-IITM Earth System Grid Federation (ESFG) Data Node for public access and use (Sanjay et al., 2017). The RCP 4.5 and RCP 8.5 scenarios are used for the present study. In CORDEX, the static bias correction was performed utilizing real-time data, and RCP 4.5 is the most suitable case for the static bias correction. shows Region 6: South Asia of the CORDEX project.

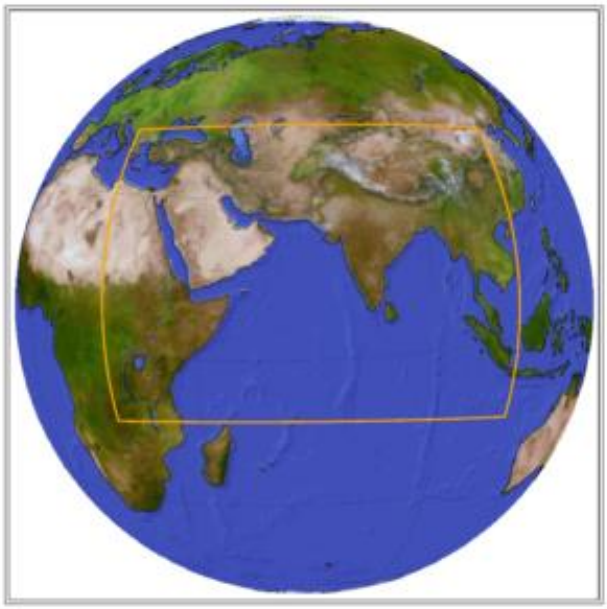

Figure 2-1: Region 6 - South Asia in Regional Climate Model (Cordex)

(Source: http://www.cordex.org/domains/region-6-south-asia/)

2.5 Bias Correction

Large-scale Global Climate Models (GCMs) with a resolution of 100-250 km is used to model atmospheric circulation patterns. To generate simulations with finer resolutions of roughly 25-50 km, downscaling techniques are required. RCMs (Regional Climate Models) are the most used downscaling technique (Eden et al., 2014). Bias correction approaches improve climate model output fitting by removing systematic errors that have a better match with observed data (Teutschbein & Seibert, 2010).

To remove systematic inaccuracies in forecast climatic parameters, several bias correction approaches are available. Some bias correction procedures are straightforward, while others are more difficult. For a single climate parameter, such as precipitation, there are some empirical bias correction approaches (Leander & Buishand, 2007). The base period of precipitation and temperature was selected as 1990-2005 for this research project.

The general recommendation is to use 30 years periods of reference for the climate studies (WMO G, 2017). Due to data unavailability, data accuracy, and economy, 15

years of reference period can be considered for climate bias correction (Sirisena et al., 2021).

2.6 Missing of Rainfall Data

Rainfall has a significant role in the hydrological cycle. Accessing accurate data is one of the first tasks in any hydrological or meteorological investigation. For the precise planning of water resources, a hydrologist considers some methods to fill the missing data. There are several methods for filling the missing data such as the arithmetic averaging method, the multiple linear regression method, and the nonlinear iterative partial least squares algorithm that performs best (Sattari et al., 2017).

2.6.1 Simple linear Regression Method

Simple linear regression can be a good solution for the problem if the number of points is less than two (2) and there is no need to cross from all points. The quantity of an unknown variable can be determined by a known variable or variables; hence regression follows a mathematical relationship computation. Due to the set of neighboring stations that have fairly high correlation coefficients with the target station dimple linear regression method selected (Caldera et al., 2016). If there is a cause-and-effect relationship between two quantitative variables that are linear, the regression equation is shown in Equation [2-1].

$$Y = A + BX \qquad [2\text{-}1]$$

where,

Y is the dependent variable (that's the variable that goes on the Y-axis), X is the independent variable, B is the slope of the line and A is the y-intercept.

2.7 Hydrological Model Classification

Generally, there are two types of hydrological models: physical models and abstract models. The scale model and the analog model are two physical models. The scales are smaller in the physical model. The model is used to lower the scales in dam

spillway hydraulic models. An analogy model is used extensively in the fields of geometry, thermodynamics, and fluid mechanics.

The mathematical or abstract model considers systems in mathematical representations. The operation of the system is based on a set of equations that connect the variables' input and output. The variation is probably both spatial and temporal. These factors can be measures of time and space, as well as probabilistic or random variables that have no fixed value at any given location in space and time and are instead defined by probability distributions. Deterministic models include lumped, semi-distributed, and distributed models. The lumped model will not take into account spatial variances, and geographical areas will be treated as a single catchment but spatial variation factors will be considered in the distributed model, such as soil maps, land use land cover maps, and so on. The geographical area is treated as a single catchment in the lumped model while in a distributed model, the catchment is divided into cells or grids, and water flows from one cell to the next as it drains through the basin. All of the above models, including lumped and distributed models, are components of the deterministic model (Chow, Maidment & Mays, 1988).

2.8 HEC-HMS Model

The hydrologic engineering center is a non-profit organization dedicated to improving water quality. The US Army Corps of Engineers developed the Hydrologic Modelling System (HEC-HMS), which is a physically-concept model. It is primarily used in a semi-distributed or lumped way, the abilities for distributed modeling are also included. It's designed to mimic the runoff mechanism in dendritic watersheds (USACE, 2018).

HEC-HMS can model both continuous and event-based hydrological phenomena while ignoring evapotranspiration and groundwater seepage flow contributions to the catchment response.

HEC-HMS has been used for various applications, comprising flood forecasting (Bhuiyan et al., 2017), response analysis of post-fire (Cydzik & Hogue, 2009), managing of stormwater (McEnroe, 2010), and assessment of climate impact (Meenu et al., 2013). The HEC-HMS model's four main input components are the

meteorological model, watershed model, control manager, and data manager. Sub-watersheds reaches, junctions, sources, sinks, reservoirs, and diversions are all represented by real-world objects in the watershed model. These elements require parameters which will enable to define the hydrological system and its interaction. These interconnected pieces allow water to flow freely and form a dendritic network (USACE, 2018).

The physical properties of a watershed's hydrologic constituents are represented by a basic model, which turns atmospheric situations into streamflow at specific watershed locations. The supplied list of infiltration losses can be used to mimic infiltration losses. Initial constant, SCS curve number, exponential, Green Ampt, and Smith Parlange are all options for event modeling. For simple continuous modeling, the one-layer deficit constant method can be employed. The canopy component has been included to indicate the canopy's interception (USACE, 2018).

There are seven different strategies for converting surplus precipitation into surface runoff. The Clark, Snyder, and SCS approaches are examples of unit hydrograph methods. Five methods are used to represent baseflow contributions to subbasin outflow. From a single or numerous sequential events, the recession approach produces an exponentially declining baseflow (USACE, 2018).

Shortwave radiation, longwave radiation, precipitation, evapotranspiration, and snowmelt are the available ways for analyzing meteorologic data using a meteorological model whereas precipitation and evapotranspiration are required as inputs for continuous events (USACE, 2018). Control Specifications determine how long a simulation lasts. A starting date and time, final date and time, and a time interval are all included. Combining a basin model, a meteorologic model, and control criteria, a simulation run is performed.

2.8.1 HEC-HMS Model Parameter Estimation

The following sub-sections are describing the model parameters which are estimated for the model set up in this study.

2.8.1.1 Simple Canopy Method

There are two parameters in the Canopy method to be estimated:

- **Initial canopy storage (%):** It's a starting condition input that shows how much of the maximum canopy storage is filled at the start. As a starting point, it is recommended to start after a period of no rain, which corresponds to 0 %. Following that, in the hydrologic modeling, this condition should be considered.
- **Max surface storage (mm):** A formalism parameter that represents the highest depth of water that vegetation may capture. It is dependent on the slope of the basin and the maximum value of surface parameters.

2.8.1.2 Estimation of Deficit and Constant Parameters

The deficit and constant methods require several parameters to be defined prior to model simulation (initial deficit, maximum storage, and constant rate). Maximum storage can be linked to maximum potential storage, which is obtained from the curve number (Madhushankha & Wijesekera, 2021). Taking soil group C as a guideline for calculating curve numbers with soil moisture antecedent condition II, the curve number for each land use is calculated using the TR55 guideline. The initial deficit is calculated as 20 % of the maximum deficit. Saturated hydraulic conductivity is an excellent estimate of a constant parameter (USACE, 2018). However, due to lack of data this parameter is estimated based on the minimum constant loss rate of a particular soil type.

2.8.1.3 Muskingum Parameter

In case of gauged flows required for calibration are not accessible, the value of K and X can be estimated from the channel characteristics, the estimation of K is as follows. Before the calculation of k, we have to estimate the flood wave velocity according to Seddon's Law which is shown in Equation [2-2].

$$v_\omega = \frac{1}{B}\frac{dQ}{d_y} \qquad [\ 2\text{-}2]$$

where B is the highest side of the water surfaces and dQ/dy is the slope of the discharge rating curve at the channel cross-section. For the estimation of the K value, Equation [2-3] is used.

$$k = \frac{L}{v_w} \quad [2\text{-}3]$$

And for calculation of the X value, Equation [2-4] is used.

$$X = \frac{1}{2}\left(1 - \frac{Q_0}{Bs_0C\Delta x}\right) \quad [2\text{-}4]$$

where the Q_0 is the initial flow from Hydrograph, B is the highest width of flow area, S_0 is bed slope, C is the flood wave speed and Δx is the length of reach the average value for the hydrograph. In other words, the midway between the base flow and the peak flow is called reference flow or initial flow.

2.8.1.4 Kirpich Equation

The Kirpich formula is the most widely used equation for the calculation of the time of concentration which is shown in Equation [2-5].

$$Tc = 0.01947L^{0.77}S^{-0.385} \quad [2\text{-}5]$$

where the T_C is a time of concentration in minutes, L is the maximum length of travel of water in meter and S=ΔH/L is the slope of the catchment in which ΔH is the most remote point of the catchment and outlet.

Lag time is calculated using the Equation [2-6].

$$T_L = 0.6 * T_C \quad [2\text{-}6]$$

2.8.1.5 Initial Abstraction

Initially, an abstraction that is influenced by many factors related to the antecedent watershed condition (AWC), is difficult to estimate due to lack of observed data. In the Soil Conservation Service curve number (SCS-CN) method, it is often assumed that Initial abstraction is 0.2 times the potential highest retention. This assumption has frequently been questioned (Zheng et al., 2020). The formula for initial abstraction is utilized in the SCS method is shown in Equations [2-7] and [2-8].

$$IA = 0.2S \quad [2\text{-}7]$$

$$S = \left(\frac{1000}{CN}\right) - 10 \quad [2\text{-}8]$$

where S = Potential maximum retention (inches)

2.8.1.6 Snyder Unit Hydrograph Transform

A synthetic unit hydrograph method is the Snyder unit hydrograph. In 1938, Snyder published a description of a parametric UH that he had developed for the analysis of ungauged watersheds in the Appalachian Highlands in the US. More importantly, he provided relationships for estimating the UH parameters from watershed characteristics (USACE, 2018). The initial data only allowed for the calculation of peak flow as a function of a unit of precipitation.

2.8.2 Calibration of Hydrological Model

The basic objective of calibrating a hydrologic model is to estimate parameter values so that the simulated model outputs match the observed data as closely as possible. The hydrologic model's technical capabilities and the quality of the input dataset allow for accurate calibration and successful implementation of the hydrologic watershed model (Verma et al., 2010).

To obtain simulated outcomes in HEC-HMS modeling, each component requires a parameter value as an input. Some metrics can be approximated exactly by monitoring stream and basin features, but others cannot. Calibration is used to approximate parameters that cannot be accurately estimated. The calibrated values are established by a systematic exploration for the best fit of the observed and simulated streamflow hydrographs.

2.8.3 Validation of Hydrological Model

Verification (also known as validation) is performed on a piece of the dataset that was not utilized for calibration. The goal of model validation is to ensure the model's robustness and accuracy in describing the catchment's hydrological response, as well as to discover any bias in the calibrated parameters (Gupta et al., 2005).

If the model's performance during verification is unacceptable, the starting assumptions must be revised, and the model structure must be evaluated, according to Pechlivanidis et al. (2013). During the calibration period, the model performs better than during the validation period.

2.9 Objective Function

For various purposes, a variety of performance indicators are used. The choice of a certain metric is determined by the modeling purpose. Higher values of NSE are recommended, for example, when peak flow must be properly simulated.

The Nash Sutcliffe Efficiency (NSE) is a well-known performance metric widely used in calibrating/validating a hydrologic model. It determines the relative error in the variance of simulated discharge compared to the observed one. The NSE values lie between -∝ and 1.

Values close to 1 imply good calibration while a value below 0.5 is not acceptable. The indicator can be calculated by Equation [2-9]. In all equations, $Qobs$, $Qsim$, and $\overline{Q_{obs}}$ $b$stand for observed simulated, and the average of observed streamflow, respectively.

$$NSE = 1 - \frac{\sum(Q_{sim} - Q_{obs})^2}{\sum(Q_{obs} - \overline{Q_{obs}})^2} \quad [2\text{-}9]$$

The percentage bias (Pbias) performance indicator indicates how well the model can simulate total runoff volume. When the simulated discharge is positive, it is overvalued, and vice versa. How much the value of Pbias is close to zero, it shows a good performance. This indicator is calculated using Equation [2-10].

$$Pbias = 1 - \frac{\sum(Q_{sim} - Q_{sim})^2}{\sum Q_{obs}} x100 \quad [2\text{-}10]$$

The R^2 coefficient of determination reflects whether the model captures the variation of observed data. There is a strong correlation between observed and simulated data when the values are close to 1. The equation used to calculate the performance metric is shown in Equation [2-11].

$$R^2 = \frac{\sum(Q_{obs} - \overline{Q_{obs}}) \times \sum(Q_{sim} - \overline{Q_{sim}})}{\sqrt{\sum(Q_{obs} - \overline{Q_{obs}})^2} \times \sqrt{\sum(Q_{sim} - \overline{Q_{sim}})^2}} \quad [2\text{-}11]$$

This objective function's optimum values are close to zero. Equation [2-12] is used to determine the indicator, where n represents the total number of observations.

$$MARE = \frac{1}{n} \left| \frac{(Q_{obs} - Q_{sim})}{Q_{obs}} \right| \quad [2\text{-}12]$$

CHAPTER 3

3 MATERIALS AND METHODS

The methodology followed to achieve the objectives of this study is explained in sub-section 3.1.

3.1 Methodology Flowchart

The methodology flowchart is shown in Figure 3-1.

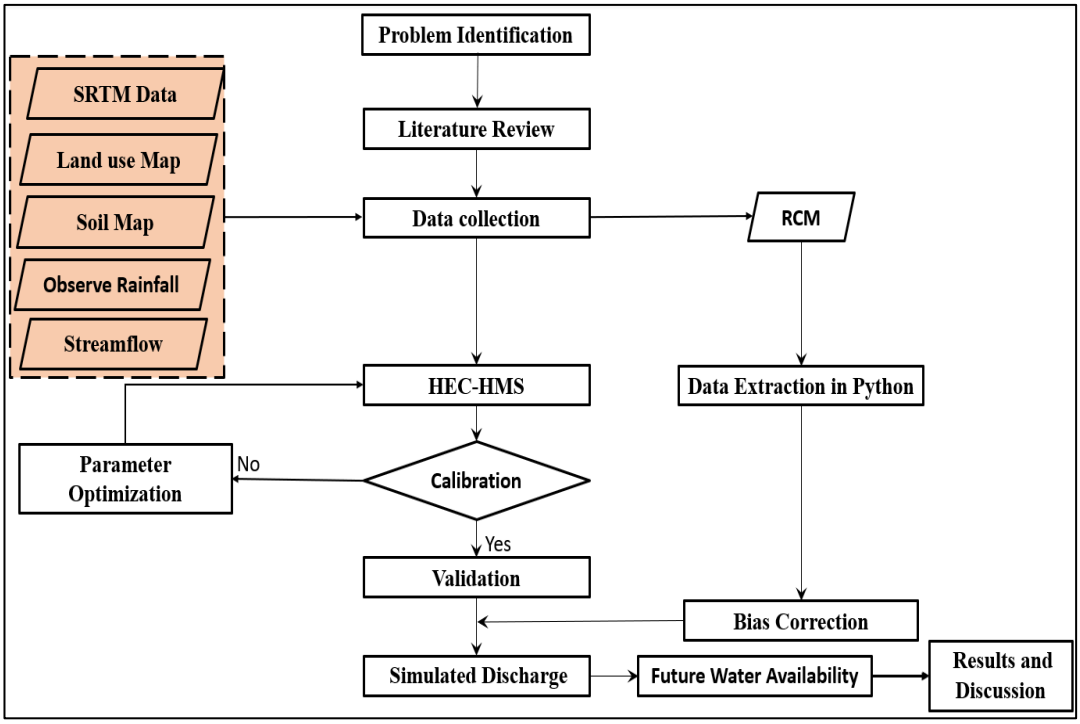

Figure 3-1: Methodology flowchart of the study

According to the methodology flowchart, the problems were identified in the study area and a literature review of the site is accomplished. Then, all required data were collected and checked for errors and biases. Then the datasets were prepared for modeling in the HEC-HMS model. The model parameters optimization was performed using manual and automatic methods. The model is calibrated and validated using the

optimum values for each parameter and water availability is checked in the study area. Finally, results and discussion are presented and subsequently, the conclusions and recommendations are suggested.

3.2 Overview of Study Area

The Mahaweli River is Sri Lanka's longest river with a length of 335 kilometers. It is covering an estimated area of 10,448 km^2 or nearly 16 percent of the country's land area. The basin receives 281.09 m^3 of precipitation per year, of which 109 m^3 is released to the sea. The Mahaweli has an annual flow of 881.09 m^3 and provides one-seventh of the total runoff of all Sri Lankan rivers. Rainfall in the MRB is highly varied in both time and space (Shelton & Lin, 2019).

The Mahaweli basin is divided into two parts, Upper Mahaweli River Basin (UMRB) and Lower Mahaweli River Basin (LMRB). The UMRB falls into the wet climatic zone and a small portion of the intermediate zone. The Mahaweli's upper reaches are found in the western region of the central highlands, with total annual precipitation of 6,000 mm. The typical annual precipitation in the MRB's lower levels ranges from 1,600 to 1,900 mm. In the lowlands, Mahaweli water irrigates 3,650 km^2 of paddy crops, with a total of 10,049 km of canal networks. In addition, the Mahaweli hydropower complex contains seven large power stations with a combined capacity of 775 MWs, which yearly contributes roughly 17 % electrical energy (or 40 % of the island's total hydropower potential) to the national grid. At the current, almost 15 % of the Sri Lankan population (2.8 million people) resides in MRB, and about 166,269 households are settled in the Mahaweli settlement areas.

The upper reaches of MRB include three sub-catchments: Calidoniya, Nawalapitiya, and Peradeniya (UMRB, 2,917.3 km^2). In the lower areas of the MRB, there are three catchments: Laggala, Thaldana, and Manampitiya (LMRB, 7,345.7 km^2). In the Upper Mahaweli River basin, Calidoniya covers an area of (185.1 km^2), Nawalapitiya (143.7 km^2), and Peradeniya (1146 km^2), whereas in the Lower Mahaweli River basin, Loggala covers an area of (117.9 km^2), Thaldana (276.3 km^2), and Manampitiya (5929 km^2) (Shelton & Lin, 2019).

3.3 Delineation of the Catchment by GIS

Following are the processes which are used to delineate the study area boundary using ArcGIS 10.3. Version.

1. Fill Sinks: The filling of the depression or pit cells is handled by the fill sinks command.
2. Flow direction: This step determines the sharpest slope direction for each terrain cell which is performed after filling the sinks in the digital elevation model.
3. Flow accumulation: The flow accumulation tool estimates the flow to each cell by determination of upstream cells that flow into the downslope cell.
4. Stream delineation: All cells with a flow accumulation greater than the user-defined threshold are classified as stream network cells in this step.
5. Catchment grid delineation: For each stream section, this step creates a subbasin.
6. Catchment polygon processing: Using the watershed grid computed in the previous step, this step of the process builds a vector layer of the sub-basins.
7. Drainage line processing: A vector stream layer is generated in this step.

After processing all the above steps, the sub-catchment boundary is delineated which is shown in Figure 3-2.

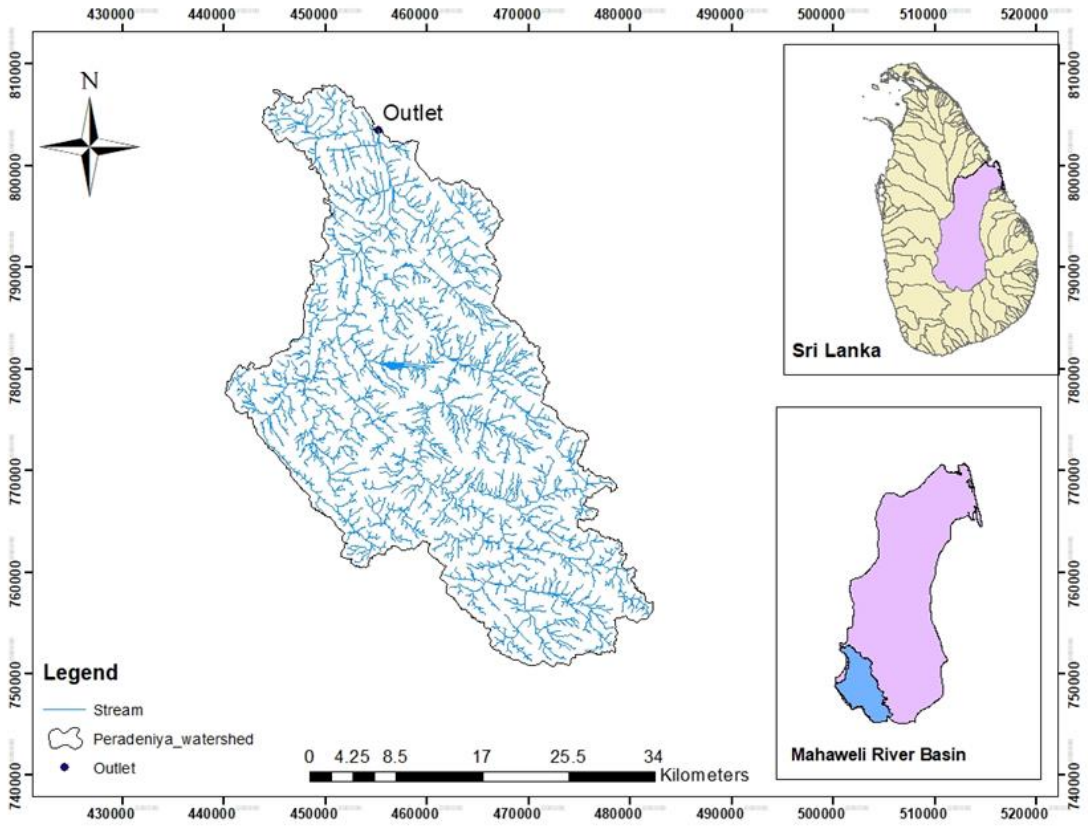

Figure 3-2: Peradeniya sub-catchment located at the upper Mahaweli river basin

3.4 Data and Data Sources

The various datasets like land use maps, digital elevation models, soil maps of the study area are required to give input to the model and generate parameters for the model. In this study, daily precipitation data for four meteorological stations were collected from 1990 to 2015 from the Meteorological Department of Sri Lanka, and missing data were filled by creating a linear regression method. In this study, the daily streamflow data of all four river gauge stations were collected from the Irrigation Department from the period 1990 to 2015. The Regional Climate Model (RCM) data is downloaded from the ESGF website, in which the historical data is downloaded from 1990-2005, and for future climate assessment, the period 2020-2100 regional climate data is considered. Thiessen polygons were created using data collected from all stations to determine the distribution of rainfall. The USGS website was used to obtain a 30 m resolution Digital Elevation Model (DEM) for this study.

The soil and land use data are collected from the Survey Department of Sri Lanka. In this study, the statistical comparison is performed with raw RCM at the basin level. For hydrological modeling, the United States Army Corps of Engineers (USACE) a semi-distributed hydrological model HEC-HMS version 4.8. is set up. The bias-corrected rainfall from RCP 4.5 and RCP 8.5 is input into HEC- HMS to forecast the future decadal availability of water. Clark unit hydrograph transformation, constant monthly baseflow, and lag routing methods are selected to prepare the model. The meteorological model was developed by the Thiessen Polygon weight method. Observed hydrological and meteorological data from the period of 1990-1994 and 1994-2000 is chosen for the calibration and validation of the model, respectively. The general data required for this study is as mentioned in Table 3-1. The details of rainfall and streamflow gauging stations is as mentioned in Table 3-2.

Table 3-1: Data sources and resolution

No.	Data	Spatial Resolution	Data Source
1	Land Use	1:500,000	Survey Department of Sri Lanka (1999)
2	Digital Elevation Model	30 m	Shuttle Radar Topography Mission
3	Soil Map	1:500,000	Survey Department of Sri Lanka (1999)
4	Rainfall	Daily	Department of Meteorology (1990-2015); GFDL-RegCM4 (IITM)
5	Streamflow	Daily	Irrigation Department (1990-2020)
6	Evaporation	Daily	Meteorological Department (1990-2015)

Table 3-2: Rainfall and streamflow gauging stations

Gauging Stations	Data type	Time Period
Helbodde Estate	Rainfall	1990-2015
Nawalapitiya	Rainfall	1990-2015
Peradeniya Bot	Rainfall	1990-2015
Annfield Estate	Rainfall	1990-2015
Kotmale	Evaporation	1990-2015
Peradeniya	Streamflow	1990-2020
Nawalapitiya	Streamflow	1990-2020

3.5 Tools/Software Used

1. HEC-HMS 4.8 (Product of Hydrologic Engineering Center, US Army Corps of Engineers)
2. ArcGIS 10.3 (Product of Environmental System Research Institute)
3. Python 3.7

3.6 Data Checking and Analysis

Good quality hydrological data are required to develop and calibrate simulation models, which are used to plan, design, and upgrade urban stormwater drainage systems. These good quality data can be obtained from a successful data collection program. The outcome of data analysis depends on the quality and completeness of data. The complete series (with no missing values) are used to predict monthly precipitation. There are many methods for filling out missing data such as the arithmetic averaging method, the multiple linear regression method, and the non-linear iterative method (Bai et al., 2018).

Rainfall is an important part of the hydrological cycle. One of the first steps in any hydrological and meteorological study is accessing reliable data. However, precipitation data is frequently incomplete. The incompleteness of precipitation data may be due to damaged mensuration of instruments, measurement errors and geographical scarcity of data (data gaps) or changes to instrumentation over time, a change in the measurement site, a change in data collectors, the irregularity of measurement, or severe topical changes in the climate of a zone. The accurate estimation of the missing data makes a great contribution in accurately assessing the capacity of flood control structures in rivers and dam spillovers (Chen & Liu, 2012).

3.6.1 Data Filling Using Linear Regression Technique

To fill the data, linear regression methods are commonly applied. By fitting a linear equation to observable data, this method demonstrates the link between variables.

The graphs are presented from Figure 3-3 to Figure 3-6 shows the scatter plot before and after filling the missing data, for Helbodde Estate, Nawalapitiya, Peradeniya Bot, and Annfield Estate rainfall station. The missing data are estimated at 1 %, 4 %, 10 %, 2 % for Helbodde Estate, Nawalapitiya, Peradeniya Bot, and Annfield Estate rainfall stations, respectively. For the Helbodde rainfall station, the extreme value of rainfall is above 200 mm/day and the R^2 has increased after filling the data from 0.58 to 0.62.

For Nawalapitiya rainfall station the extreme rainfall value is above 200 mm/day and the R^2 has increased after filling the data from 0.47 to 0.56. for the Peradeniya Bot rainfall station, the extreme rainfall value is above 150 mm/day and the R^2 has increased after filling the data from 0.40 to 0.47.

For the Annfield rainfall station, the extreme value of rainfall value is above around 170 mm/day, but the R^2 has decreased from 0.60 to 0.40 because of 10 % of missing data.

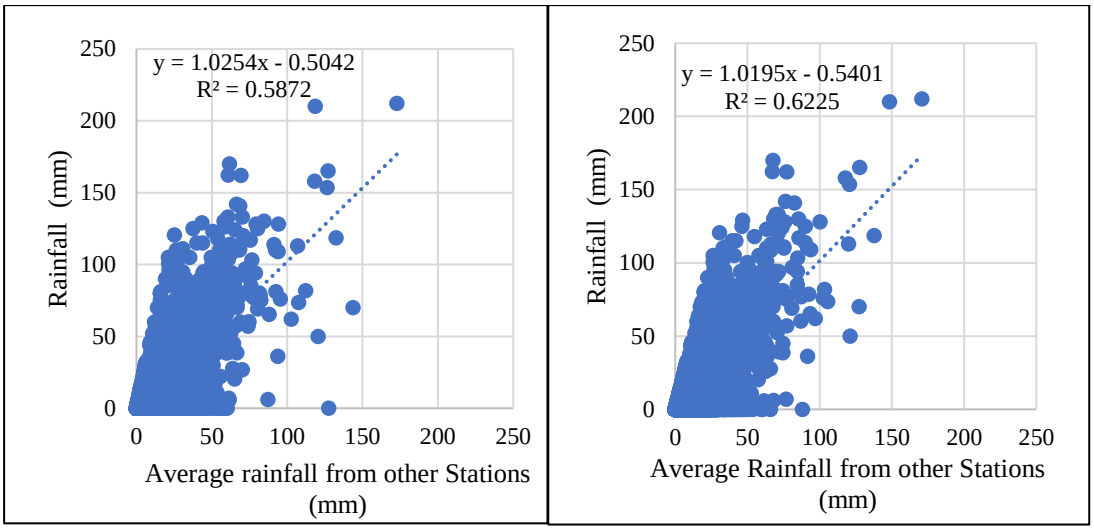

Figure 3-3: Scatter plot for Helbodde Estate rainfall station before filling (left) and after filling (right) of missing data

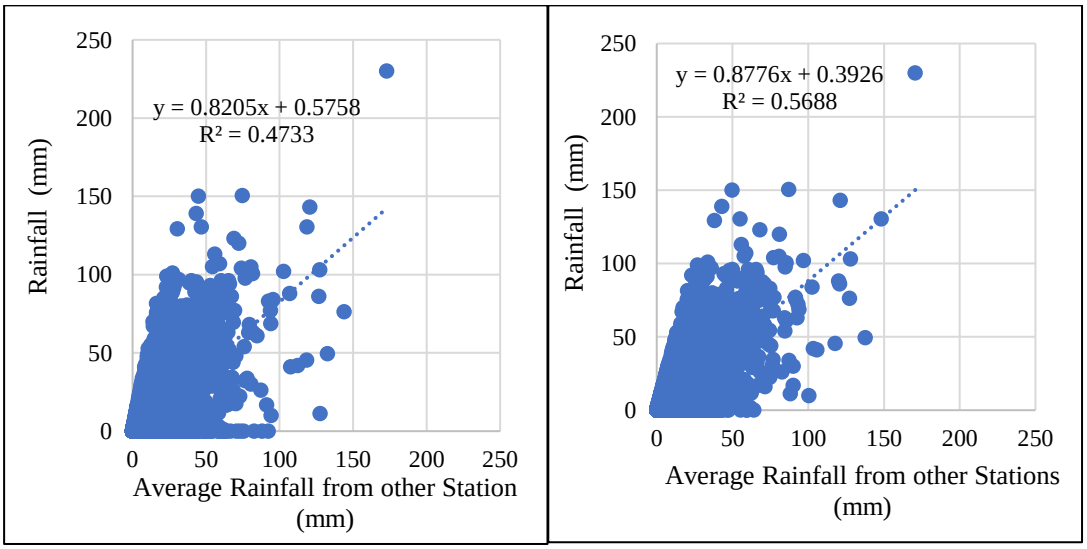

Figure 3-4: Scatter plot for Nawalapitiya rainfall station before filling (left) and after filling (right) of missing data

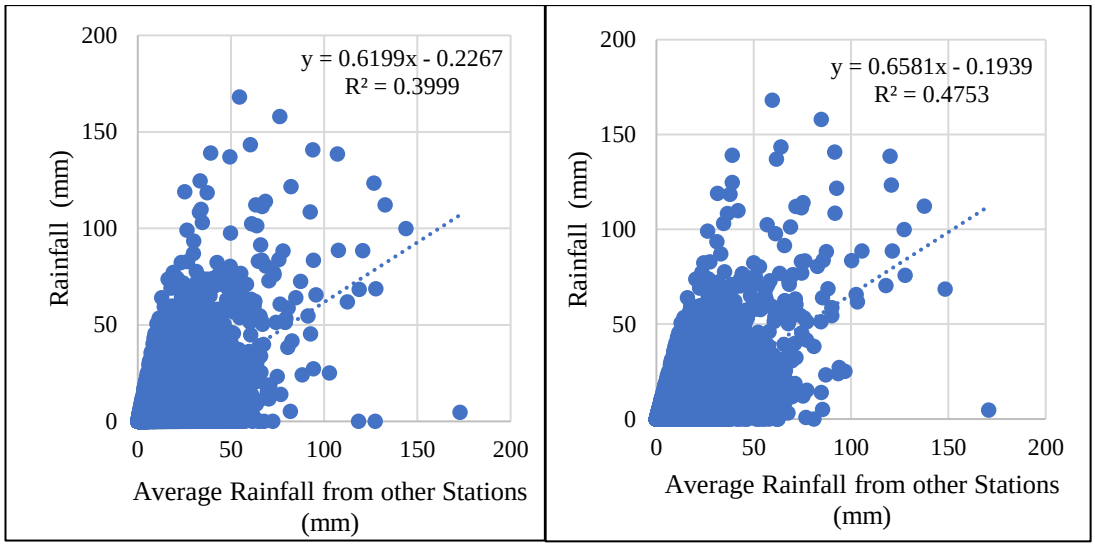

Figure 3-5: Scatter plot for Peradeniya Bot rainfall station before filling (left) and after filling (right) of missing data

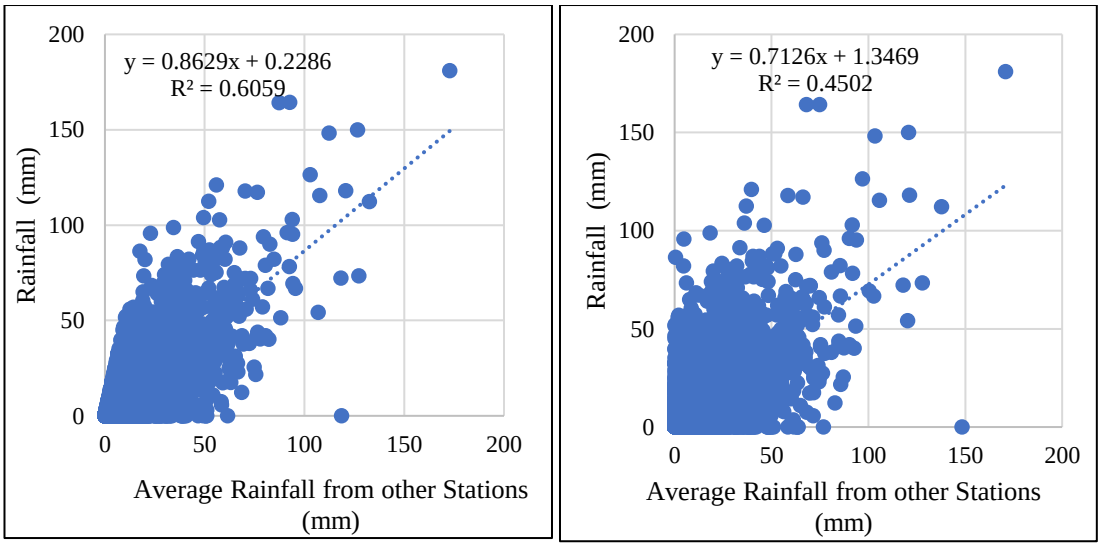

Figure 3-6: Scatter plot for Annfield Estate rainfall station before filling (left) and after filling (right) of missing data

3.6.2 Inconsistency Check Using Mass Curves

It is vital to evaluate the data for consistency and continuity before adopting the rainfall records of stations. The application of a Single mass curve aims to find out the correlations between rainfall stations. It means that this curve will help us to identify the rainfall stations' similarities in terms of their data.

By contrasting data from a particular station to a trend built of data from multiple other stations in the vicinity, the double mass curve technique can be used to validate the consistency of several types of hydrologic data. Depending on a variety of factors, such as damage or a failure in the rain gauge throughout a time, the continuity of a record can be interrupted with missing data (Grigsby & McLawhorn, 2019).

The single mass curve for Peradeniya and Helboda state stations is plotted and shown in Figure 3-7 and Figure 3-8. The graph indicated consistent and homogenous rainfall data with fewer quirks and deviations in the line in both stations.

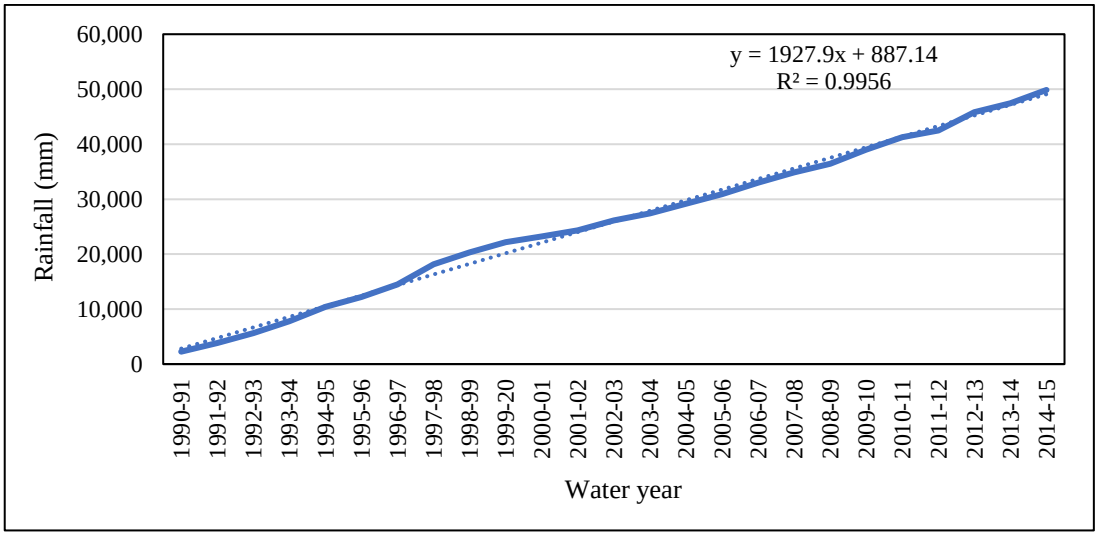

Figure 3-7: Single mass curve after filling data for Peradeniya Bot rainfall station

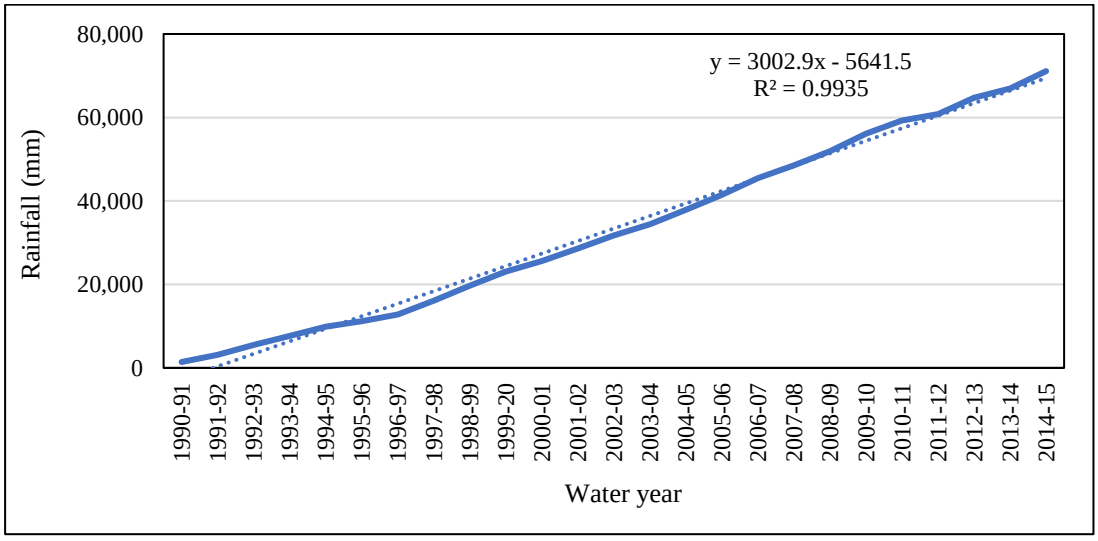

Figure 3-8: Single mass curve after filling data for Helboda Estate rainfall station

The double mass curve for the Peradeniya station is plotted and shown in Figure 3-9. A straight line was obtained indicating consistent data throughout the study period in the basin.

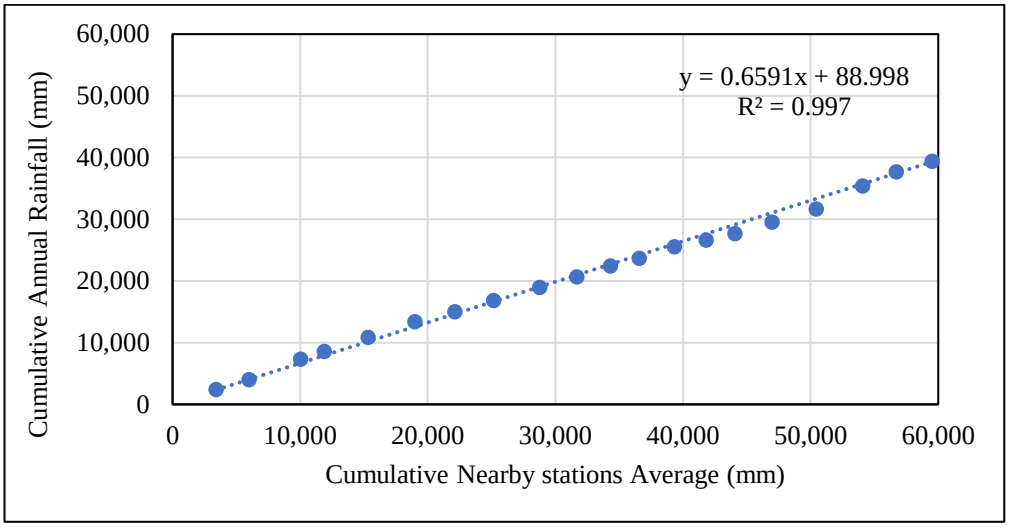

Figure 3-9: Double mass curve for Peradeniya Bot rainfall station after filling

3.6.3 Rainfall Variation Based on Monthly and Annual Timescale Periods

From Figure 3-10 to Figure 3-12, The variation of maximum, minimum, and mean rainfall is based on the monthly period for Helbodde, Peradeniya, Nawalapitia stations before filling the data. The annual variation of rainfall is plotted before filling the data from Figure 3-13 to Figure 3-15.

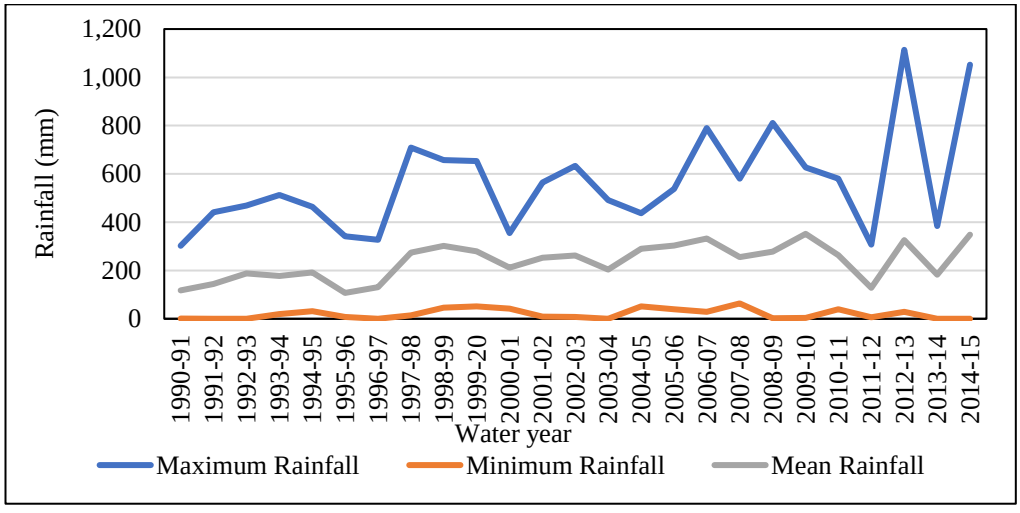

Figure 3-10: Variation of maximum, minimum, and mean monthly rainfall for Helbodde Estate station

The variation of rainfall in the Helbode throughout the study period is as shown in Figure 3-10. The maximum rainfall is exhibiting an increasing trend along with the mean rainfall. The average rainfall during the study period is between 100 mm to 400 mm.

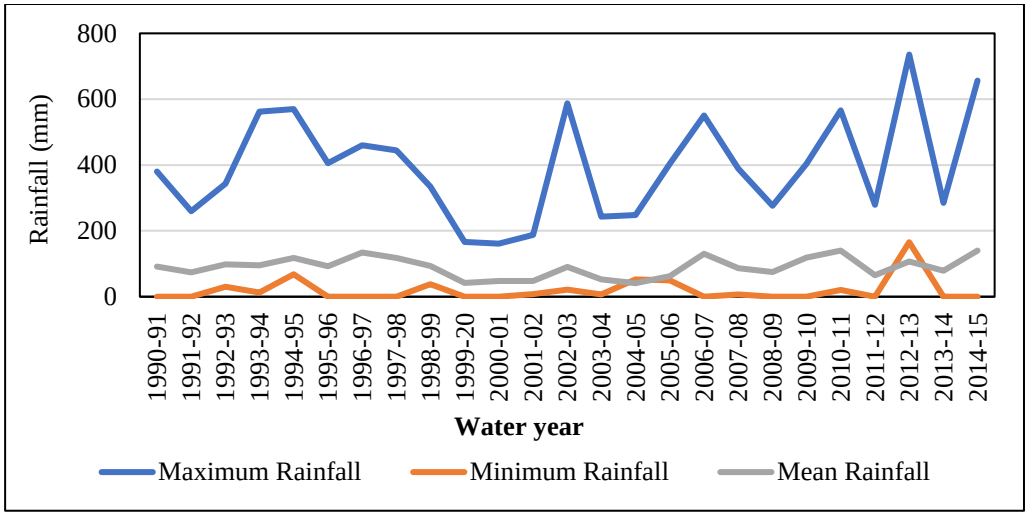

Figure 3-11: Variation of maximum, minimum, and mean monthly rainfall for Peradeniya station

The variation of rainfall in the Peradeniya station throughout the study period is as shown in Figure 3-11. The maximum rainfall is exhibiting an increasing trend along with the mean rainfall. The average rainfall during the study period is between 100 mm to 200 mm.

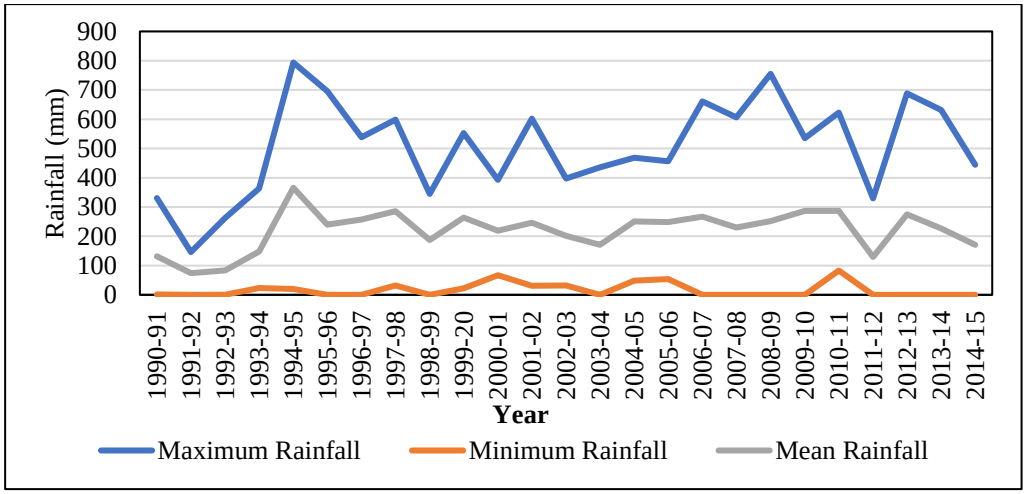

Figure 3-12: Variation of maximum, minimum, and mean monthly rainfall for Nawalapitia station

The variation of rainfall in the Nawalapitia throughout the study period is as shown in Figure 3-12. The maximum rainfall is exhibiting an increasing trend along with the mean rainfall. The average rainfall during the study period is between 100 mm to 400 mm.

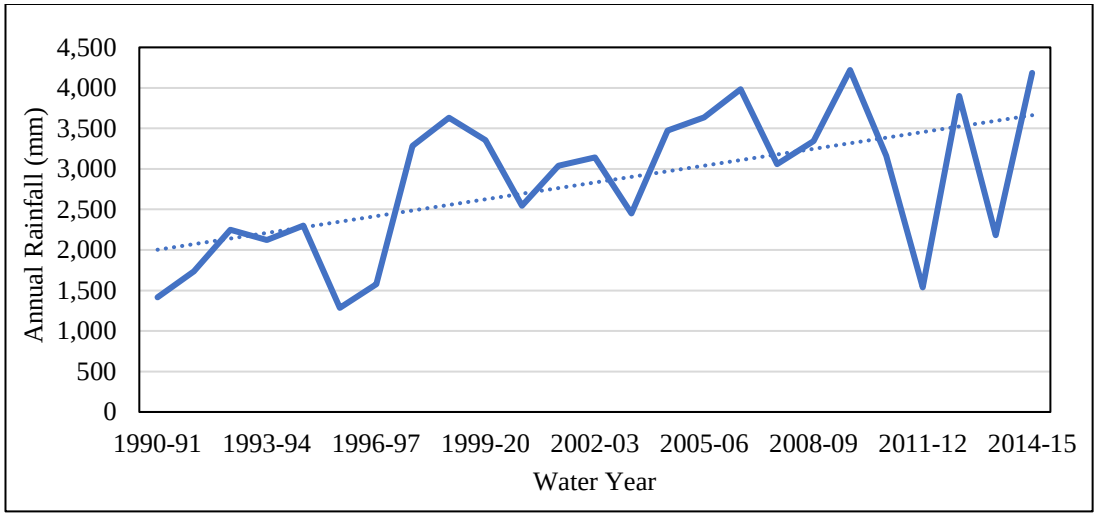

Figure 3-13: Annual variation of rainfall in Helbodde Estate rainfall station

The annual variation of rainfall in Helbode state is as shown in Figure 3-13 which indicates an upward trend for the study period. The maximum value of rainfall in the station is 4,220 mm in the water year 2009/10 and the minimum value is 1,285 mm in the water year 1995/96.

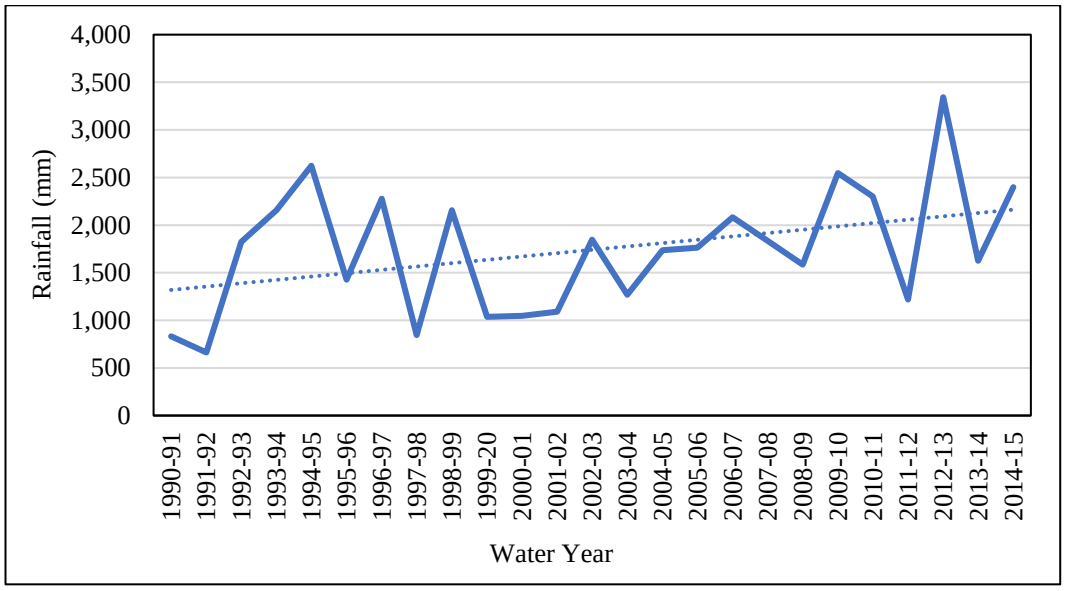

Figure 3-14: Annual variations of rainfall in Peradeniya Bot rainfall station

The annual variation of rainfall in the Peradeniya Bot rainfall station is as shown which indicates an upward trend for the study period. The maximum value of rainfall in the station is 3,343 mm in the water year 2012/13 and the minimum value is 662.6 mm in the water year 1991/92.

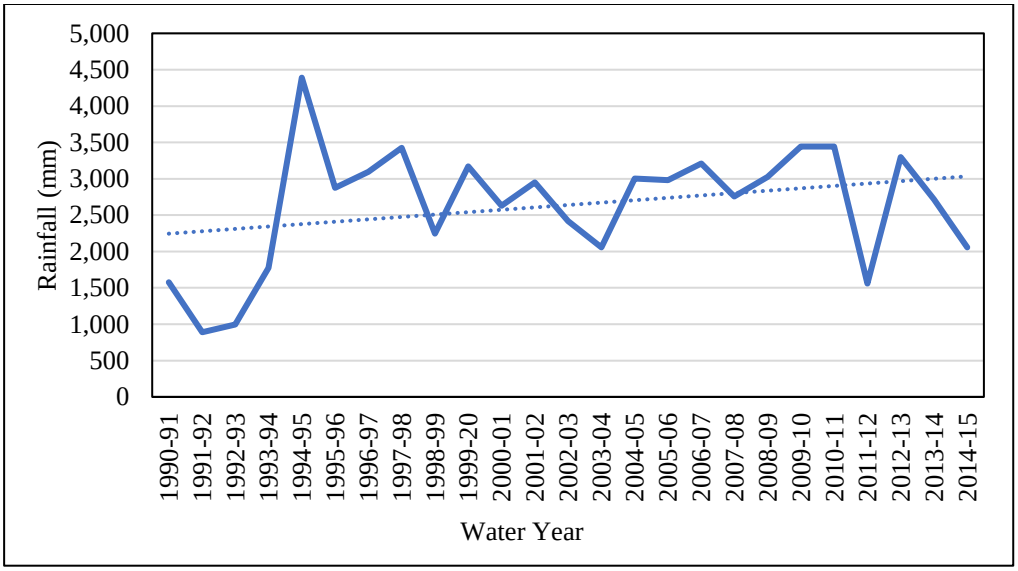

Figure 3-15: Annual variations of rainfall in Nawalapitia rainfall station

The annual variation of rainfall in the Peradeniya Bot rainfall station is as shown in Figure 3-15 which indicates an upward trend for the study period. The maximum value of rainfall in the station is 4,390 mm in the water year 1994/95 and the minimum value is 889.4 mm in the water year 1991/92.

3.6.4 Seasonal Rainfall Variation

The figures below show the streamflow varies according to the season. Therefore, the average of each season is calculated by the average streamflow involved in a particular month. The Northeast monsoon is a wet period with high variability. Further, the variability of successive years is also high, and the fluctuation range is large. The Southwest monsoon, First Inter monsoon, and Second Inter-monsoon are dry periods with less variability, which means the fluctuation range is small from successive years.

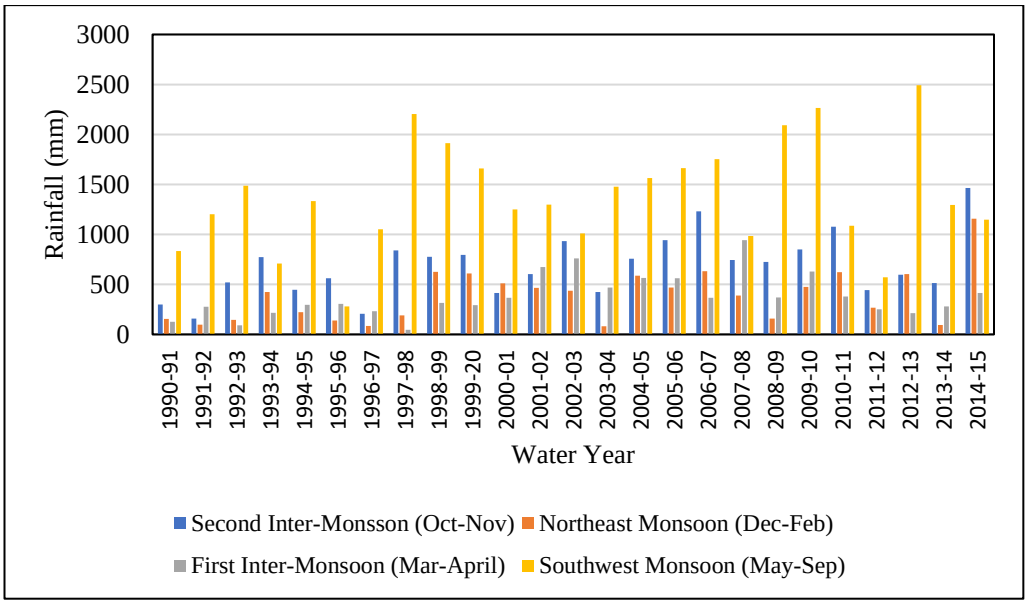

Figure 3-16: Seasonal variation of rainfall at Helbodde Estate station

According to the seasonal graph shown in Figure 3-16, the southwest monsoon receives more rainfall (maximum rainfall during the study period is 2,492 mm) compared to other seasons.

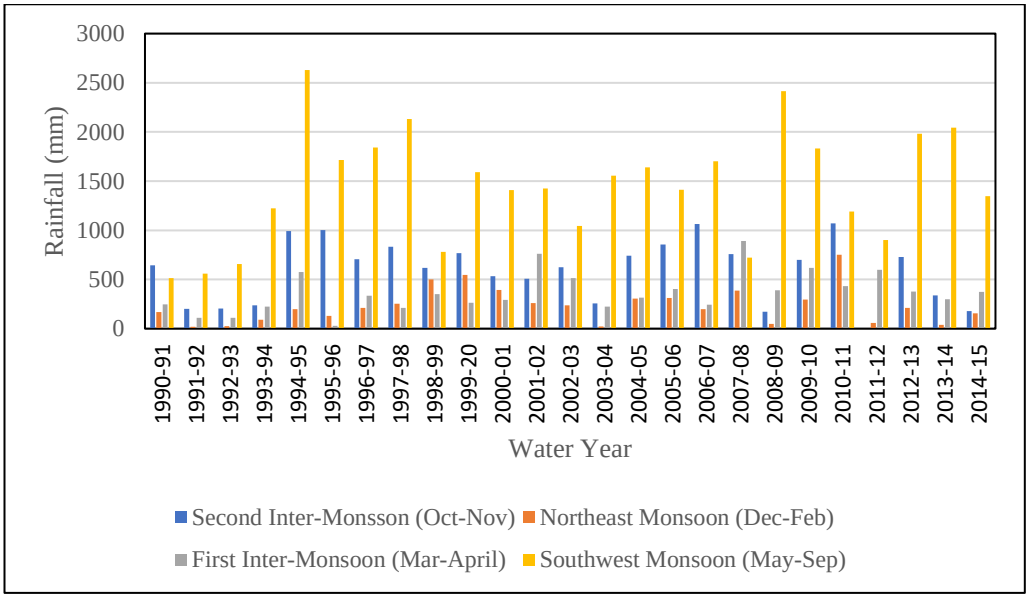

Figure 3-17: Seasonal variation of rainfall at Nawalapitiya station

According to the above-plotted graph shown in Figure 3-17, the Southwest monsoon receives more rainfall (maximum rainfall during the study period is 2,628.2 mm) compared to other seasons. Further, the First-inter monsoon and Northeast monsoon

receive less rainfall. But, in some years, likewise, 1991/92, 1995/96, 2003/04, 2011/12 the station has missing data.

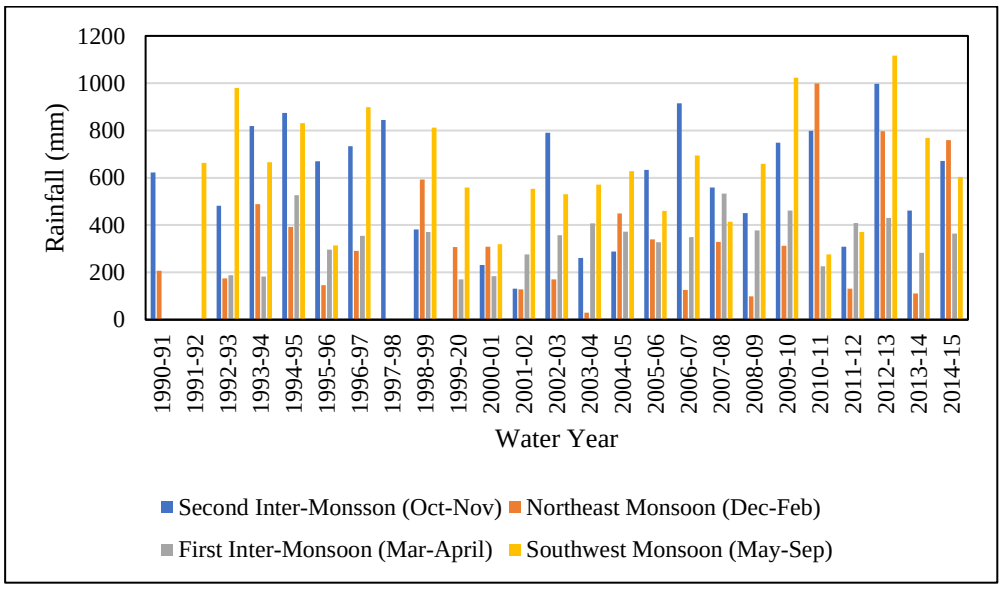

Figure 3-18: Seasonal variation of rainfall at Peradeniya station

According to the above-plotted graph shown in Figure 3-18, the southwest monsoon most receives more rainfall (maximum rainfall during the study period is 1,117.3 mm) compared to other seasons. Further, the First-inter monsoon and Northeast monsoon receive less rainfall. But, in some years, likewise, 1991/92, 1998/99, 1999/2000, the station has missing data.

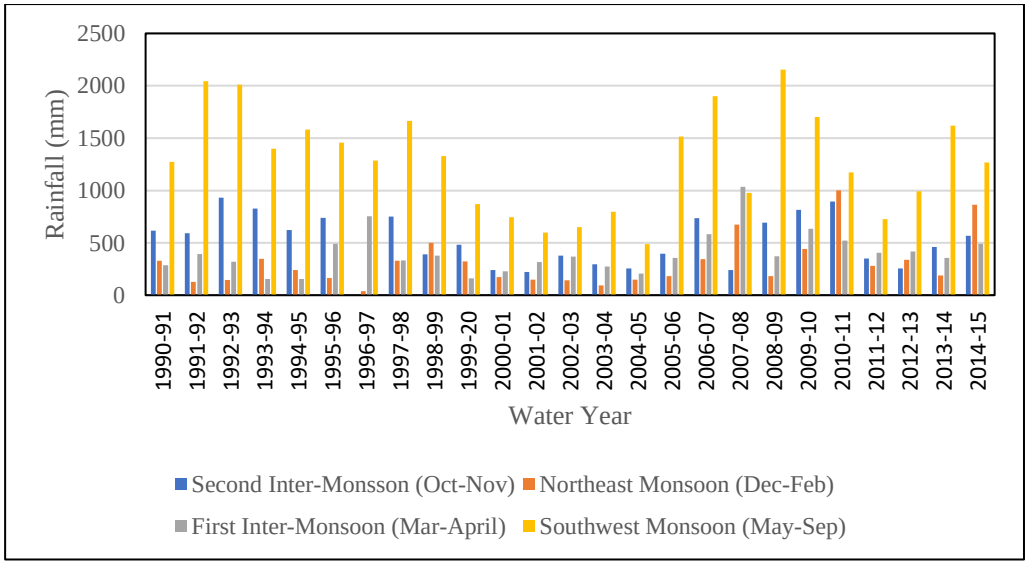

Figure 3-19: Seasonal variation of rainfall at Annfield Estate station

According to the above-plotted graph shown in Figure 3-19, the southwest monsoon most receives more rainfall (maximum rainfall during the study period is 2,153.7 mm) compared to other seasons. Further, the First-inter monsoon and Northeast monsoon receive less rainfall in the water year. But in some years likewise, 1996/97, the station has missing data.

3.7 Bias Correction

The regional climate model, CORDEX, was chosen for this study to examine the impact of climate change on future water supply. Domain WAS-44i with a resolution of 44 km is the model chosen from CORDEX. Python was used to extract the climatic data, and the CMhyd model was used for the verification of extracted climate data.

Bias correction can be accomplished in a variety of ways. Delta-Change Correction is a linear scaling approach. The bias correction methods are based on the assumption that the correction algorithm and parameterization for present climate conditions are also applicable for future climate conditions, i.e., all bias correction methods are stationary.

$$X'_M(i) = X_M(i) * \frac{\mu_o}{\mu_M} \qquad [3\text{-}1]$$

where i is a day in the month, μ_o and μ_M are monthly means of observed and model (RCM) data for the baseline period, respectively. X_M is the raw daily model data and X'_M is the bias-corrected daily data. The study conducted by Sirisena et al. (2021) for future periods, monthly values of $\frac{\mu_o}{\mu_M}$ were taken from the baseline period and utilized in Equation [3-1] to correct the bias in the data.

The base period of precipitation and temperature was selected as 1990-2005 for a research project. The general recommendation is to use 30 years periods of reference for the climate (*WMO*, 2017).

Due to data unavailability, data accuracy, and economy 15 years of reference period can be considered for climate bias correction (Sirisena et al., 2021). The research title (Evaluation of future climate and potential impact on streamflow in the upper nan river

basin of northern Thailand) considers 1988-2005 climate and streamflow value with future time scale (Gunathilake et al., 2020).

3.8 Location of the Catchment and Climate Model Grids

According to Figure 3- 20, the Peradeniya sub-catchment is located between 6.67-7.330 latitude and 80.33-80.83-degree longitude. The precipitation grid of the climate model reveals that most of the Peradeniya sub-catchment is located in two right grids (80.5-810 E, and 6.5-7.50N). A small portion of the catchment is located in another two grids (80-80.50 E, and 6.5-7.50N. And also the location of rainfall station is located in that part of the climate projection map which covers around all parts of the Peradeniya sub-catchment.

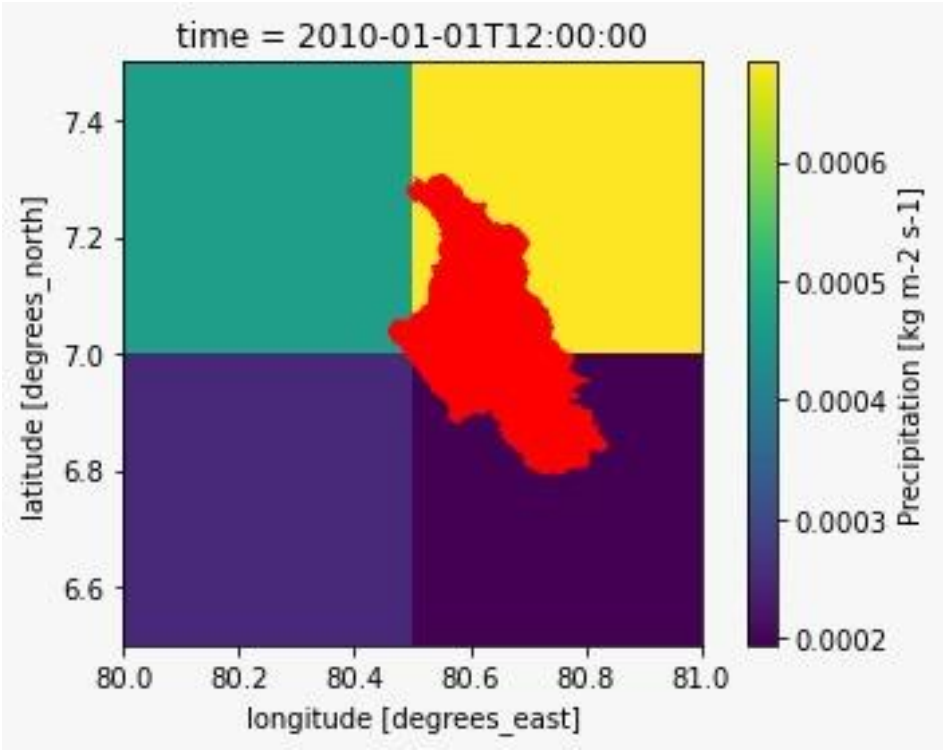

Figure 3- 20: Climate projection grids number which covers Peradeniya-sub catchment

According to Table 3-2 Climate data for each station (Helbodde Estate, Nawalapitia, Peradeniya. Bot) is extracted from the coordinate of 7.250 North and 80.750 East. Similarly, climate data for Annefiled Estate is extracted from the coordinates of 6.250 North 80.750 East. Coordinate of each rain gauge with their corresponding grid of climate data from which data were extracted are summarized in the Table.

Additionally, climate data for a particular gauge is extracted from the center of the nearest grid to that corresponding gauge. As we can see the nearest grid to Helbodde Estate, Nawalapitia, Peradeniya. Bot stations are 7.250 North and 80.750 East, which is also shown in the Figure of climate grids.

Table 3-3: Coordinate of the station and coordinate of extracted climate data

Rainfall Station	Coordinates of the rainfall station		Coordinates of extracted climate data	
	latitude	longitude	latitude	longitude
Helbodde Estate	7.08°	80.67°	7.25°	80.75°
Nawalapitia	7.07°	80.53°	7.25°	80.75°
Peradeniya.Bot	7.27°	80.60°	7.25°	80.75°
Annfield Estate	6.87°	80.63°	6.25°	80.75°

3.9 Development of the HEC-HMS Model

The hydrologic processes of the Peradeniya watershed in the upper Mahaweli basin were modeled using the HEC-HMS version 4.8 created by the US army corps of engineers. The HEC-HMS Model was used for continuous modeling in this research.

The 30 m DEM was used to compute the basin slope, drainage area, and watershed delineation. The deficit and constant methods are used as loss methods in this study. For the HEC-HMS Model, the initial deficit, maximum deficit, maximum storage, constant rate, and impervious percentage are required. Maximum storage can be linked to maximum potential storage, which is obtained from curve numbers (Madhushankha & Wijesekera, 2021). Using guidelines from TR55 for calculation of curve number with soil moisture antecedent condition II, curve number for each land use is determined by taking soil group as C. The initial deficit parameter is taken as 20 % of the maximum deficit. A good estimate of the constant parameter is saturated hydraulic conductivity (USACE, 2018).

However, due to lack of data this parameter is estimated based on the minimum constant loss rate of a particular soil type. For reaches, the Muskingum-Cunge approach is employed as the routing method. One of the most common and simple routing methods is the Muskingum-cunge approach. The conservation of mass and the diffusion representation of the conservation of mass and the diffusion representation of the conservation of momentum are the basis of this method (USACE, 2018).

The parameters required are length (total length of the reach element), slope (average slope of the entire reach), Manning's n (average value for the entire reach), and cross-section of the shape profile. For the baseflow method, the constant monthly baseflow method is applied, which specifies the baseflow into a constant flow for each month of the year. A time of concentration (T_C) and a storage coefficient are necessary parameters (Bai et al., 2018).

The study area is divided into three sub-catchments in the HEC-HMS model which is shown in Figure 3-21.

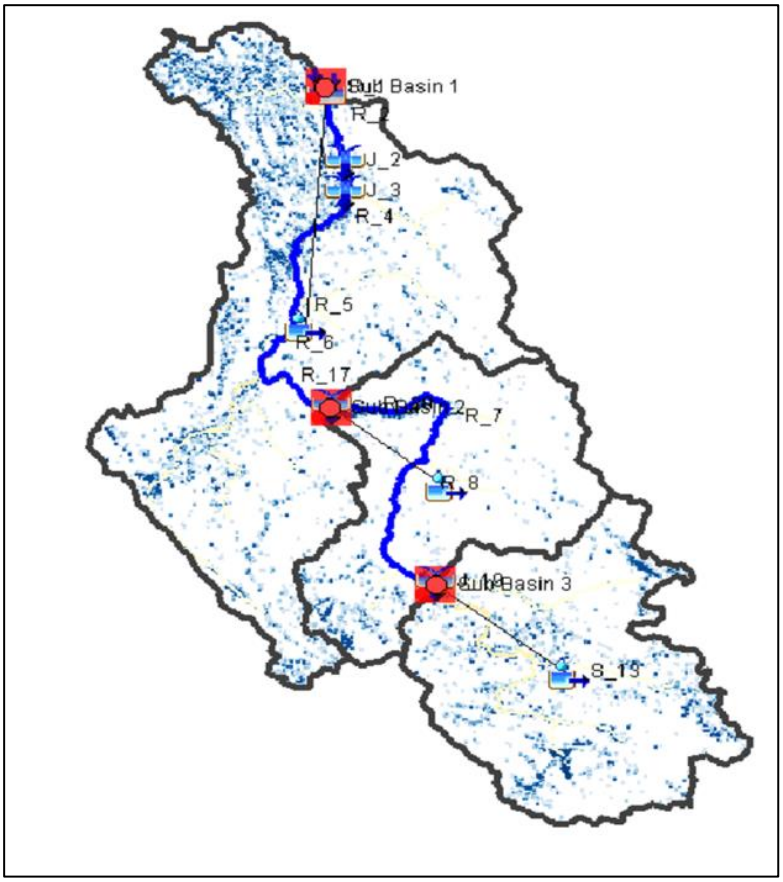

Figure 3-21: Division of study area for HEC-HMS modeling

The area of each sub-catchments is shown in Table 3-4.

Table 3-4: Sub-catchments division of Peradeniya sub-catchment

Sub-catchments	Area (km^2)
Sub-catchment 1	567.22
Sub-catchment 2	257.52
Sub-catchment 3	312.41

3.9.1 Application of Thiessen Polygon

Thiessen polygons are used to calculate the average precipitation over an area or watershed. The advent of geographic information systems (GIS) has significantly simplified the difficulty of determining spatial statistics, however, GIS is not always applicable. The fundamental idea is to divide the watershed into numerous polygons, each with a measurement point in the center, and then calculate a weighted average of the measurements based on the size of each polygon. The weighted average is calculated by Equation [3-2] according to Johnson & Sharma, (2010).

$$P = \frac{P_1A_1 + P_2A_2 + P_3A_3 + \cdots P_nA_n}{A_1 + A_2 + A_3 + \ldots + A_n} \quad [3\text{-}2]$$

where,

P is the weighted average, Ps are measurements, and A are areas of each polygon.

The Thiessen polygons of the study area are delineated and shown in Figure 3-22.

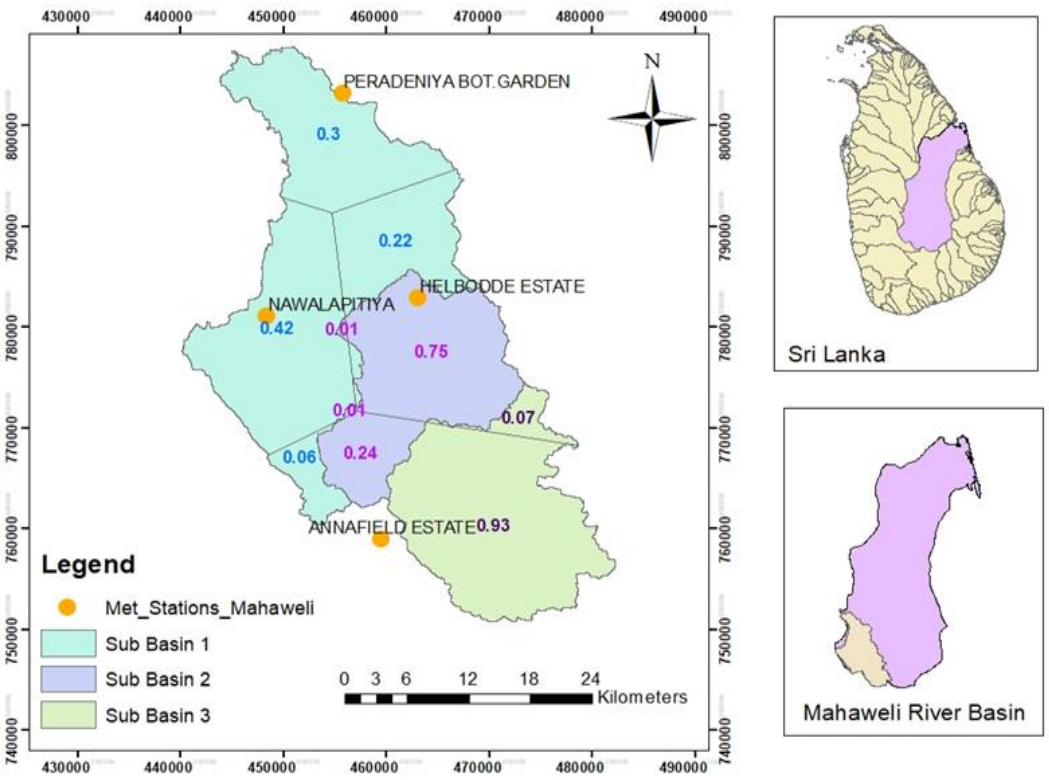

Figure 3-22: Thiessen weightage for each sub-basin

3.9.2 Canopy Storage Estimation

The precipitation intercepted by trees and other vegetation is called canopy storage. Initial canopy storage (percent) is an initial condition input that indicates how much of the maximum canopy storage is filled at the start of the simulation. it is recommended to start the simulation after a term of no rainfall, which makes a value of 0 % acceptable as an initial value. This assumption should be respected in the choice of the simulation periods later in the hydrologic modeling. The maximum depth of water that can be intercepted by plants is represented by the max canopy storage (mm) (Ahbari et al., 2018).

Table 3-5: Canopy interception by vegetation type

Vegetation type	Canopy interception (mm)
General vegetation	1.27
Grasses and deciduous trees	2.03
Trees and coniferous trees	2.54

Source: Bennett & Peters (2000)

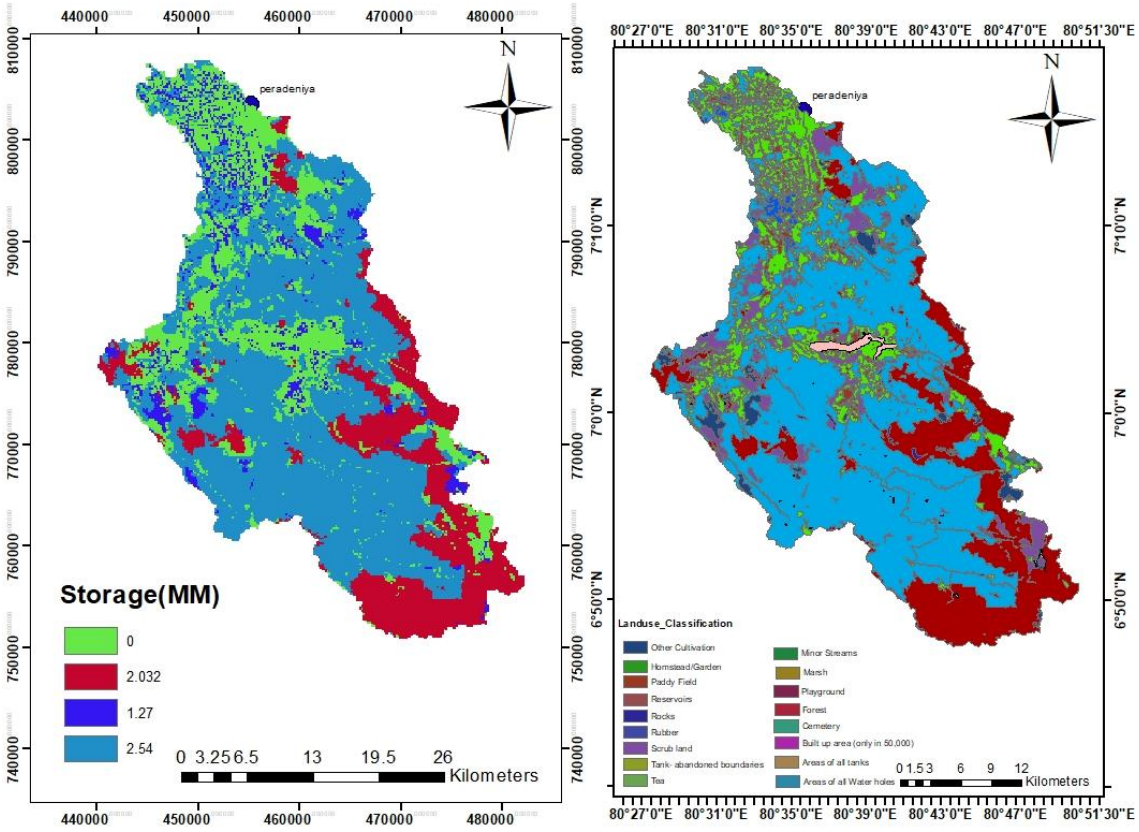

Figure 3-23: Canopy storage for Upper Mahaweli river basin at Peradeniya sub-catchment

3.9.3 Surface Storage Parameter Estimation

The volume of water stored on the surface of the ground, or the total volume of water held on the earth's surface in lakes, ponds, and puddles is known as depression storage or surface storage. It is calculated based on the slope of the catchment surface (in percent). Some precipitation will fall to the ground and either seep into the soil or flow as runoff across the land surface. The surface runoff will either flow into a body of

water or a wetland, or it will be held in depressions that allow for soil infiltration. The slope of the land affects surface storage capacity. The surface storage for the Peradeniya sub-catchment of upper Mawawili is shown in Figure 3-24.

Table 3-6: Surface depression storage values

Description	Slope %	Surface storage (mm)
Paved impervious areas	NA	3.20 - 6.40
Steep and smooth slopes	>30	1.00
Moderate to gentle slope	5-30	12.70 - 6.50
Flat and furrowed land	0-5	50.80

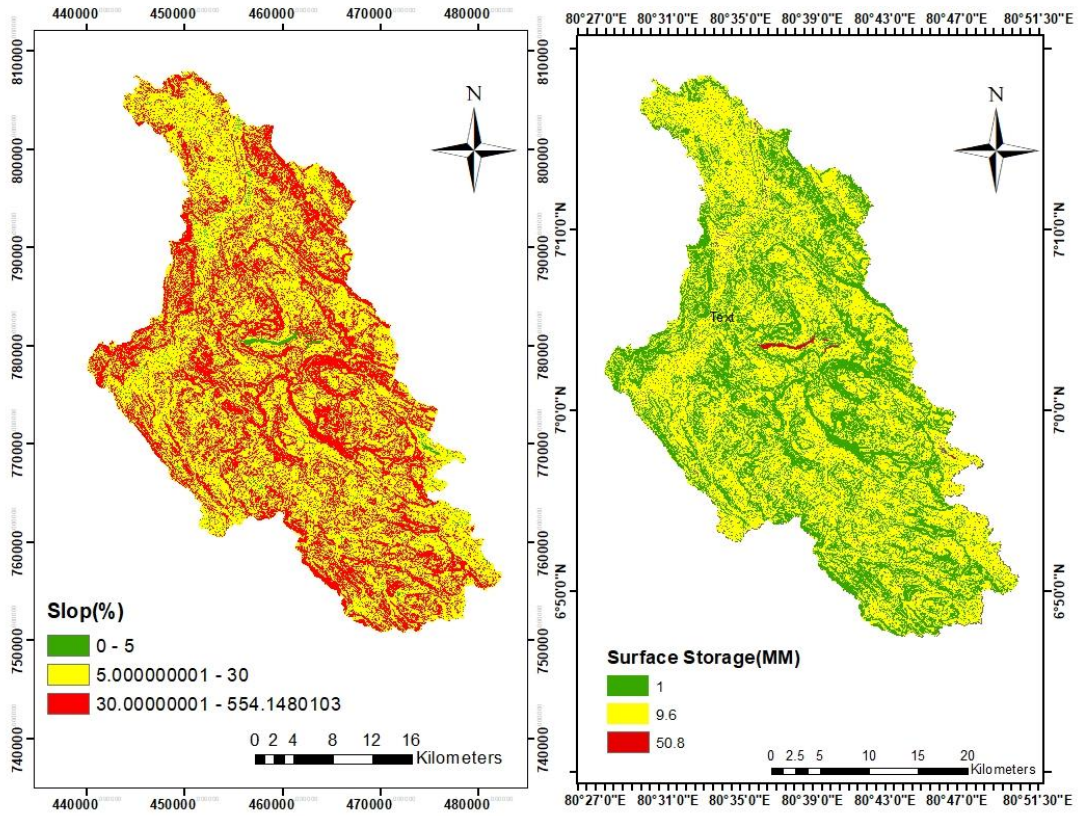

Figure 3-24: Surface storage raster for Upper Mahaweli river basin at Peradeniya sub-catchment

Table 3-7: Canopy storage and surface storage for each sub-basin

Sub Basin	Maximum Canopy Storage (mm)	Maximum Surface Storage (mm)
Sub-catchment 1	2.82	7.41
Sub-catchment 2	2.98	6.93
Sub-catchment 3	2.93	7.40

3.9.4 Impervious Surface Calculations

Roofs, roads, and decks are examples of impervious surfaces, which prevent precipitation from infiltrating the earth and instead cause rain or snowmelt to runoff. All or most of the water that falls on it is released as runoff.

The surface area of proposed existing impervious surfaces on the fraction of a lot or parcel which is in under 300 feet of the regular top watermark shall be divided by the overall surface area of that segment of the lot or part that is inside 300 feet of the regular topwater sign and multiplied by 100 to determine the values of impervious surface (Li et al., 2011).

Table 3-8: is used to calculate the impervious area for each sub-basin which mentioned the coefficient of different types of land use. Table 3-9 calculated, the impervious area for each sub-basin.

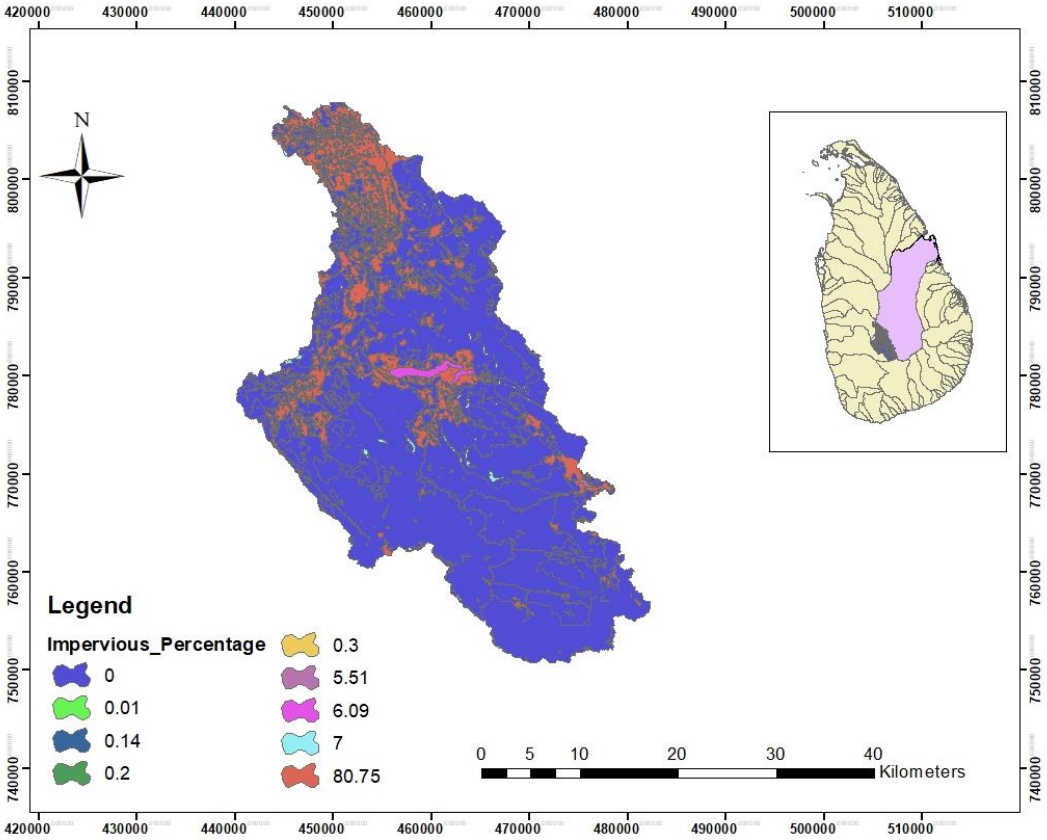

Figure 3-25: Impervious area percentage for Peradeniya sub-catchment

Table 3-8: Land use coefficient for the calculation of impervious area

	TYPE	Coefficient		Type	Coefficient
Farmland	Paddy Field	1	Unused land	Sand	0.1
	Dray land	0.7		Gobi	0.1
	Forest Land	0.6		Sali and alkali land	0.2
Wood-land	Shrubbery	0.6		Swampland	0.5
	Scattered woodland	0.4		Bare land	0.2
	Others	0.4			
Grassland	High Coverage	0.6		Stone land	0.1

TYPE		Coefficient	Type		Coefficient
Water Area	Medium Coverage	0.6	Construction Land	Others	0.3
	Low coverage	0.6			
	River and canal	0.6		Bottomland	0.4
	Lake	0.6		Urban land	0.8
	Reservoir and pond	0.6		Rural residential land	0.6
	Glaciers and Snow field	0.1		Others	0.4

Table 3-9: Impervious surface area for each sub-basin

Sub Basin	Impervious %
Sub-catchment 1	14.43
Sub-catchment 2	10.95
Sub-catchment 3	2.9

3.9.5 Calculation of SCS Curve Number

The soil of the Peradeniya watershed was classified as hydrological group C. Initially, CN value was determined using standardized tables, by evaluation of antecedent moisture condition and hydrological soil group. For each sub-catchment, a weighted CN value was determined. For better calculation, the Peradeniya sub-catchment is divided into three sub-catchments. The curve number for all three (3) sub-basin is calculated and shown in Table A - 1, Table A - 2, and Table A - 3 of Annexure 1.

Table 3-10: Estimation of SCS curve number for each sub-catchment

Sub Basin	CN
Sub-catchment 1	79.20
Sub-catchment 2	75.64
Sub-catchment 3	69.58

According to Table 3-1, the value of the SCS curve number for sub-catchment 1 (one) is 79.20, and the SCS curve number for sub-catchment two (2) and sub-catchment three (3) is 75.64, 69.58, respectively. The SCS Curve number depends on land use/surface cover and the soil type of a catchment. In particular, When the catchment is highly impervious and the soil type has less infiltration capacity, the volume of precipitation that infiltrates will be less, consequently causing more SCS curve numbers. In contrast, when the catchment has large green areas, more precipitation will be lost due to evapotranspiration from plants, as a result, the SCS curve number will decrease.

Based on the above argument, the SCS curve number varies in each sub-catchment due to land use and soil characteristics of the given sub-catchment. Therefore, in sub-catchment 1 (one), the SCS curve number is more than the other two sub-catchments. it means that in sub-catchment one is highly impervious, and the soil type has less infiltration, consequently causing more SCS curve numbers. But, in subbasement 3 (three) the SCS curve number is less than sub catchment 1 (one) and sub-catchment 2 (two). Because the green area is more than sub catchment 1 (one) and 2 (two) and more precipitation will be lost due to the evaporation and infiltration.

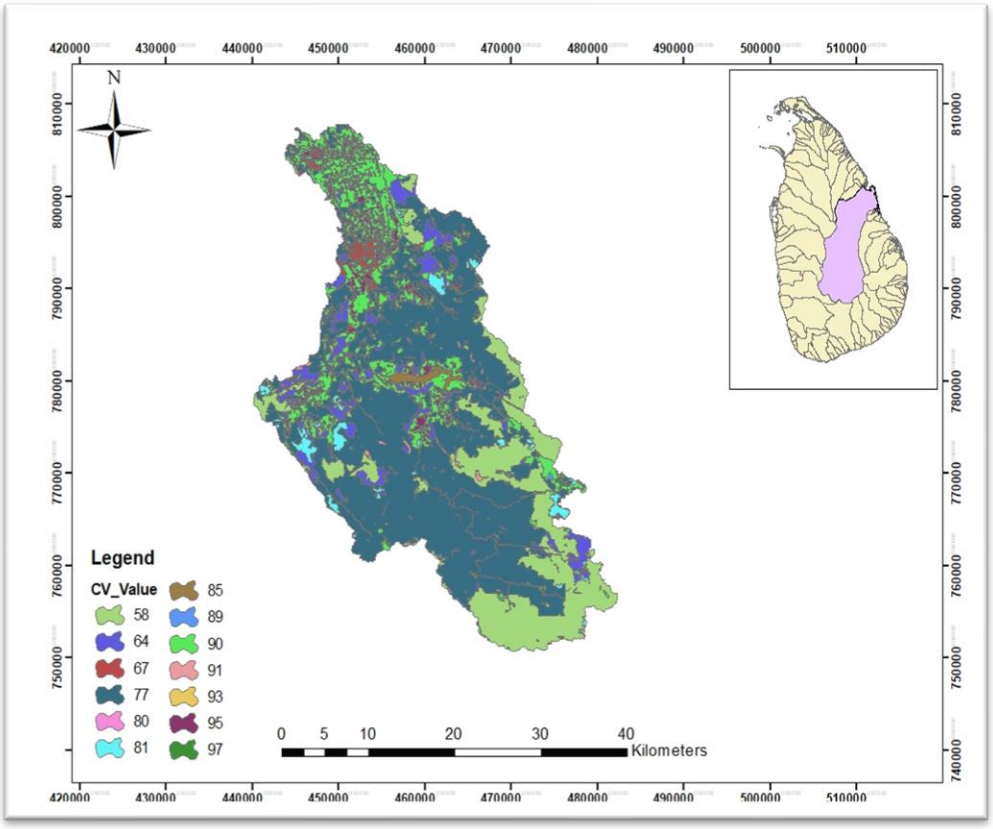

Figure 3-26: CN Grid for the Upper Mahaweli river basin at Peradeniya sub Catchment

3.9.6 Estimation of Initial Abstraction for Hydrological Modeling

According to equation [2-7], initial abstraction was calculated for every sub-basin and is shown in Table 3-11. For sub-catchment one (1) the value of initial abstraction is 13.34 mm and initial abstraction for sub-catchment two (2) and sub-catchment three (3) is 16.36 mm, 22.2 mm, respectively. The initial abstraction is the volume of precipitation lost due to initial infiltration, evapotranspiration, and surface depression. Therefore, initial abstraction depends on land use/surface cover and the soil type of a catchment. In particular, When the catchment is highly impervious and has soil type has less infiltration capacity, the volume of precipitation that infiltrates will be less, consequently causing less initial abstraction. In contrast, when the catchment has large green areas, more precipitation will be lost due to evapotranspiration from plants, as a result, initial abstraction will increase. Based on the above argument, the initial abstraction varies in each sub-catchment due to land use and soil characteristics of the given sub-catchment. Therefore, in sub-catchment 1 (one) the initial abstraction is less

than the other two sub-catchments. it means that in sub-catchment one is highly impervious and the soil type has less infiltration, consequently causing less initial abstraction. But, in subbasement 3 (three) initial abstraction is more than sub catchment 1 (one) and sub-catchment 2 (two). Because the green area is more than sub catchment 1 (one) and 2 (two) and more precipitation will be lost due to the evaporation and infiltration.

Table 3-11: Initial abstractions for different sub-basin

Sub Basin	Initial Abstraction (mm)
Sub-catchment 1	13.34
Sub-catchment 2	16.36
Sub-catchment 3	22.21

3.9.7 Development of the Transform Model

The value of T_c was calculated using the Kirpich formula as shown in Equation

[2-5] and the Lag time for the Padiyathalawa watershed was calculated using Equation [2-6]. The lag time for sub-basin one (1) two (2) three (3) is 1.60 hr 1.01 hr and 1.09 hr, respectively and the time of concentration for sub-catchment one (1) two (2) three (3) is 2.67 hr, 1.67 hr, 1.82 hr, respectively.

Table 3-12: Time of concentration and lag time for each sub-basin

	Sub Basin	K	$L^{0.77}$	$S^{-0.385}$	Tc (hr.)	Lag Time (hr)
Time of Concentration	1	0.02	5035.79	1.63	2.672	1.603
	2	0.02	3304.60	1.56	1.676	1.005
	3	0.02	3422.03	1.64	1.828	1.097

3.9.8 Estimation of Initial Deficit Constant Parameters

Estimation of maximum storage, initial deficit, and initial constant rate parameters is in table Table 13.

Table 13:Estimation of deficit constant parameters

Sub-basin	Maximum Storage (mm)	Initial Deficit (mm)	Initial Constant Rate (mm/hr)
Sub catchment 1	66.70	13.34	1.27
sub catchment 2	81.80	16.36	1.27
sub catchment 3	111.06	22.21	1.27

CHAPTER 4

4 RESULTS AND ANALYSIS

4.1 Sensitivity Analysis of the Model

Understanding the model-sensitive parameters is important for model calibration and validation. It will enable to make the model optimized very easily by analysis of sensitive parameters and changing them gradually. Figure 4-1 and Figure 4-2 show which parameters are more sensitive with respect to discharge and volume, respectively.

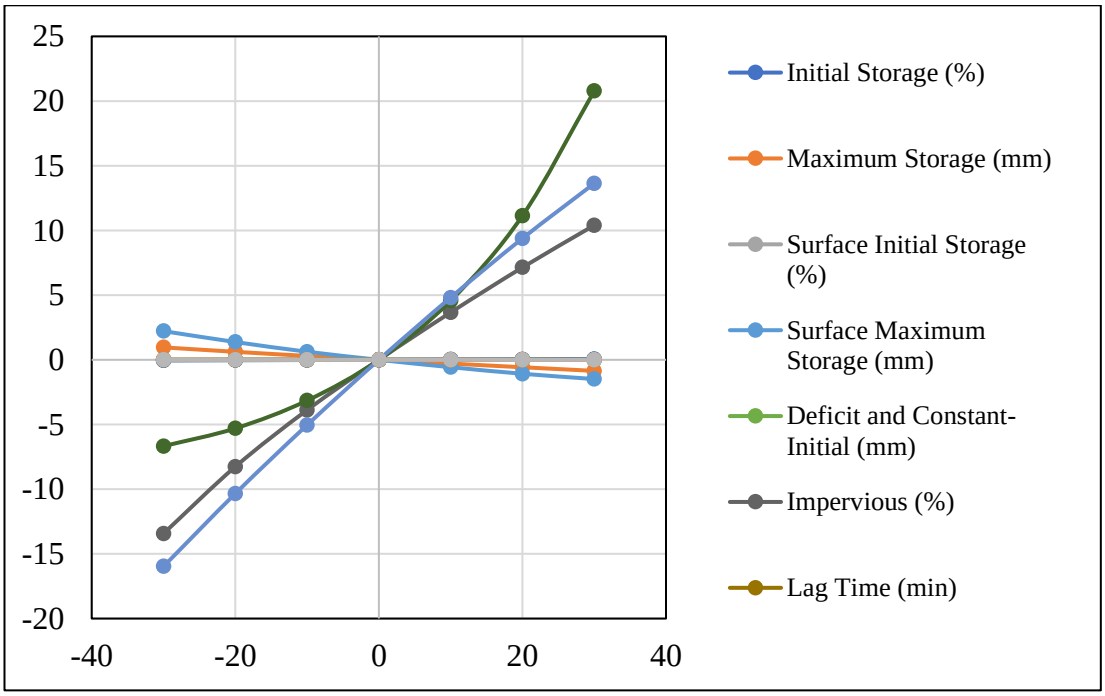

Figure 4-1: Sensitivity analysis of the model based on changing streamflow volume

According to Figure 4-1, the sensitivity analysis of the model based on streamflow volume shows that the more sensitive parameters are rescission constant surface maximum storage (mm) and the least sensitive parameters are surface initial storage, Muskingum X, Muskingum K (H), and threshold flow (m^3/s).

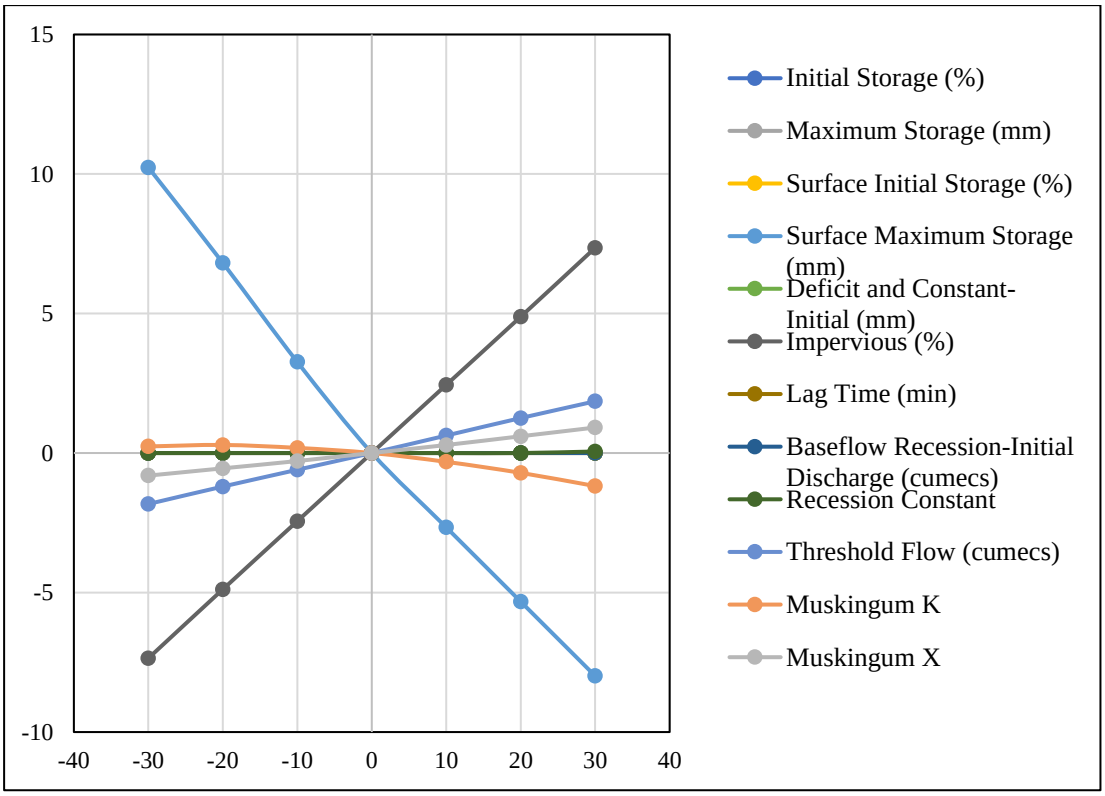

Figure 4-2: Sensitivity analysis of the model based on changing streamflow discharge

According to Figure 4-2, sensitive analysis of the model based on changing streamflow discharge, more sensitive parameters are threshold impervious (%) and the least sensitive parameters are surface initial storage, Muskingum X, and Deficit and constant.

4.2 Model Calibration and Validation

For the calibration of the model, the period 1990-1994 is selected for model calibration, and from 19994 till 2000 is selected for model validation. The historical data for the regional climate model is up to 2005, therefore the selected duration is considered between 1990-2005. Table 4-1 indicates of initial and optimized parameters in the model.

Table 4-1: Summary of initial and optimized Parameters in the model

Components		Methods	Basin	Initial Parameter	Optimized Parameter
Canopy	Simple Canopy	Initial Storage (%)	Sub 1	10.00	9.03
			Sub 2	10.00	6.35
			Sub 3	10.00	8.89
		Maximum Storage (MM)	Sub 1	2.82	2.54
			Sub 2	2.98	2.50
			Sub 3	2.97	2.54
		Crop Coefficient	Sub 1	1.00	1.00
			Sub 2	1.00	1.00
			Sub 3	1.00	1.00
Surface	Simple Surface	Initial storage (%)	Sub 1	7.41	8.53
			Sub 2	6.93	5.66
			Sub 3	7.40	9.43
		Maximum Storage (MM)	Sub 1	53.01	41.09
			Sub 2	33.53	25.99
			Sub 3	62.38	48.36

Table 4-2: Summary of Initial and optimized parameters in the model continues

Component		Method	Basin	Initial Parameter	Optimized Parameter
Loss Method	Deficit and Constant	Initial Deficit (mm)	Sub 1	13.34	19.64
			Sub 2	16.36	12.93
			Sub 3	22.21	14.43
		Maximum Storage (mm)	Sub 1	66.70	266.16
			Sub 2	81.80	187.51
			Sub 3	111.06	230.25
		Constant Rat (mm/hr)	Sub 1	2.50	2.08
			Sub 2	1.90	2.98
			Sub 3	1.27	0.63
		Impervious	Sub 1	14.43	15.00
			Sub 2	10.95	17.50
			Sub 3	2.90	10.50
Transform	SCS Unit Hydrograph	Lag Time (Min)	Sub 1	96.21	1445.70
			Sub 2	60.32	658.18
			Sub 3	65.80	1141.30
Baseflow	Recession	Rececian and Constant	Sub 1	0.96	0.97
			Sub 2	0.84	0.34
			Sub 3	0.84	0.67
		Initial Discharge(m^3/sec)	Sub 1	16.77	17.93
			Sub 2	14.51	10.85
			Sub 3	13.17	10.01
		Threshold	Sub 1	34.78	33.39
			Sub 2	61.57	41.50
			Sub 3	32.11	26.84

Table 4-3: Objective function of the model calibration

RMSE	Nash-Sutcliff	Percent Bias
0.60	0.62	-15%

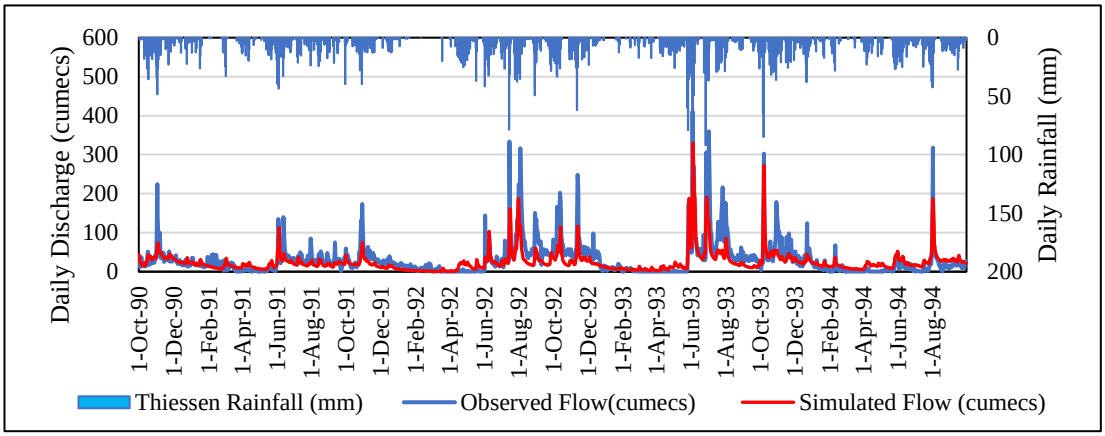

Figure 4-3: Observed versus simulated hydrograph for calibration 1990-1994 (Normal)

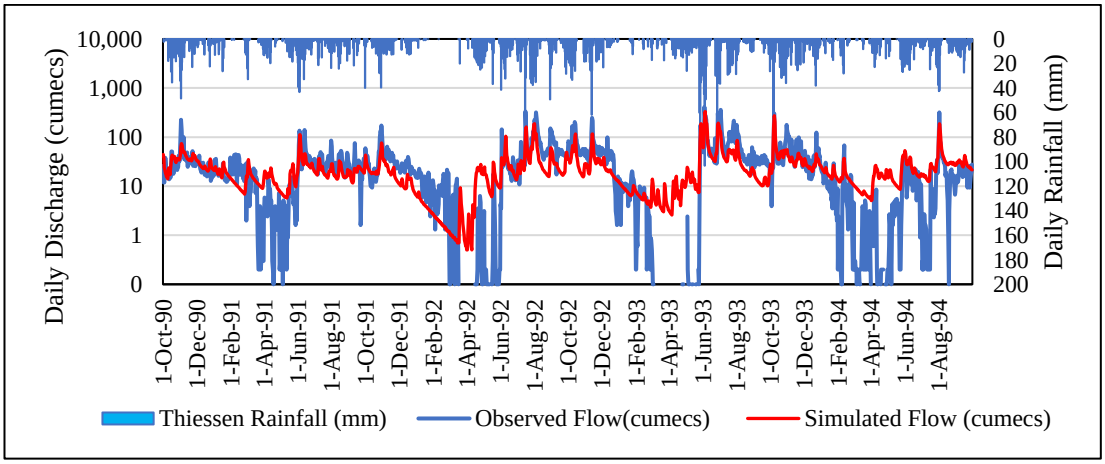

Figure 4-4: Observe versus simulated hydrograph for calibration from 1990-1994 (Simi-Log)

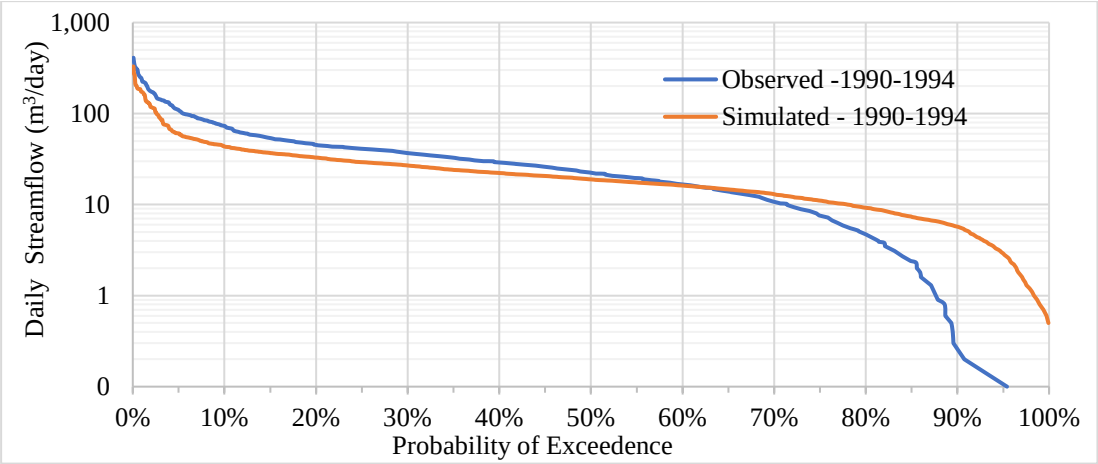

Figure 4-5: Flow duration curve of observed discharge and simulated discharge started in descending order for calibration period of 1990 to 1994

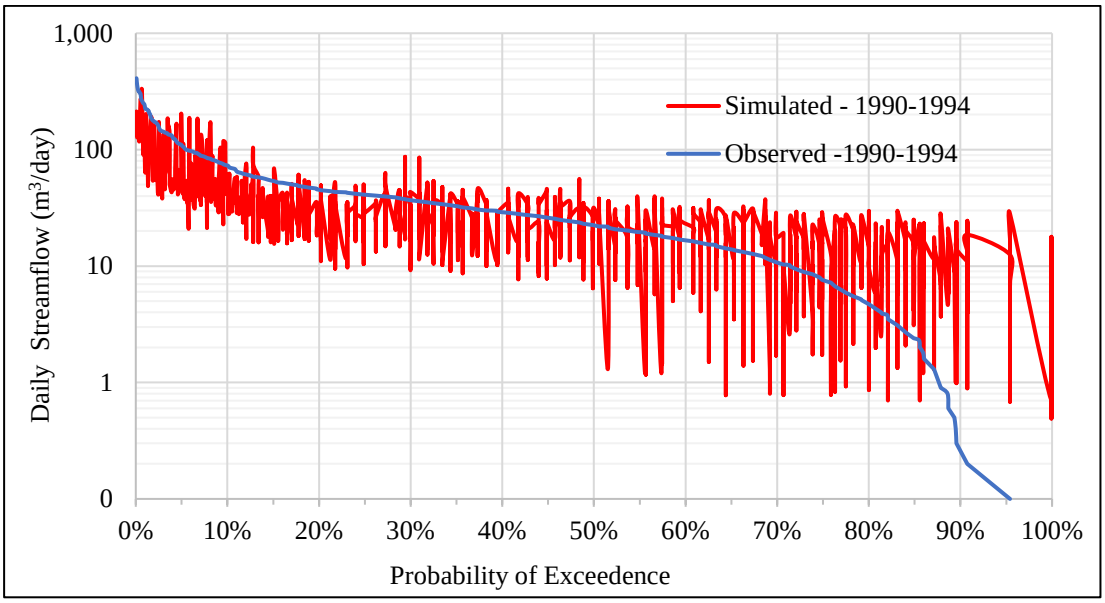

Figure 4-6: Flow duration curve of observed discharge and simulated discharge sorted against the observed for calibration period of 1990 to 1994

The observed discharge versus simulated hydrograph for the calibration period of 1990 to 2004 is presented in Figure 4-3 to Figure 4-4 where the model is able to match most of the peak discharges. Conversely, the model is unable to capture low flow during the calibration period. The flow values below 10 m^3/s are not well matched throughout the period. Further, the flow duration curve is drawn for the calibration period as shown in Figure 4-5 and Figure 4-6 well indicated the matching of high flows and

intermediate flows. The mismatch in the low flow can be well identified from both flow duration curves.

Table 4-4: Objective functions after model validation

The objective function of the model in case of validation		
RMSE	Nash-Sutcliff	Percent Bias
0.60	0.55	13.90 %

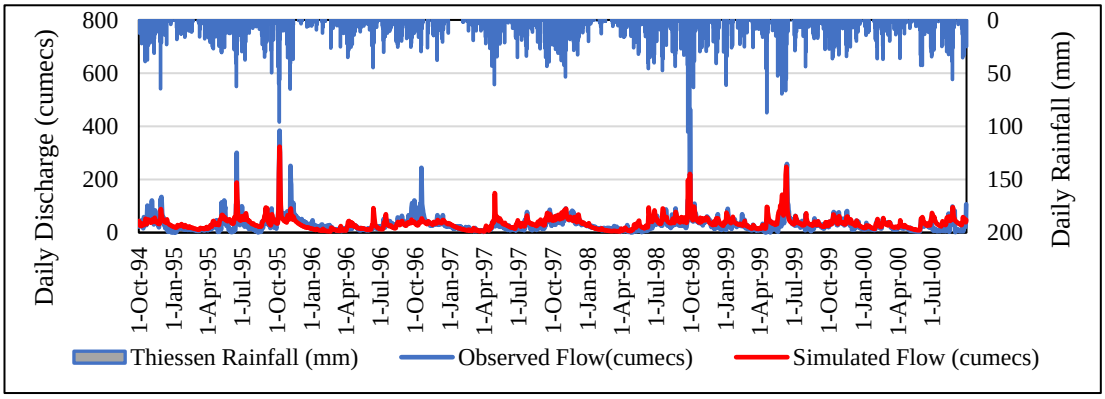

Figure 4-7: Observed versus simulated hydrograph for validation from 1994-2000 (Normal)

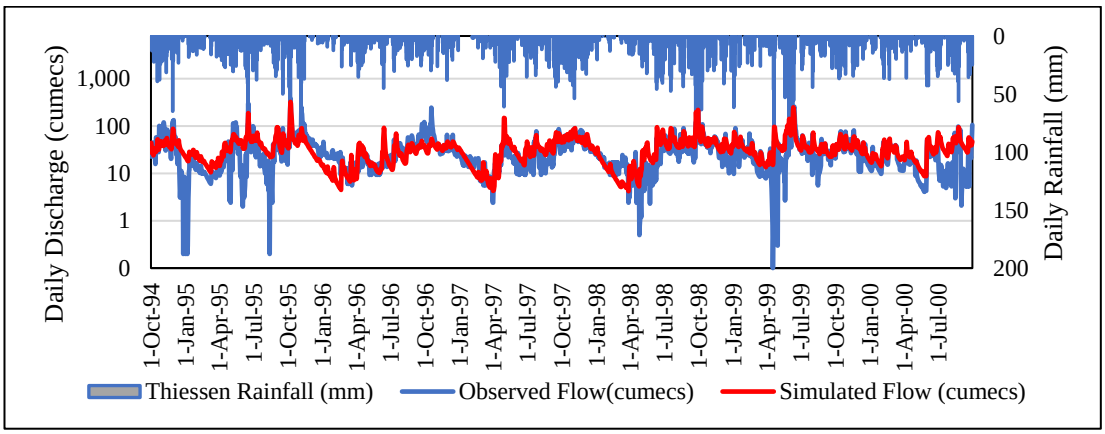

Figure 4-8: Observed versus simulated hydrograph for validation from 1994-2000 (Semi Log)

The observed versus simulated hydrograph for the calibration period of 1994 to 2000 is presented in Figure 4-3 and Figure 4-8 where the model is able to match most of the peak discharges but the low flow and intermediate flow are not matching. Further, the model is unable to capture low flow during the validation period. Moreover, the

flow duration curve is drawn for the validation period as shown in Figure 4-9 and Figure 4-10 well indicated the matching of high flows and intermediate flows. The mismatch in the low flow can be well-identified from both flow duration curves.

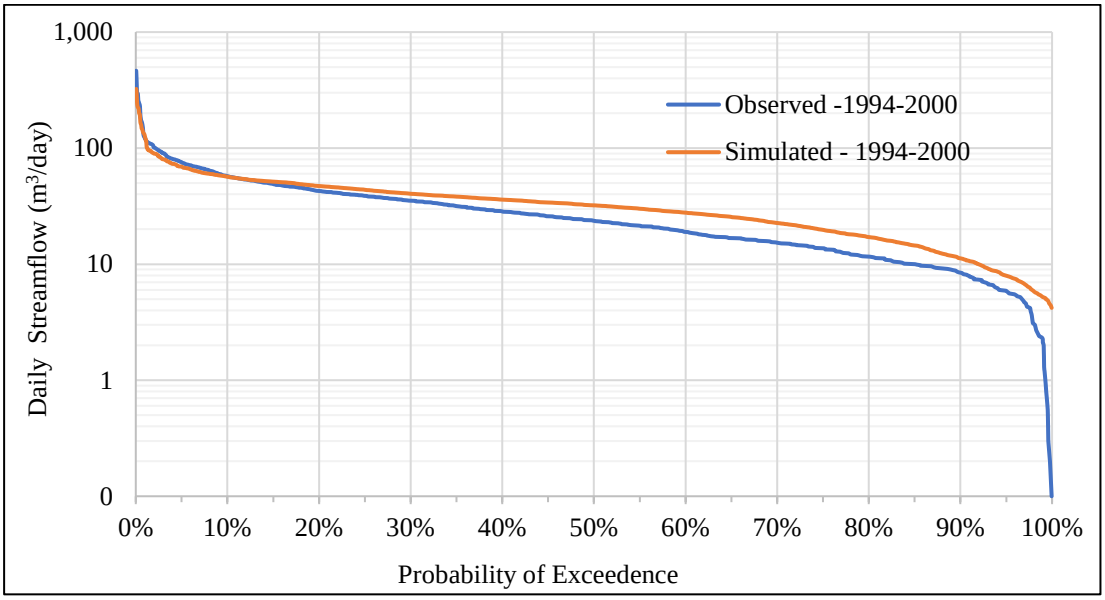

Figure 4-9: Flow duration curve of observed discharge and simulated discharge sorted in descending order for validation period of 1994 to 2000

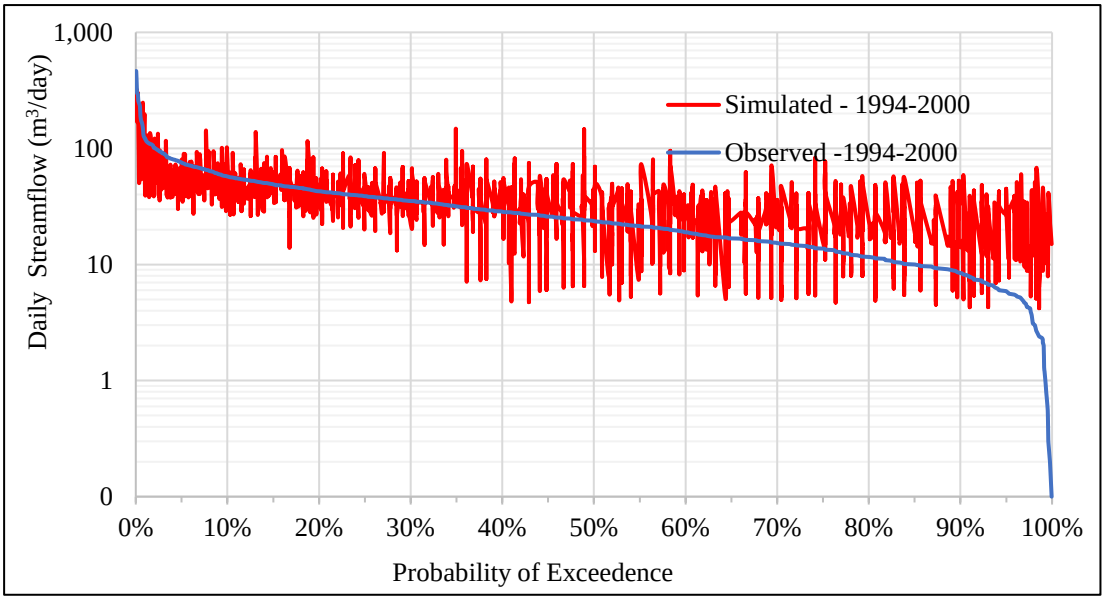

Figure 4-10: Flow duration curve of observed discharge and simulated discharge sorted against the observed for validation period of 1994 to 2000

4.3 Future Runoff Forecasting

After the calibration and validation of the model for observing flow, the model is justified based on the optimized parameter for the future runoff simulation, the model simulation is carried out for both RCM scenarios (RCP4.5 and RCP 8.5). The duration of the model simulation for mid-century from 2040 to 2060 and the end-century from 2080 to 2100 is selected.

4.3.1 Mid-Century Period

The future water availability in the basin during the mid-century period considering the RCP 4.5 scenario is as presented in Figure 4-11 and Figure 4-12. During the 20 years, the peak discharge obtained is 1,577 m^3/s. Similarly, for the same period considering the RCP 8.5 scenario as presented in Figure 4-13 and Figure 4-14, the peak discharge obtained is 1,550 m^3/s. Although the peak discharge magnitude during RCP 8.5 is lesser than the RCP 4.5 in the mid-century period, the frequency of occurrence of the peak discharge is higher in the RCP 8.5 scenario.

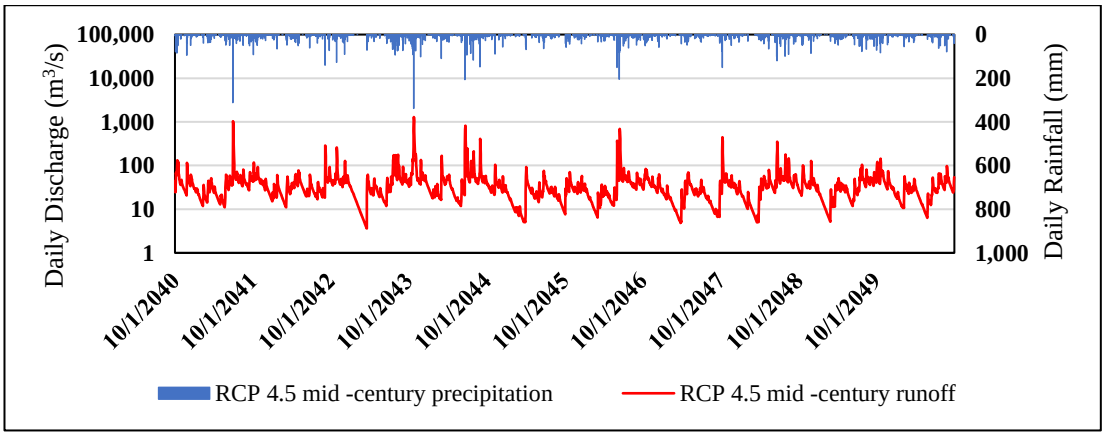

Figure 4-11: Future rainfall vs. simulated runoff for the mid-century (2040 – 2050) for RCP 4.5 scenario

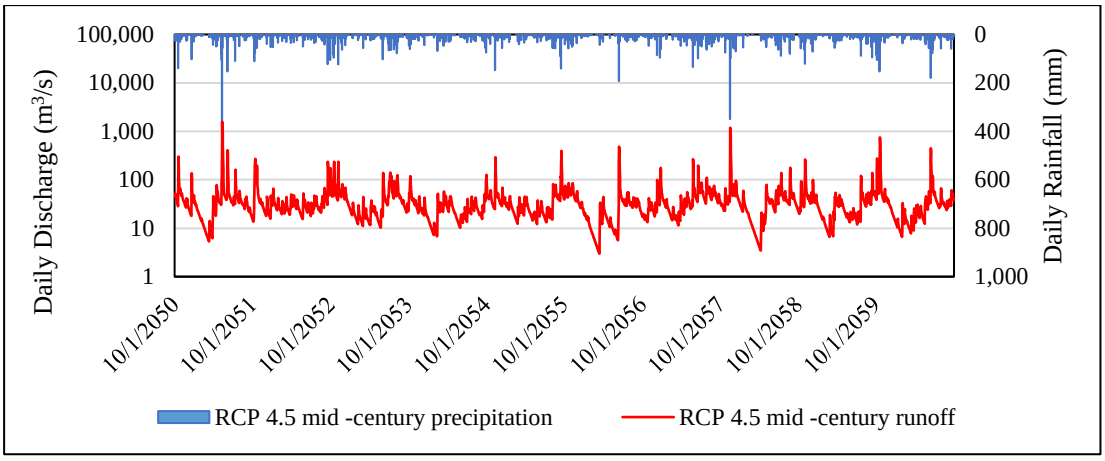

Figure 4-12: Future rainfall vs. simulated runoff for the mid-century (2050 – 2060) for RCP 4.5 scenario

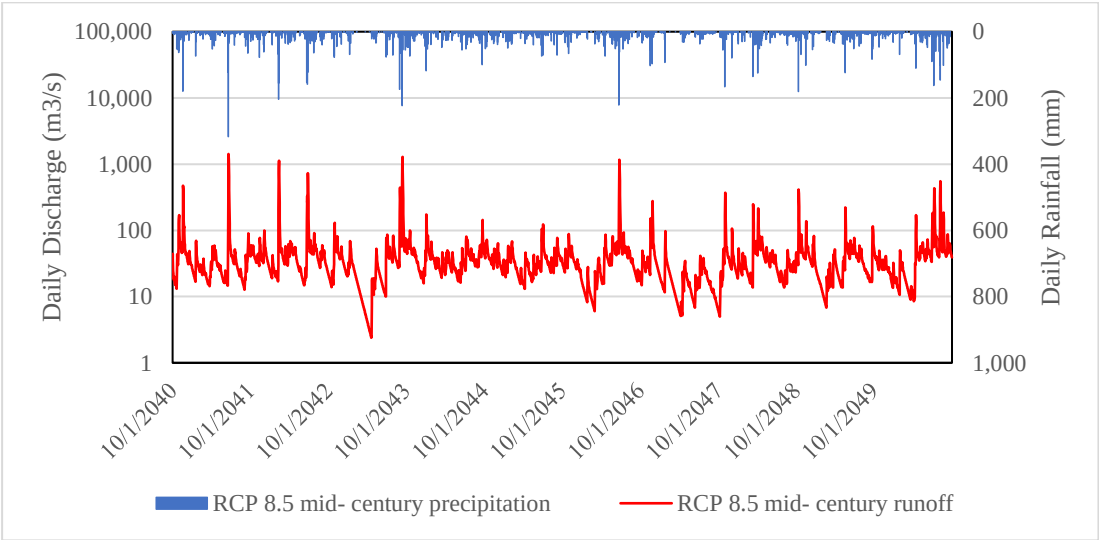

Figure 4-13: Future rainfall versus simulated runoff for mid-century (2040 – 2050) for RCP 8.5 scenario

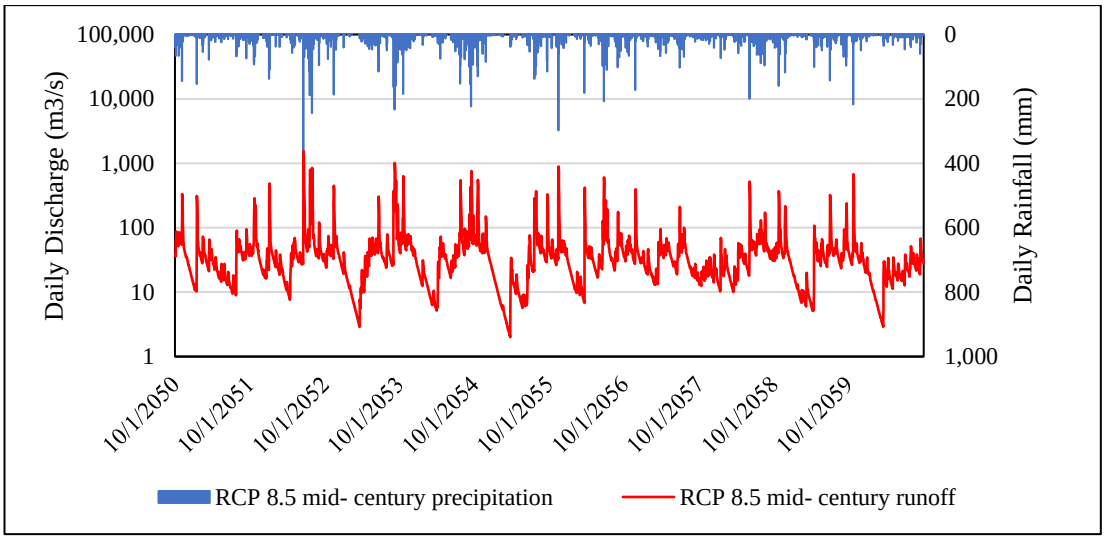

Figure 4-14: Future rainfall versus simulated runoff for mid-century (2050 – 2060) for RCP 8.5 scenario

4.3.2 End-Century Period

The future water availability in the basin during the end-century period considering the RCP 4.5 scenario is presented in Figure 4-15 and Figure 4-16. During the 20 years, the peak discharge obtained is 1,452 m^3/s. Similarly, for the same period considering the RCP 8.5 scenario as presented in Figure 4-17 and Figure 4-18, the peak discharge obtained is 1,9175 m^3/s. Here, the peak discharge magnitude during RCP 8.5 is higher than the RCP 4.5 in the end-century period, the frequency of occurrence of the peak discharge is higher in the RCP 8.5 scenario.

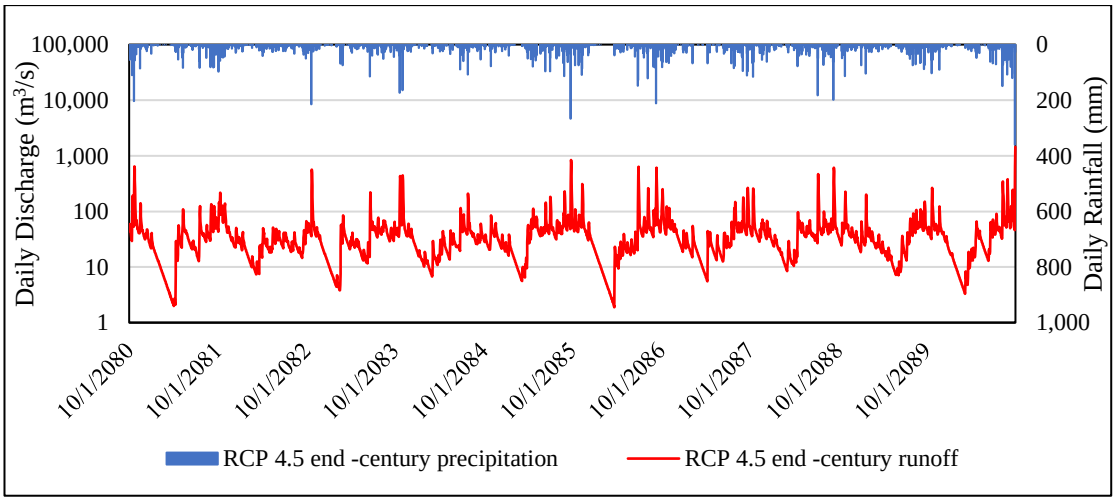

Figure 4-15: Future rainfall versus simulated runoff for end century (2080 – 2089) for RCP 4.5 scenario

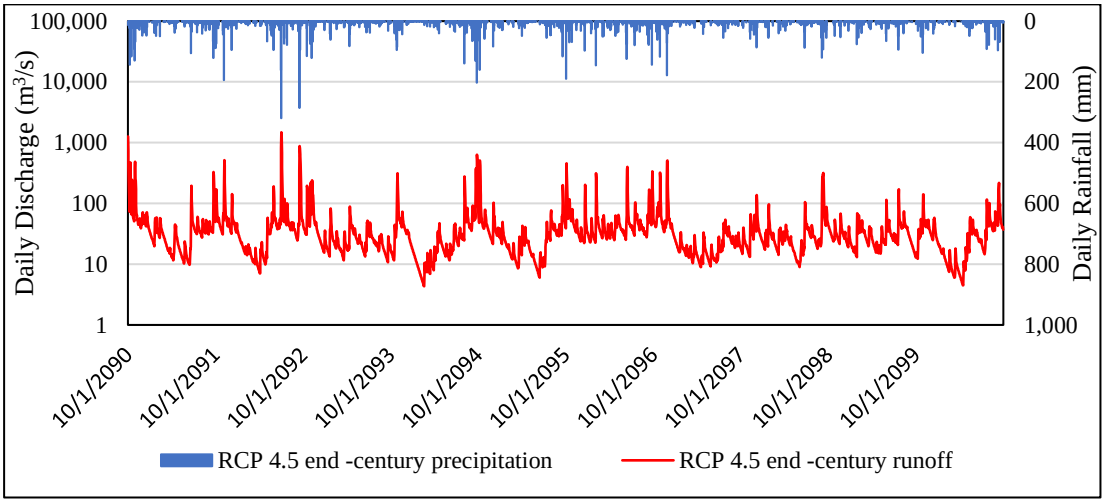

Figure 4-16: Future rainfall versus simulated runoff for end century (2090 – 2100) for RCP 4.5 scenario

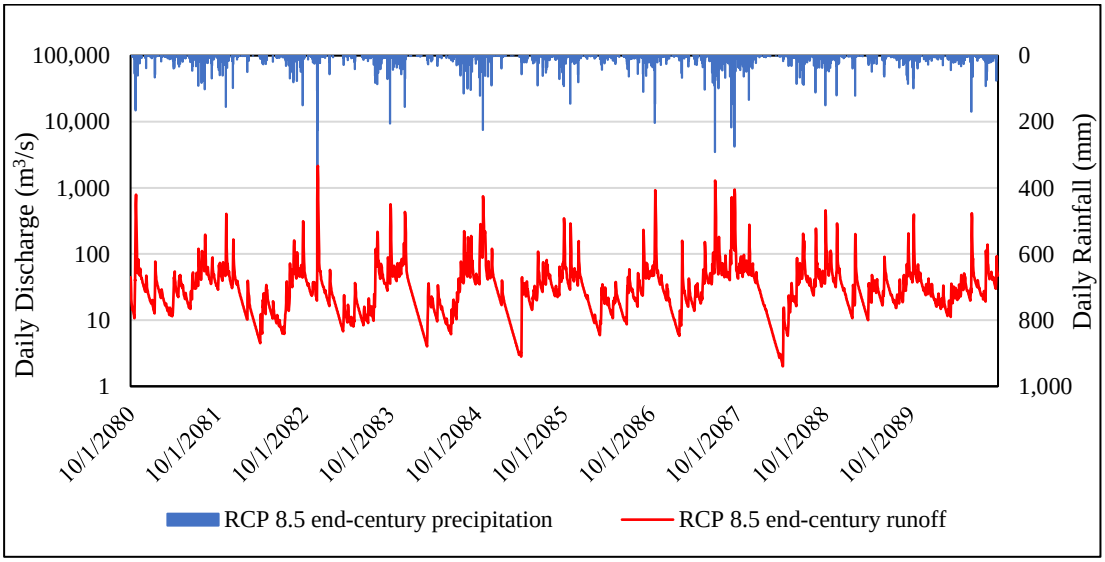

Figure 4-17: Future rainfall versus simulated runoff for end century (2080 – 2090) for RCP 8.5 scenario

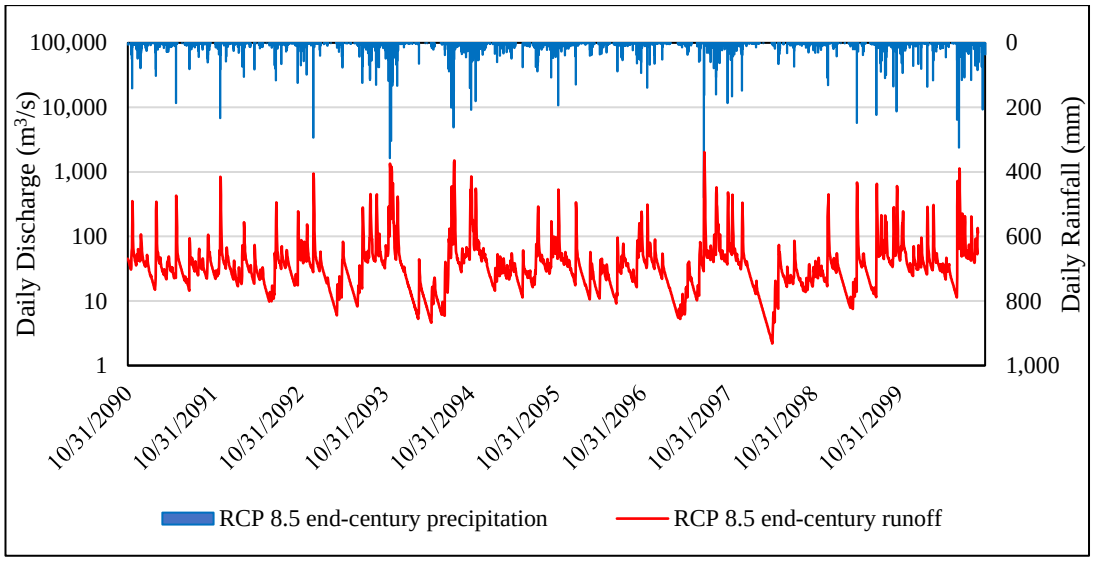

Figure 4-18: Future rainfall versus simulated runoff for end century (2090 – 2100) for RCP 8.5 scenario

4.4 Analysis of Water Availability Based on Observed Streamflow and Regional Climate Model Scenarios

In this analysis, the assessment of water availably based on decadal and seasonal periods was analyzed using the runoff simulated using the climate data in the HEC-HMS model.

4.4.1 Analysis of Water Availability in Case of the Annual Period

According to Figure 4-19, the average decadal water availability based on historical observed flow, for the mid-century in RCP 4.5 is indicating that the water availability is increasing by 17.96 %, but according to the RCP 8.5 scenario, it represents that the water availability is increasing by 6.66 %. The summary table is attached in Table A - 4 Annexure 2.

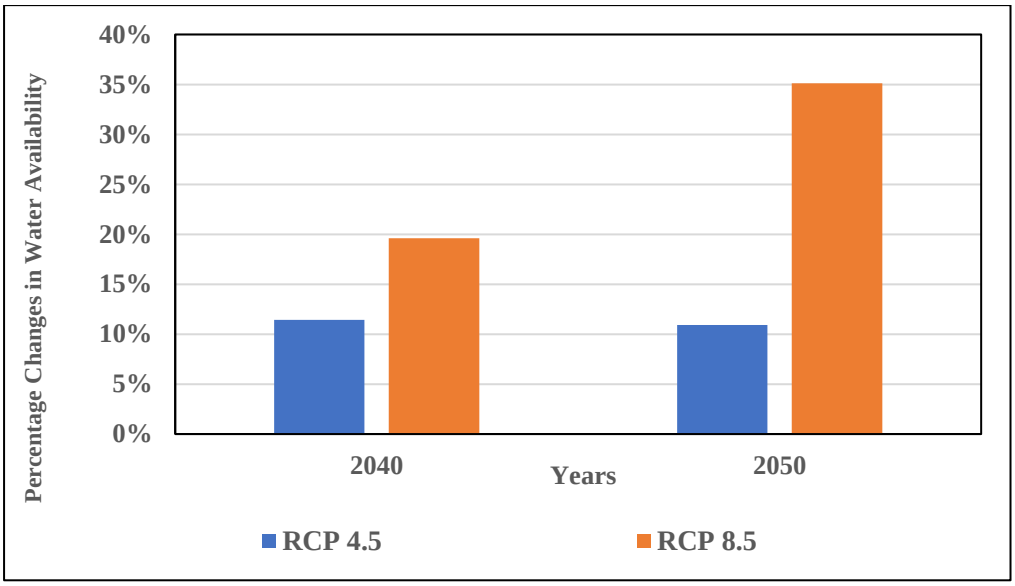

Figure 4-19: Increasing of water availability based on historical observed streamflow in mid-century for both scenario RCP 4.5 and RCP 8.5

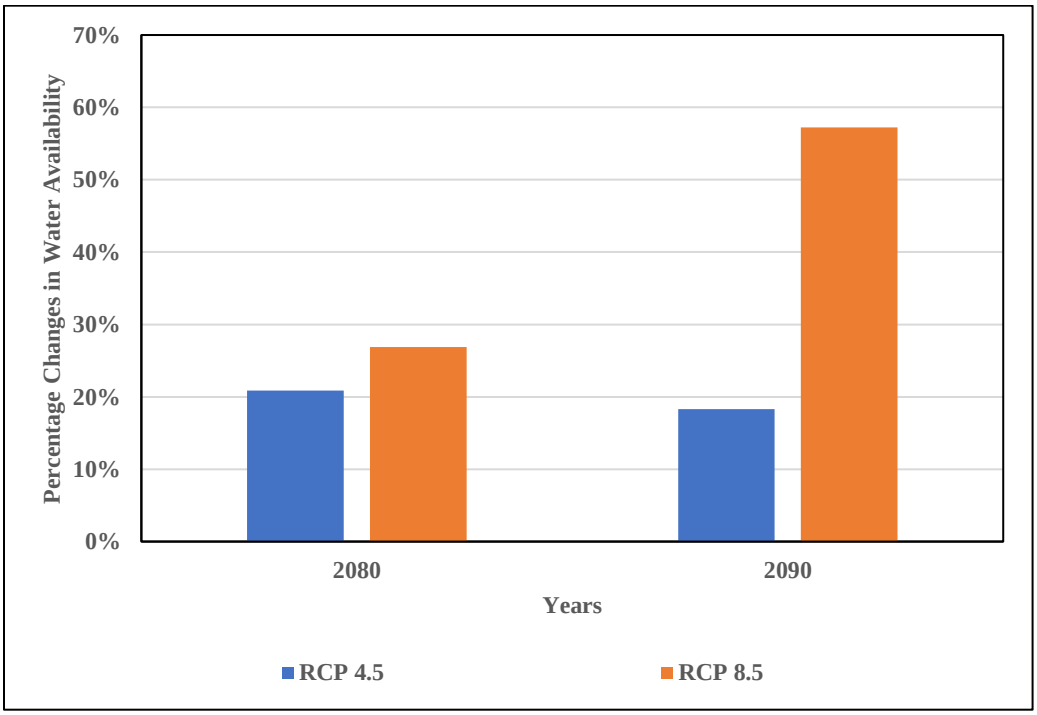

Figure 4-20: Increasing of water availability based on historical observed streamflow in end century for both scenario RCP 4.5 and RCP 8.5

According to Figure 4-20, variation of decadal average water availability based on historical observe flow for the end century in RCP 4.5 is indicating that the water

availability is increasing 11.49 % per decade, but according to the trend analysis, in the case of the RCP 8.5 scenario, it represents that the water availability is increasing 28.27 % per decade. The summary table is attached in Table A - 5Annexure 2.

4.4.2 Analysis of Water Availability in Case of the Seasonal Period

Figure 4-21 shows that the variation of water availability in the first inter-monsoon seasonal based on historical observed flow for the mid-century in RCP 4.5 is showing that the water availability is increasing 38.8 %. But in the case of the RCP 8.5 scenario, it represents that the water availability is increasing 46.48 %. Therefore, the water availability is more enlarging in the RCP 8.5 scenario than the RCP 4.5 scenario for the first inter-monsoon season. The summary table is attached in Table A - 6 Annexure 2.

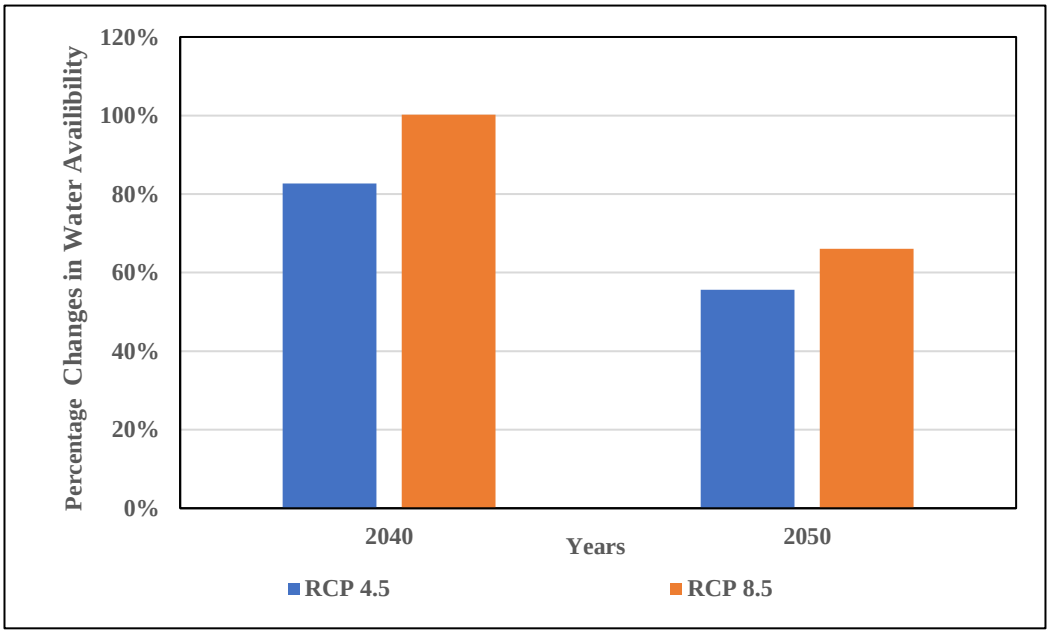

Figure 4-21: Water availability for the First Inter monsoon (March-April) based on historical observed streamflow in midcentury for both scenario RCP 4.5 and RCP 8.5

Figure 4-22 shows the variation of water availability in Southwest monsoon (May-Sep), based on historical observe flow for the mid-century in RCP 4.5 is indicating that the water availability is increasing 4.20 %, but in the case of the RCP 8.5 scenario, it represents that the water availability is increasing 22.41 %. therefore, the water

availability is more increasing in the RCP 8.5 scenario than in the RCP 4.5 scenario. The summary table is attached in Table A - 6 Annexure 2.

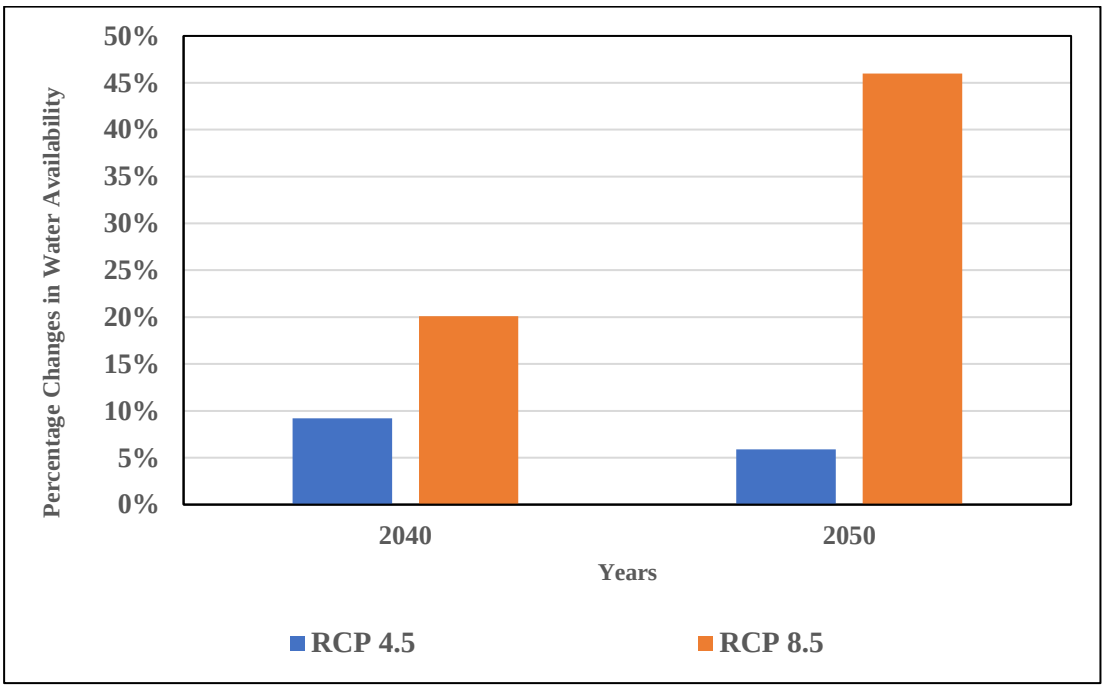

Figure 4-22: Water availability for the Southwest monsoon (May-Sep) based on historical observed streamflow in midcentury for both scenario RCP 4.5 and RCP 8.5

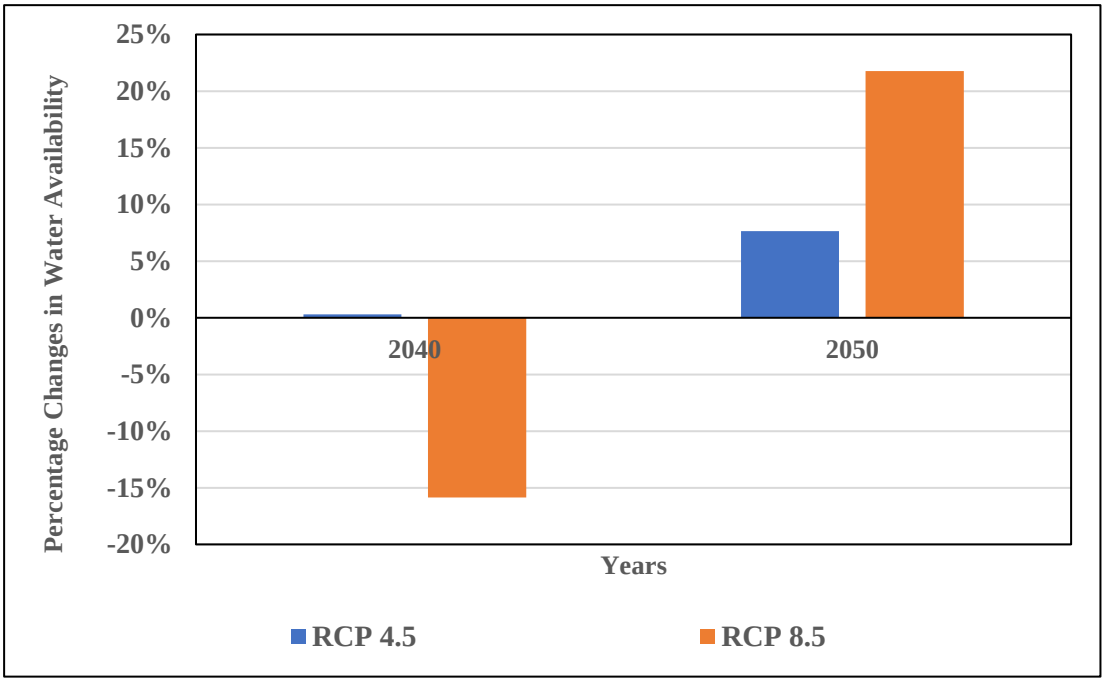

Figure 4-23: Water availability for the Second Inter monsoon (Oct-Nov) on historical observed streamflow in midcentury for both scenario RCP 4.5 and RCP 8.5

Figure 4-23 shows the variation of water availability in the Second Inter monsoon (Oct-Nov), based on historical observe flow for the mid-century in RCP 4.5 is showing that the water availability is increasing 3.12 %, but according to the trend analysis the variation of water availability for RCP 8.5 scenario, it represents that the water availability is increasing by 5.53 %. Therefore, the water availability is more increasing in the RCP 8.5 scenario than in the RCP 4.5 scenario. The summary table is attached in Table A - 8 Annexure 2.

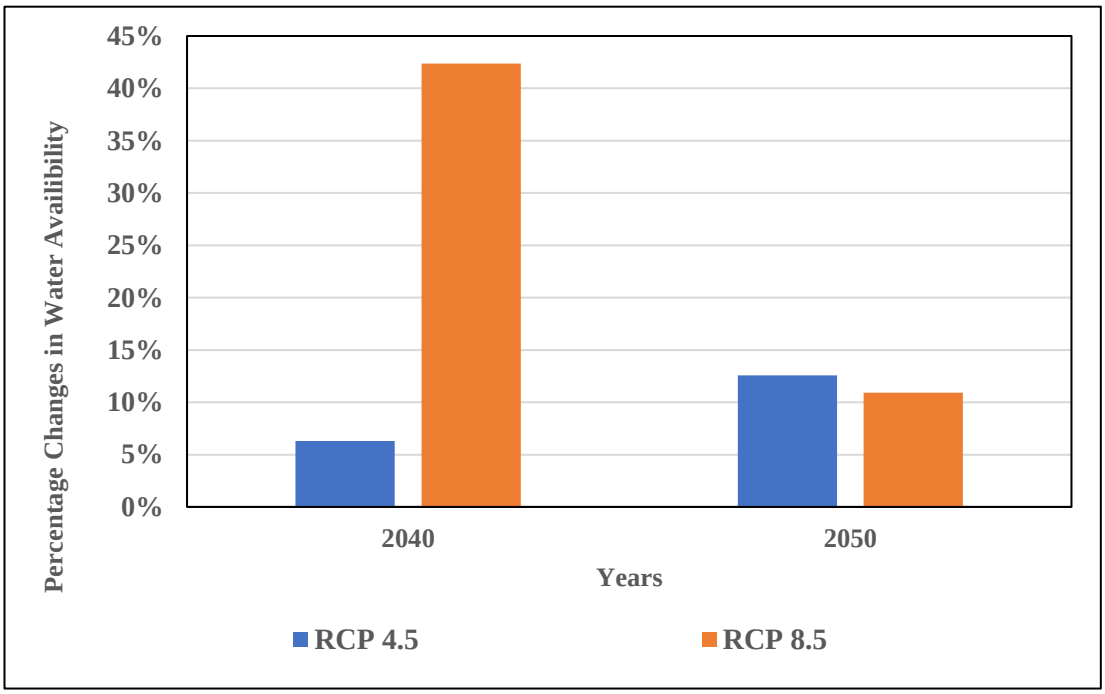

Figure 4-24: Water availability for the Northeast monsoon (Dec-Feb) based on historical observed streamflow in mid-century for both scenario RCP 4.5 and RCP 8.5

Figure 4-24 shows the variation of water availability in Northeast monsoon (Dec-Feb), based on historical observe flow for the mid-century in RCP 4.5 is points ou that the water availability is increasing 6.28 %, but in the case of RCP 8.5 scenario, it shows that the water availability is increasing 12.83 %. Therefore, the water availability is more augmented in the RCP 8.5 scenario than in the RCP 4.5 scenario. The summary table is attached in Table A - 9 Annexure 2.

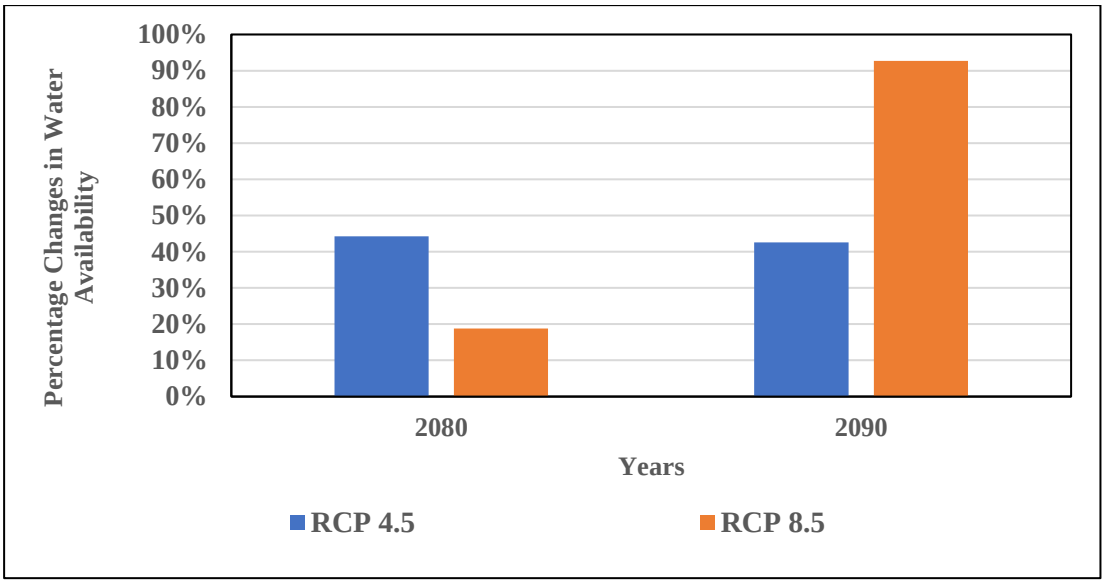

Figure 4-25: Water availability for the First Inter monsoon (March-April) based on historical observed streamflow in end century for both scenario RCP 4.5 and RCP 8.5

Figure 4-25 shows the variation of water availability in the first Inter monsoon (March-April), based on historical observed flow for the end century in RCP 4.5 is showing that the water availability is increasing 25.90 %, but in the case of the RCP 8.5 scenario, it represents that the water availability is increasing 40.83 %. Therefore, the water availability is more augmented in the RCP 8.5 scenario than in the RCP 4.5 scenario The summary table is attached in Table A - 10 Annexure 2

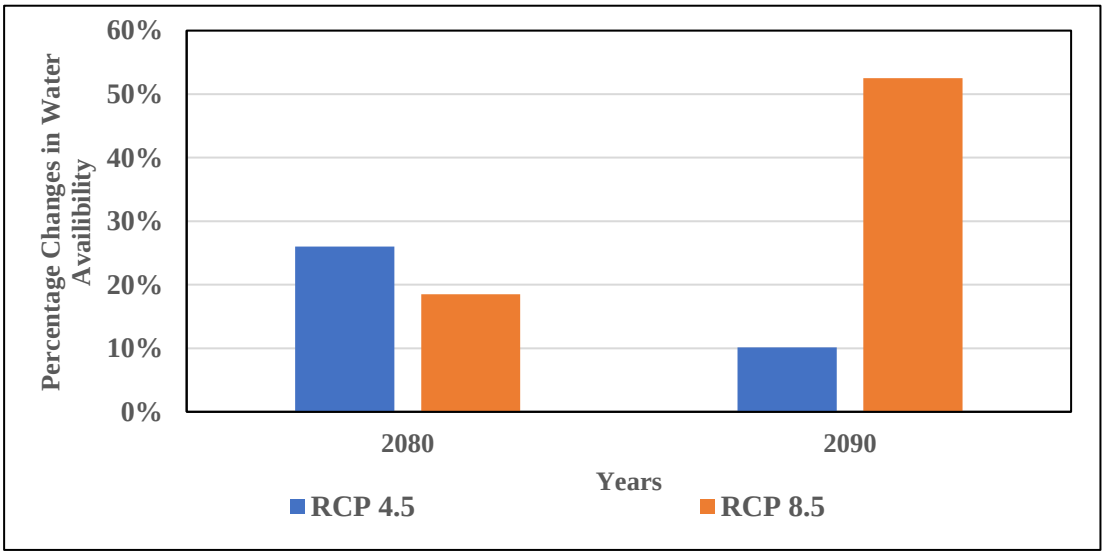

Figure 4-26: Water availability for the Southwest monsoon (May-Sep) based on historical observed streamflow in end-century for both scenario RCP 4.5 and RCP 8.5

Figure 4-26 variations of water availability in Southwest monsoon (May-Sep) based on historical observed flow for the end century in RCP 4.5 is indicating that the water availability is increasing 9.26 %, but in the case of the RCP 8.5 scenario, it represents that the water availability is increasing 24.71 %. Therefore, the water availability is more increasing in the RCP 8.5 scenario than in the RCP 4.5 scenario. The summary table is attached in Table A - 11 Annexure 2.

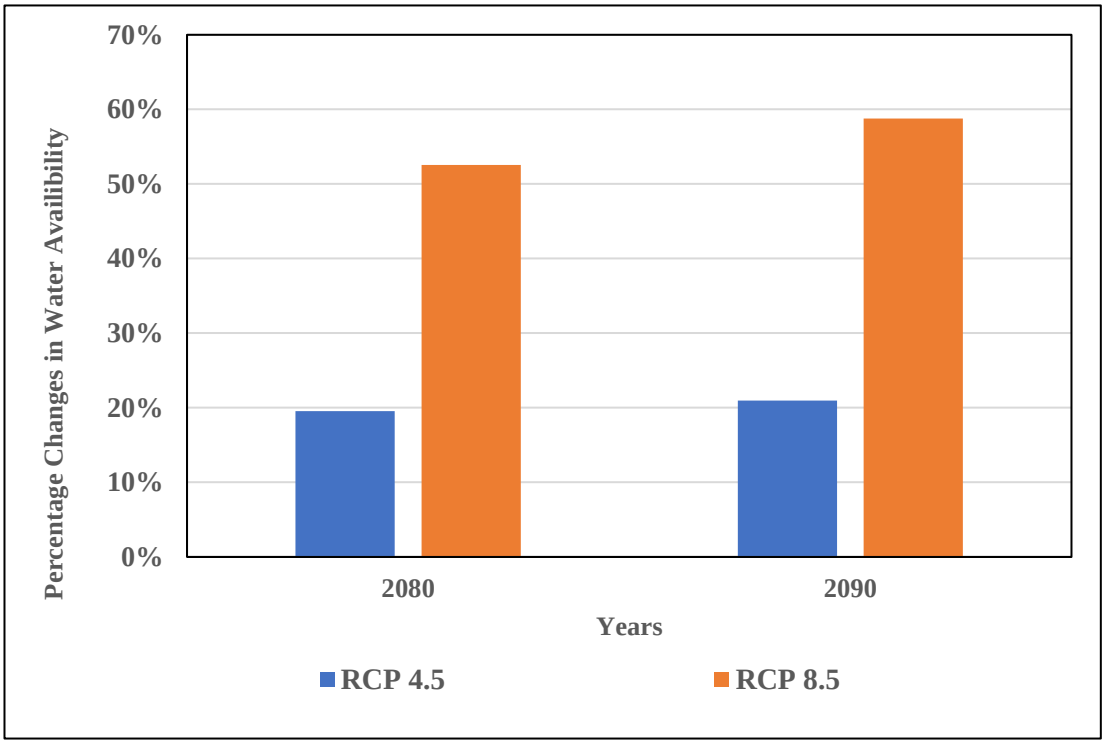

Figure 4-27: Water availability for the Second Inter monsoon (Oct-Nov) based on historical observed streamflow in end century for both scenario RCP 4.5 and RCP 8.5

Figure 4-27 shows the variation of water availability in the Second Inter monsoon (Oct-Nov) based on historical observe flow for the end century in RCP 4.5 is points out that the water availability is increasing 12.28 %, but according to the trend analysis, the variation of water availability for the RCP 8.5 scenario represents that the water availability is increasing 34.02 %. Therefore, the water availability is more increasing in the RCP 8.5 scenario than in the RCP 4.5 scenario. The summary table is attached in Table A - 12 of Annexure 2.

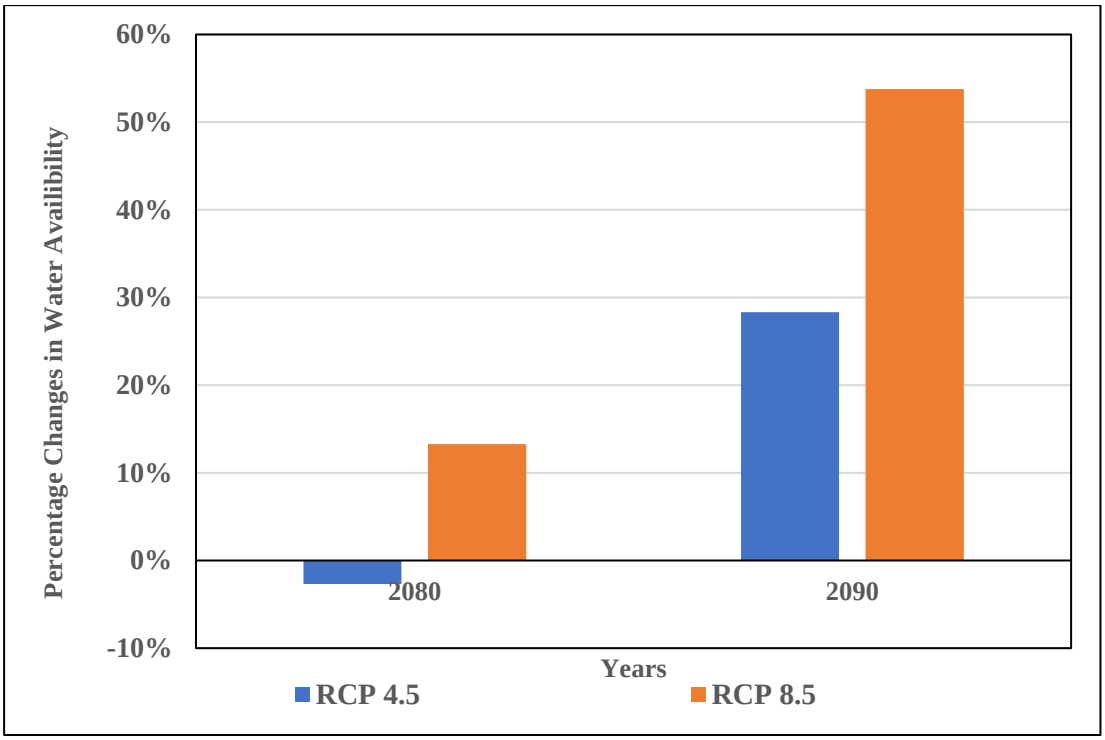

Figure 4-28: Water availability for the Northeast monsoon (Dec-Feb) on historical observe streamflow in end century for both scenario RCP 4.5 and RCP 8.5

Figure 4-28 shows the variation of water availability in Northeast monsoon (Dec-Feb) based on historical observe flow for the end century in RCP 4.5 is showing that the water availability is increasing 10.79 %, but according to the trend analysis, in the case of the RCP 8.5 scenario, it represents that the water availability is increasing 24.16 %. Therefore, the water availability is more increasing in the RCP 8.5 scenario than in the RCP 4.5 scenario. The summary table is attached in Table A - 13 Annexure2.

CHAPTER 5

5 DISCUSSION

In this study, the HEC-HMS was calibrated and validated for the Peradeniya sub-catchment in the Upper Mahaweli basin, in which the period of 1990 - 1994 and 1994 - 2000 was chosen for the model calibration and validation, respectively. Further, The future runoff for the mid-century and end-century periods was estimated using the climate data which was bias-corrected using the observed data.

The findings of this study depend on several aspects to be considered like the accuracy of input data, selection of future climate data, bias correction processes, and model optimization which are discussed in the following sub-sections.

5.1 Data Checking and Analysis

5.1.1 Filling of Missing Data

The data collected for the study are daily rainfall, daily streamflow, and daily evaporation from different available stations nearby. The rainfall data were collected from 1990 to 2015 for stations Peradeniya Bot, Helbode Estate, Nawalapitiya, and Annfield Estate. The rainfall data collected for the Peradeniya Bot station had 10 % of missing data, which is the highest percentage compared to other stations (other stations < 5% missing). If the missing data is below 10 %, it can be filled using the arithmetical average of the rainfall of nearby stations, and missing above 10 % can be filled using the normal ratio method as suggested by Chow, Maidment, and Mays (1988). But here the missing data is filled using the linear regression method as there is a variation in the spatial distribution of the rainfall magnitude from the top of the basin to the outlet.

5.1.2 Consistency Check

After the filling of missing data, the consistency and homogeneity test performed using the single mass curve and double mass curve indicated that the data is consistent and fit for the study. The annual rainfall is highest at the Helbode station (average annual rainfall around 3500 mm) which is situated in the upper part of the basin whereas the Peradeniya station (average annual rainfall around 2500 mm) situated at the outlet of the basin experiences less annual rainfall compared to the other rainfall stations.

5.1.3 Bias Correction of Climate Data

The climate data were obtained from the coordinated regional climate downscaling experiment (CORDEX) program and the dataset adopted for this study was WAS-44i with a resolution of 44 km. The climatic datasets that are huge and are highly compressed, are extracted using Python and the extracted data was verified using the CMhyd model. The climate data was bias corrected adopting the linear scaling technique where the coefficient of determination value (R^2) was obtained to be 0.34.

Although different bias-correction methods were used, the R^2 value obtained for the different methods was unacceptable (R^2 for LOCI method is 0.09, R^2 for transform method is 0.06) and finally the linear scaling technique was adopted for the bias correction of the climate data set. The bias correction was carried out using the rainfall data of the historical period from 1990 to 2015 where the historical data of the model is compared with the observed data for the same period and a multiplication factor is obtained. This factor is in turn is employed for the future period to correct the climate data for the mid-century and end-century periods.

5.2 HEC-HMS Model Development

5.2.1 Parameter Estimation

The HEC-HMS model was developed for this study with canopy storage and surface storage layers storing water as the upper layers. The maximum storage parameters and maximum surface storage parameters are obtained using the land use map and the digital elevation model (DEM). The maximum canopy storage was obtained in the upstream ridges where there is more vegetation with higher storage. Conversely, the

surface storage is maximum in the middle part of the basin in a small area which can be referred to as Section 3.9.3. The precipitation loss model was selected as a deficit and constant method where the curve number was computed using the land-use properties, antecedent soil moisture condition, and soil properties. The curve number obtained for the sub-basin 1 is 79.20 which is higher than the other two (2) sub-basins. The reason for the higher curve number in sub-basin 1 is that the basin lies in the lower part of the basin where there is a more impervious area due to the increased human settlement.

Here, the baseflow was calculated by adopting the recession model and the parameters were calculated using the streamflow recession analysis. Later, the parameters computed were adjusted during the calibration and validation of the model performance. The lag time was calculated using the Kirpich formula and the maximum lag time in the sub-basin was 97 minutes. This indicates that the discharge is approaching rapidly towards the outlet of the catchment.

5.2.2 Sensitivity Analysis

Finding the sensitive parameters in the model is the most important task for getting good results for calibration, where the most sensitive parameters were identified through sensitivity analysis of the model. For the sensitivity analysis, the model parameters were varied in the rages of – 30 % up to +30 % and the changes in the model performance were observed. The performance metrics adopted in the sensitivity analysis are the total runoff volume and the peak discharge. The impervious (%), surface storage (mm), and recession constant are the most sensitive parameters in the model affecting the runoff generation in the catchment.

5.2.3 Model Optimization and Future Simulation

After obtaining the sensitive parameters in the models, the calibration and validation process was carried out in the HEC-HMS model to optimize the model parameters to ensure that correct result is obtained from the model and a higher degree of uncertain results are avoided. The calibration is carried out from 1990 to 1994 where the parameters are optimized by comparing the observed discharge with the simulated discharge. Thereafter, the optimized parameters were used to run the model for the

period of 1994 to 2000 and the performance was measured with different objective functions.

After calibration and validation of the model for observing data sets and optimizing all parameters. The optimized parameters fix for the climate data sets and generate the future runoff for both scenarios RCP 4.5 and RCP 8.5. The model generates the runoff for future mid and end centuries. In this study, we considered from 2040-2060 as mid-century and 2080-2100 as the end century. The period is considered for the annual and seasonal periods. The runoff for RCP 4.5 and RCP 8.5 scenarios for mid and end century generated by the HEC HMS 4.8 is considered. According to the historical observation of flow data, an increase in the annual flow is observed for both scenarios is considered. In this comparison, we considered how much the water availability is increasing for both scenarios RCP 4.5 and RCP 8.5. According to the evaluation of mentioned parameters in comparison to RCP 4.5, in the case of RCP 8.5, the runoff is more increasing for both seasonal and annual duration. The impact of global warming is the reason for rising runoff. This climate change impact is directly related to the increase in air temperature and greenhouse gases. Therefore, for a longer period the basin may experience droughts but for the short period, more runoff and frequent flooding. For controlling this future critical condition, there are some solutions like adaptation and mitigation. Mitigation is employed by developed countries to decrease the emission of CO_2 gases in the atmosphere. And for developing countries, adaptation is the preferable solution and it can be achieved through the development of integrated water resources management (IWRM) plan with sustainable development in the mind. Construction of the dam and hydraulic structure to control and store the water in flood season will help to minimize drought in the study area and reduce potential inundation and other cascade effects due to the flooding. (Shrestha, 2014)

5.1 Annual Variation in Future Water Availability

The variation of average annual water availability based on historical observe flow for the midcentury in RCP 4.5 is indicating that the water availability is increasing 17.96 % in decadal period scale, but according to the trend analysis in the case of the RCP

8.5 scenario, it represents that the water availability is increasing by 6.66 % every decade.

The variation of annual average water availability based on historical observed flow for the end century in RCP 4.5 is indicating that the water availability is increasing by 11.49 % per year, but in the case of the RCP 8.5 scenario, it indicates that the water availability is increasing 28.27 % per decade.

5.2 Seasonal Variation in Future Water Availability

The variation of water availability in the First Inter monsoon (March-April) season based on historical observe flow for the midcentury in RCP 4.5 is indicating that the water availability is increasing 38.80 %, but in the case of the RCP 8.5 scenario, it represents that the water availability is increasing 46.48 %.In Southwest monsoon (May-Sep) for RCP 4.5,4.2 % and for RCP 8.5 scenario 22.41 %.For the Second Inter monsoon (Oct-Nov) in RCP 4.5 and RCP 8.5, it increases from 3.12 % to 5.53 %, and for the Northeast monsoon (Dec-Feb) in both scenarios RCP 4.5 and RCP 8.5, it increases 6.28 % to 12.38 % respectively. The variation of water availability for the end century for the First Inter monsoon (March-April) for both scenario RCP 4.5 and RCP 8.5 increases from 25.90 % to 40.83 % respectively. And for Southwest monsoon (May-Sep) 24.71 % to 9.26 %, Second Inter monsoon (Oct-Nov) 12.28 % to 34.02 %, Northeast monsoon (Dec-Feb) 10.79 % to 24.16 % accordingly.

Table 5-1: Percentage change in future water availability in different seasons

Seasons	Mid Century		End Century	
	RCP 4.5	RCP 8.5	RCP 4.5	RCP 8.5
First Inter Monsoon (March-April)	69 %	83 %	43 %	56 %
Southwest Monsoon (May-Sep)	8 %	33 %	18 %	36 %
Second Inter Monsoon (Oct-Nov)	4 %	3 %	20 %	56 %
Northeast Monsson (Dec-Feb)	9 %	27 %	13 %	34 %

According to Table 5-1, the percentage change in water availability indicates an increase for the first inter monsoon for RCP 4.5 and RCP 8.5 by 69 % and 83 %, respectively, for the mid-century (2040-2060) period scale. For southwest monsoon, the percentage increase is around 8 % and 33 % for RCP 4.5 and RCP 8.5, respectively. For the second inter monsoon, the percentage change in future water availability is 4 % and 3 % and for northeast monsoon percentage change in future water, availability is 9 %, 27 %, respectively. Whereas the percentage change in water availability indicates an increase for the first inter monsoon for RCP 4.5 and RCP 8.5, 43 % and 56 % for the end-century (2080-2100) period scale. For southwest monsoon, the percentage increase is around 18 % and 36 % for RCP 4.5 and RCP 8.5 respectively. For the second inter monsoon, the percentage change in future water availability is 20 % and 56 % and for northeast monsoon percentage change in future water, availability is 13 %, 34 % respectively.

CHAPTER 6

6 CONCLUSION AND RECOMMENDATIONS

6.1 Conclusion

- Through this study, an HEC-HMS model was successfully developed with the deficit and constant as a precipitation loss method to simulate the future runoff in the Peradeniya sub-catchment of the Upper Mahaweli basin of Sri Lanka.
- For the future simulation, the climate data WAS-44i with a resolution of 44 km obtained from the CORDEX program was employed for obtaining the future precipitation and temperature data. The climate data obtained was successfully bias-corrected using a linear method with an agreeable coefficient of determination (R^2) of 0.34 compared to other methods of bias correction. Based on raw RCM data outputs and bias-corrected results purpose that, the future climate data can be significantly corrected by linear scaling of bias correction. The linear scaling method can be used for hydrologically similar basins in the region to bias-correct the climatic data.
- The HEC-HMS model developed for the Peradeniya sub-catchment of the Mahaweli basin performed well during the calibration with objective functions yielding satisfactory to good results. The root means square error standard deviation ratio (RMSE std dev) was obtained to be 0.60 along with nash Sutcliffe efficiency (NSE) of 0.62 indicating a satisfactory result from the model. The percentage bias of -15 % indicated a satisfactory performance of the model.
- Further, the model during the validation furnished satisfactory results as the RMSE std dev was obtained to be 0.60 along with NSE of 0.55 indicating a satisfactory result from the model. The percentage bias of 14 % indicated a good performance of the model.

- The First-Inter Monson likely experienced increasing flood occurrence because the increase in streamflow ranged from 43 to 83 %. While the lowest changes occurred in the Northeast monsoon (9-34 %) under both scenarios, therefore water availability might become a serious concern for the Northeast monsoon.
- This study's results indicate the increasing streamflow for the projected period; therefore, water availability is not a serious concern. However, this can cause extreme events such as floods. therefore might be vulnerable to flood damage.

6.2 Recommendations

- The model developed in this study used 3 sub-basins. Dividing into more sub-basins like that will help to analyze the water availability on a local scale and provide recommendations for effective water management.
- It is exceedingly suggested to go for finer resolution of climate data for better results. In case of bias correction, it is recommended to try different methods, and select methods giving better results for further analysis.
- It is recommended to use multiple climate models for climate change studies since the output from one model is not sufficiently reliable.

BIBLIOGRAPHY

Abdo, K. S., Fiseha, B. M., Rientjes, T. H. M., Gieske, A. S. M., & Haile, A. T. (2009). Assessment of climate change impacts on the hydrology of Gilgel Abay catchment in Lake Tana Basin, Ethiopia. *Hydrological Processes*, n/a-n/a. https://doi.org/10.1002/hyp.7363

Abu-Taleb, M. F. (2000). Impacts of Global Climate Change Scenarios on Water Supply and Demand in Jordan. *Water International*, *25*(3), 457–463. https://doi.org/10.1080/02508060008686853

Ahbari, A., Stour, L., Agoumi, A., & Serhir, N. (2018). Estimation of initial values of the HMS model parameters: Application to the basin of Bin El Ouidane (Azilal, Morocco). *Journal of Materials and Environmental Sciences*, *9*(1), 305–317. https://doi.org/10.26872/jmes.2018.9.1.34

Ahmed, F. (2012). A Hydrologic Model of Kemptville Basin—Calibration and Extended Validation. *Water Resources Management*, *26*(9), 2583–2604. https://doi.org/10.1007/s11269-012-0034-0

Bai, Y., Zhao, N., Zhang, R., & Zeng, X. (2018). Storm Water Management of Low Impact Development in Urban Areas Based on SWMM. *Water*, *11*(1), 33. https://doi.org/10.3390/w11010033

Chen, F.-W., & Liu, C.-W. (2012). Estimation of the spatial rainfall distribution using inverse distance weighting (IDW) in the middle of Taiwan. *Paddy and Water Environment*, *10*(3), 209–222. https://doi.org/10.1007/s10333-012-0319-1

Chow, V. T., Maidment, D. R., & Mays, L. W. (1988). *Applied Hydrology*.

Dhital, Y. P., Kayastha, R. B., & Eslamian, S. (2011). PRECIPITATION AND DISCHARGE PATTERN ANALYSIS: A CASE STUDY OF BAGMATI RIVER BASIN, NEPAL. 13.

Giorgi, F., & Gutowski, W. J. (2016). Coordinated Experiments for Projections of Regional Climate Change. *Current Climate Change Reports*, *2*(4), 202–210. https://doi.org/10.1007/s40641-016-0046-6

Grigsby, T. J., & McLawhorn, J. (2019). Missing Data Techniques and the Statistical Conclusion Validity of Survey-Based Alcohol and Drug Use Research Studies: A Review and Comment on Reproducibility. *Journal of Drug Issues*, *49*(1), 44–56. https://doi.org/10.1177/0022042618795878

Johnson, F., & Sharma, A. (2010). A Comparison of Australian Open Water Body Evaporation Trends for Current and Future Climates Estimated from Class A Evaporation Pans and General Circulation Models. *Journal of Hydrometeorology*, *11*(1), 105–121. https://doi.org/10.1175/2009JHM1158.1

Kristvik, E., Muthanna, T. M., & Alfredsen, K. (2019). Assessment of future water availability under climate change, considering scenarios for population growth and ageing infrastructure. *Journal of Water and Climate Change*, *10*(1), 1–12. https://doi.org/10.2166/wcc.2018.096

Madhushankha, J. M. L., & Wijesekera, N. T. S. (2021). Application of HEC-HMS Model to Estimate Daily Streamflow in Badddegama Watershed of Gin Ganga Basin Sri Lanka. *Engineer: Journal of the Institution of Engineers, Sri Lanka*, *54*(1), 89. https://doi.org/10.4038/engineer.v54i1.7438

Mirrah, A. A., & Kusratmoko, E. (2017). Application of GIS for Assessment of Water Availability in the Cianten Watershed, West Java. *IOP Conference Series: Earth and Environmental Science*, *98*, 012018. https://doi.org/10.1088/1755-1315/98/1/012018

Molden, D. J., Vaidya, R. A., Shrestha, A. B., Rasul, G., & Shrestha, M. S. (2014). Water infrastructure for the Hindu Kush Himalayas. *International Journal of Water Resources Development*, *30*(1), 60–77. https://doi.org/10.1080/07900627.2013.859044

Pachauri, R. K., Meyer, L. A., & Intergovernmental Panel on Climate Change. (2014). IPCC, 2014: Climate Change 2014: Synthesis Report. Contribution of Working Groups I, II, and III to the Fifth Assessment Report of the Intergovernmental Panel on Climate Change.

Sampath, D. S., Weerakoon, S. B., & Herath, S. (2015). HEC-HMS model for runoff simulation in a tropical catchment with intra-basin diversions – a case study of the Deduru Oya river basin, Sri Lanka. *Engineer: Journal of the Institution of Engineers, Sri Lanka*, *48*(1), 1. https://doi.org/10.4038/engineer.v48i1.6843

Seneviratne, S. I., Corti, T., Davin, E. L., Hirschi, M., Jaeger, E. B., Lehner, I., Orlowsky, B., & Teuling, A. J. (2010). Investigating soil moisture–climate interactions in a changing climate: A review. *Earth-Science Reviews*, *99*(3–4), 125–161. https://doi.org/10.1016/j.earscirev.2010.02.004

Shelton, S., & Lin, Z. (2019). Streamflow Variability in Mahaweli River Basin of Sri Lanka during 1990–2014 and Its Possible Mechanisms. 21.

Shrestha, S. (2014). Assessment of Water Availability under Climate Change Scenarios in Thailand. *Journal of Earth Science & Climatic Change*, *05*(03). https://doi.org/10.4172/2157-7617.1000184

Sophocleous, M. (2004). Global and Regional Water Availability and Demand: Prospects for the Future. *Natural Resources Research*, *13*(2), 61–75. https://doi.org/10.1023/B:NARR.0000032644.16734.f5

Tekleab, S., Uhlenbrook, S., Mohamed, Y., Savenije, H. H. G., Temesgen, M., & Wenninger, J. (2011). Water balance modeling of Upper Blue Nile catchments using a top-down approach. *Hydrology and Earth System Sciences*, *15*(7), 2179–2193. https://doi.org/10.5194/hess-15-2179-2011

Tolisano, J., Abeygunewardene, P., Athukorala, T., Davis, C., Fleming, W., Goonesekera, K., & Rusinow, T. (2009). *Lessons Learned And Donor Opportunities For Improved Assistance*. 120.

USACE. (2018). Hydrologic Modeling System HEC-HMS User's Manual (p. 640). USACE.

Xiong, W., Holman, I., Lin, E., Conway, D., Jiang, J., Xu, Y., & Li, Y. (2010). Climate change, water availability, and future cereal production in China. *Agriculture, Ecosystems & Environment*, *135*(1–2), 58–69. https://doi.org/10.1016/j.agee.2009.08.015

ANNEXURE 1

CURVE NUMBER

Table A - 1 Curve Number Calculation for Sub Catchment one (1)

	GFCODE	Area (sq. km)	Area in Percentage	Soil Group	Curve Number (CN)	CN x A
Sub catchment 1 (one)	BLTPA	0.173	0.03	C	85	14.67
	CMTYA	0.017	0.00	C	80	1.39
	FRSUA	33.534	5.95	C	58	1944.97
	HOMSA	123.183	21.87	C	90	11086.50
	MRSHA	0.024	0.00	C	89	2.18
	OTHRA	17.787	3.16	C	81	1440.75
	PDDYA	41.640	7.39	C	95	3955.82
	RBBRA	12.293	2.18	C	67	823.65
	ROCKA	2.931	0.52	C	91	266.75
	RSVRA	0.032	0.01	C	95	3.03
	SCRBA	46.179	8.20	C	64	2955.46
	STRMA	6.411	1.14	C	97	621.85
	TANKA	0.270	0.05	C	97	26.22
	TEAA	278.567	49.47	C	77	21449.67
	TNKAA	0.012	0.00	C	90	1.12
	WTRHA	0.092	0.02	C	93	8.58
Total		563.15	100.00	Weighted Average C		79.20

Table A - 2 Curve Number Calculation for Sub Catchment Two (2)

	GFCODE	Area (sq. km)	Area in Percentage	Soil Group	Curve Number (CN)	CN x A
Sub Catchment 2 (two)	CMTYA	0.02	0.01	C	80	1.62
	FRSUA	49.67	19.30	C	58	2880.84
	HOMSA	27.83	10.81	C	90	2504.70
	MRSHA	0.12	0.05	C	89	10.69
	OTHRA	2.70	1.05	C	81	218.54
	PDDYA	8.65	3.36	C	95	821.36
	ROCKA	3.71	1.44	C	91	337.62
	RSVRA	6.64	2.58	C	95	631.05
	SCRBA	11.03	4.28	C	64	705.92
	STRMA	1.65	0.64	C	97	159.89
	TANKA	0.12	0.05	C	97	11.26
	TEAA	145.24	56.42	C	77	11183.50
	WTRHA	0.05	0.02	C	93	4.49
	Total	257.42	100.00	Weighted Average C		75.64

Table A - 3 Curve Number Calculation for Sub Catchment Three (3)

	GFCODE	Area (sq. km)	Area in Percentage	Soil Group	Curve Number (CN)	CN x A
Sub Catchment 3 (Three)	FRSUA	126.40	40.75	C	58	7331.08
	HOMSA	8.63	2.78	C	90	776.43
	MRSHA	0.18	0.06	C	89	15.87
	OTHRA	5.86	1.89	C	81	475.00
	PDDYA	0.07	0.02	C	95	7.07
	PLGDA	0.31	0.10	C	89	27.58
	ROCKA	1.32	0.43	C	91	120.52
	RSVRA	0.62	0.20	C	95	58.67
	SCRBA	10.30	3.32	C	64	659.27
	STRMA	2.94	0.95	C	97	284.89
	TANKA	0.02	0.01	C	97	1.78
	TEAA	153.42	49.46	C	77	11813.70
	WTRHA	0.09	0.03	C	93	8.71
Total		310.17	100	Weighted Average C		69.58

ANNEXURE 2

FUTURE WATER AVAILABILITY IN THE BASIN

Table A - 4 Annual Percentage variation of Streamflow for RCP 4.5 and RCP 8.5 in mid-century

Midcentury RCP8.5 and 4.5				
Years	RCP 4.5	Percentage increase	RCP 8.5	Percentage increase
2040	1258.74	30.10%	1355.43	40.1%
2041	1002.19	3.58%	1586.69	64.0%
2042	1118.87	15.64%	1253.47	29.6%
2043	1914.54	97.88%	1077.37	11.4%
2044	688.56	-28.83%	958.17	-1.0%
2045	1114.25	15.17%	1226.65	26.8%
2046	709.44	-26.68%	667.84	-31.0%
2047	1166.38	20.55%	1068.32	10.4%
2048	898.23	-7.16%	1080.56	11.7%
2049	911.43	-5.80%	1296.28	34.0%
2050	1470.15	51.95%	1046.34	8.1%
2051	1033.96	6.87%	2027.84	109.6%
2052	1133.38	17.14%	1564.20	61.7%
2053	728.53	-24.70%	1612.98	66.7%
2054	1019.48	5.37%	1191.05	23.1%
2055	882.06	-8.83%	1508.02	55.9%
2056	1109.99	14.72%	1092.01	12.9%
2057	1275.34	31.81%	1050.57	8.6%
2058	923.39	-4.56%	1178.54	21.8%
2059	1156.80	19.56%	799.61	-17.4%

Table A - 5 Annual percentage variation of water available for RCP 4.5 and RCP 8.5 in end-century

End century RCP 8.5 and RCP 4.5				
Year	RCP 4.5	Percentage increase	RCP 8.5	Percentage increase
2080	1114.28	15.17%	1170.14	20.9%
2081	922.30	-4.67%	954.86	-1.3%
2082	1031.41	6.60%	1387.09	43.4%
2083	1067.60	10.34%	1138.63	17.7%
2084	1315.04	35.92%	1267.06	31.0%
2085	1307.10	35.10%	940.28	-2.8%
2086	1153.46	19.22%	2186.85	126.0%
2087	1372.16	41.82%	1050.21	8.5%
2088	1043.68	7.87%	1110.45	14.8%
2089	1365.85	41.17%	1071.29	10.7%
2090	1535.29	58.68%	1237.78	27.9%
2091	1833.85	89.54%	1207.55	24.8%
2092	913.87	-5.55%	1462.98	51.2%
2093	1086.19	12.26%	2361.08	144.0%
2094	923.92	-4.51%	1496.24	54.6%
2095	1512.36	56.31%	1116.46	15.4%
2096	923.96	-4.50%	1760.17	81.9%
2097	972.35	0.50%	925.80	-4.3%
2098	874.34	-9.63%	1595.30	64.9%
2099	870.35	-10.04%	2049.05	111.8%

Table A - 6 Percentage variation of water availability for RCP 4.5 and RCP 8.5 in mid-century in case of First Inter monsoon (March-April)

Midcentury RCP 8.5 and RCP 4.5 First Inter monsoon (March-April)				
Years	RCP 4.5	Percentage increase	RCP 8.5	Percentage increase
2040	122.28	81.01%	138.79	105.4%
2041	159.18	135.62%	209.11	209.5%
2042	115.16	70.47%	31.56	-53.3%
2043	216.50	220.48%	142.51	111.0%
2044	104.22	54.27%	107.47	59.1%
2045	92.72	37.25%	133.46	97.6%
2046	71.05	5.17%	54.99	-18.6%
2047	102.25	51.36%	302.53	347.8%
2048	127.09	88.13%	110.05	62.9%
2049	123.75	83.18%	122.40	81.2%
2050	112.50	66.52%	137.93	104.2%
2051	138.67	105.27%	89.47	32.4%
2052	99.66	47.53%	61.35	-9.2%
2053	148.33	119.57%	93.80	38.8%
2054	125.62	85.95%	49.39	-26.9%
2055	71.52	5.87%	221.05	227.2%
2056	109.49	62.08%	188.06	178.4%
2057	40.48	-40.08%	116.86	73.0%
2058	128.70	90.51%	97.53	44.4%
2059	76.49	13.22%	66.38	-1.7%

Table A - 7 Percentage variation of water availability for RCP 4.5 and RCP 8.5 in mid-century in case of Southwest monsoon (May-Sep)

Midcentury RCP 8.5 and RCP 4.5 southwest monsoon (May-Sep)				
Years	RCP 4.5	Percentage increase	RCP 8.5	Percentage increase
2040	713.46	48.65%	687.82	43.3%
2041	444.30	-7.43%	659.60	37.4%
2042	562.92	17.29%	852.88	77.7%
2043	840.26	75.07%	442.64	-7.8%
2044	280.62	-41.53%	416.63	-13.2%
2045	719.41	49.89%	797.29	66.1%
2046	263.59	-45.08%	193.01	-59.8%
2047	637.01	32.72%	349.25	-27.2%
2048	427.19	-10.99%	491.15	2.3%
2049	351.98	-26.66%	874.04	82.1%
2050	943.07	96.49%	334.64	-30.3%
2051	413.24	-13.90%	1323.33	175.7%
2052	521.74	8.71%	1071.44	123.2%
2053	277.52	-42.18%	933.16	94.4%
2054	438.60	-8.62%	604.55	26.0%
2055	434.37	-9.50%	710.17	48.0%
2056	639.15	33.17%	434.82	-9.4%
2057	518.51	8.03%	684.55	42.6%
2058	373.17	-22.25%	613.86	27.9%
2059	523.04	8.98%	295.92	-38.3%

Table A - 8 Percentage variation of water available for RCP 4.5 and RCP 8.5 in midcentury in case of Second Inter Monsoon (Oct-Nov)

Midcentury RCP8.5 and RCP 4.5 Second Inter Monsoon (Oct-Nov)				
	RCP 4.5	Percentage increase	RCP 8.5	Percentage increase
2040	233.89	-10.74%	316.86	20.9%
2041	231.89	-11.50%	197.12	-24.8%
2042	250.39	-4.44%	180.06	-31.3%
2043	641.43	144.80%	223.50	-14.7%
2044	164.68	-37.15%	193.30	-26.2%
2045	147.14	-43.84%	183.32	-30.0%
2046	211.63	-19.23%	228.45	-12.8%
2047	282.27	7.73%	207.10	-21.0%
2048	196.49	-25.01%	319.59	22.0%
2049	268.44	2.45%	155.19	-40.8%
2050	243.60	-7.03%	314.68	20.1%
2051	286.11	9.19%	300.59	14.7%
2052	335.30	27.96%	296.94	13.3%
2053	181.90	-30.58%	433.04	65.3%
2054	254.65	-2.81%	420.90	60.6%
2055	250.28	-4.48%	399.33	52.4%
2056	99.52	-62.02%	280.47	7.0%
2057	479.41	82.96%	95.44	-63.6%
2058	244.74	-6.60%	334.27	27.6%
2059	445.34	69.96%	315.03	20.2%

Table A - 9 Percentage variation of water available for RCP 4.5 and RCP 8.5 in midcentury in case of Northeast monsoon (Dec-Feb)

Midcentury RCP8.5 and RCP 4.5 Northeast monsoon (Dec-Feb)				
	RCP 4.5	Percentage increase	RCP 8.5	Percentage increase
2040	189.11	19.70%	211.97	34.2%
2041	166.83	5.59%	520.85	229.7%
2042	190.40	20.51%	188.97	19.6%
2043	216.36	36.94%	268.71	70.1%
2044	139.04	-11.99%	240.76	52.4%
2045	154.98	-1.91%	112.59	-28.7%
2046	163.17	3.28%	191.38	21.1%
2047	144.85	-8.32%	209.44	32.6%
2048	147.46	-6.67%	159.77	1.1%
2049	167.26	5.87%	144.66	-8.4%
2050	170.98	8.22%	259.08	64.0%
2051	195.94	24.02%	314.45	99.0%
2052	176.68	11.83%	134.47	-14.9%
2053	120.77	-23.56%	152.99	-3.2%
2054	200.61	26.97%	116.21	-26.4%
2055	125.88	-20.32%	177.47	12.3%
2056	261.83	65.72%	188.67	19.4%
2057	236.95	49.97%	153.71	-2.7%
2058	176.78	11.89%	132.87	-15.9%
2059	111.93	-29.15%	122.28	-22.6%

Table A - 10 Percentage variation of Water available for RCP 4.5 and RCP 8.5 in end century in case of First Inter monsoon (March-April)

End century RCP8.5 and RCP 4.5 First Inter monsoon (March-April)				
	RCP 4.5	Percentage increase	RCP 8.5	Percentage increase
2080	52.82	-21.81%	116.15	71.9%
2081	93.92	39.02%	55.59	-17.7%
2082	146.95	117.53%	48.95	-27.5%
2083	91.69	35.73%	80.77	19.6%
2084	153.88	127.78%	72.35	7.1%
2085	52.78	-21.87%	86.54	28.1%
2086	78.02	15.48%	106.44	57.6%
2087	122.17	80.85%	24.09	-64.3%
2088	99.15	46.77%	104.68	54.9%
2089	83.33	23.34%	107.03	58.4%
2090	98.23	45.40%	235.00	247.9%
2091	56.04	-17.04%	132.37	95.9%
2092	128.45	90.14%	115.34	70.7%
2093	77.16	14.21%	49.93	-26.1%
2094	91.71	35.75%	129.48	91.7%
2095	168.51	149.43%	108.44	60.5%
2096	68.74	1.75%	68.34	1.2%
2097	123.94	83.46%	26.25	-61.1%
2098	111.92	65.67%	274.00	305.6%
2099	38.79	-42.58%	162.43	140.4%

Table A - 11 Percentage variation of water available for RCP 4.5 and RCP 8.5 in end century in case of Southwest monsoon (May-Sep)

End century RCP8.5 and RCP 4.5 southwest monsoon (May-Sep)				
	RCP 4.5	Percentage increase	RCP 8.5	Percentage increase
2080	498.30	3.82%	520.95	8.5%
2081	322.05	-32.90%	407.15	-15.2%
2082	463.52	-3.42%	455.22	-5.2%
2083	458.21	-4.53%	463.61	-3.4%
2084	857.91	78.75%	466.10	-2.9%
2085	798.59	66.39%	389.21	-18.9%
2086	543.49	13.24%	1506.97	214.0%
2087	788.63	64.31%	535.00	11.5%
2088	442.64	-7.77%	396.08	-17.5%
2089	875.26	82.36%	547.23	14.0%
2090	465.28	-3.06%	413.45	-13.9%
2091	1212.53	152.63%	450.09	-6.2%
2092	278.35	-42.00%	727.62	51.6%
2093	653.07	36.07%	1065.21	121.9%
2094	338.03	-29.57%	536.92	11.9%
2095	695.75	44.96%	449.68	-6.3%
2096	251.84	-47.53%	1275.06	165.7%
2097	486.94	1.46%	297.31	-38.1%
2098	407.06	-15.19%	878.91	83.1%
2099	497.72	3.70%	1226.76	155.6%

Table A - 12 Percentage variation of water available for RCP 4.5 and RCP 8.5 in end century in case of Second Inter monsoon (Oct-Nov)

End century RCP8.5 and RCP 4.5 Second Inter monsoon (Oct-Nov)				
	RCP 4.5	Percentage increase	RCP 8.5	Percentage increase
2080	423.11	61.48%	356.53	36.1%
2081	350.87	33.91%	296.73	13.2%
2082	326.36	24.55%	656.78	150.7%
2083	385.89	47.27%	387.31	47.8%
2084	170.56	-34.91%	571.92	118.3%
2085	333.72	27.36%	312.36	19.2%
2086	344.77	31.58%	432.92	65.2%
2087	271.28	3.53%	326.57	24.6%
2088	240.16	-8.34%	390.94	49.2%
2089	285.17	8.83%	264.92	1.1%
2090	700.38	167.29%	289.91	10.6%
2091	359.30	37.12%	376.88	43.8%
2092	336.95	28.59%	329.73	25.8%
2093	249.82	-4.66%	1109.01	323.2%
2094	302.85	15.58%	634.10	142.0%
2095	328.44	25.35%	312.97	19.4%
2096	413.78	57.91%	272.78	4.1%
2097	130.05	-50.37%	405.27	54.7%
2098	154.98	-40.85%	159.63	-39.1%
2099	192.55	-26.52%	270.26	3.1%

Table A - 13 Percentage variation of water available for RCP 4.5 and RCP 8.5 in end century in case of Northeast monsoon (Dec-Feb)

End century RCP 8.5 and RCP 4.5 Northeast monsoon (Dec-Feb)			
RCP 4.5	Percentage increase	RCP 8.5	Percentage increase
140.06	-11.35%	176.52	11.7%
155.47	-1.60%	195.40	23.7%
94.57	-40.14%	226.14	43.1%
131.81	-16.57%	206.94	31.0%
132.70	-16.01%	156.68	-0.8%
122.02	-22.77%	152.17	-3.7%
187.18	18.48%	140.52	-11.1%
190.08	20.31%	164.55	4.1%
261.72	65.65%	218.75	38.5%
122.09	-22.72%	152.11	-3.7%
271.40	71.78%	299.42	89.5%
205.99	30.38%	248.20	57.1%
170.12	7.67%	290.28	83.7%
106.14	-32.82%	136.94	-13.3%
191.33	21.10%	195.74	23.9%
319.66	102.33%	245.38	55.3%
189.60	20.00%	143.99	-8.9%
231.42	46.47%	196.98	24.7%
200.38	26.83%	282.75	79.0%
141.30	-10.57%	389.60	146.6%

The findings, interpretations and conclusions expressed in this thesis/dissertation are entirely based on the results of the individual research study and should not be attributed in any manner to or do neither necessarily reflect the views of UNESCO Madanjeet Singh Centre for South Asia Water Management (UMCSAWM), nor of the individual members of the MSc panel, nor of their respective organizations.